
CENTER
FOR PHYSICAL SCIENCES
AND TECHNOLOGY
ANNUAL
REPORT
2020
MODERN PATHS TO INNOVATIONS

A YEAR OF 2020: KICKOFF OF A NEW DECADE

It was a year with its own specifics where conventional rules of evaluation or frame of accepted estimates can hardly be applied. The year marked with pandemic sign with two different Covid waves with strongly disparate amplitudes and duration. It caused an unpredictable and strongly retarded working regime in laboratories, seminars and workshops organization, arrangements and installations of a new equipment. Even a real exchange of experience directly in the laboratories was strongly complicated.

However, for us, **the Year 2020 was exceptional** – we have reached the first significant milestone, the **10 Year Anniversary** of our Center and successfully entered into the second decade of scientific and high-tech innovation activities. Because of the pandemic situation in spring, we were forced to postpone our Jubilee Conference *10 years of scientific excellence and high-tech-innovations* planned for April. The event was finally coupled with the APROPOS 17 (*Advanced Properties and Processes in Optoelectronic Materials and Systems*) conference at the end of September. The conferences were held in a mixed format (both limited participation in the conference hall and *on-line*) enabling thus a wide participation of the scientific community. The events were successful and gave us an excellent opportunity to reflect on our history: refresh the main scientific and technological achievements, remember our roots and exceptional experience gained in former Institutes of Physics, Chemistry and Semiconductor Physics.

The Year 2020 was particular – despite pandemic situation, our scientists were very active – probably, the retarded regime allowed to concentrate their efforts on results analysis and publish more than 260 articles in highly-ranked scientific journals (instead of conventional 200 on average), successfully defend 18 PhDs theses (instead of usual 10), and increase the number of PhDs up to 105. At last, but not least, the students and PhDs from different universities in Lithuania and abroad are finding the FTMC as an attractive place for their scientific carrier or their own high-tech business development. The citizens of 17 foreign countries are among the scientific staff of FTMC.

The Year 2020 was extraordinary – a totally a new amazing phenomenon, the patronage, manifested itself in the Center on the eve of the Jubilee Event: a unique numismatic collection was donated to FTMC by one of our distinguished professors. Moreover, a necessary special equipment for studies of the face masks filtration efficiency, was installed due to sincere efforts of one of our honourable guests. Just recently we got to know that the tradition of patronage will be continued in year 2021.

It is my pleasure to present **Annual Report 2020** – the collection of the activities covering the most interesting results in science and technology, highlights of breakthrough projects, as well as the numbers illustrating main achievements and progress. We are grateful to all of you contributing to the success of the Center, extending boundaries of scientific knowledge, adding new dimensions in activities, and thus inducing new inspirations to continue further our challenging scientific journey.

Gintaras Valušis

Director of Center for Physical Sciences and Technology

Editorial board:
Rasa Pauliukaitė, Evaldas Tornau,
Kristina Plauškaitė-Šukienė

Design, Layout and Cover:
Rasa Kromkutė, Algimantas Gedgaudas

Photos:
Archives of the scientific laboratories

Published by:
Printing-house "Petro ofsetas"
Vilnius, Lithuania

Photo J. Šapolaitė

CONTENTS

LASER TECHNOLOGIES

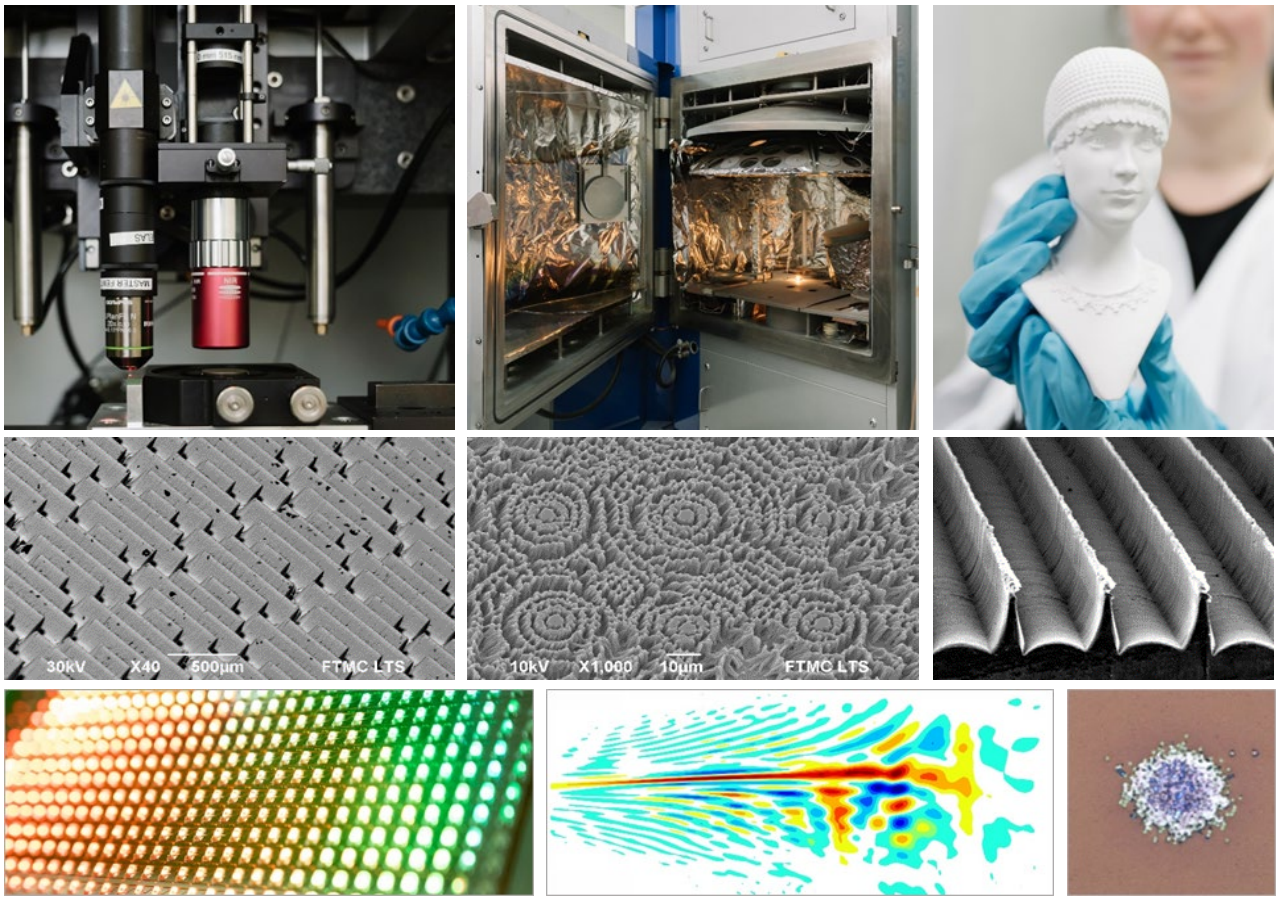

Optical coatings, solid-state and fibre lasers, laser material processing, plasmonics and nanophotonics

The Department of Laser Technologies with its seven laboratories covers a significant part of the photonics related activities, ranging from newly discovered optical effects to laser machines, and stepping through all technology readiness levels. The smart optical coatings developed in the Laboratory of Optical Coatings convert the pieces of glass into valuable products able to control spectral and temporal properties of the light. New laser sources, under development in the Fiber Laser and Solid-State Laser Laboratories, are based on tiny fibres or active bulk crystals provide not only new wavelengths of coherent radiation but high peak power, ultra-short pulses and controlled wavefront as well. Combining of the coherent beams makes the lasers even more powerful. Efficient surface texturing utilising laser beam interference, glass processing utilising smart pulsed lasers or distorted Bessel beams, nano-textures decorated by nanoparticles, 3D metal sculpturing by subtractive and additive technologies, laser-induced transformations in graphene-like materials make up the main working topics of the Laboratories of Laser Microfabrication Technologies. The scope in the material processing using ultrashort pulse lasers includes the investigations of the laser-matter interaction as well as hardware development in the Laboratory of 3D Technologies and Robotics. Significant progress was made in the validation of novel processes for electroless plating of laser-modified polymers and glasses. The Department keeps close collaboration with colleagues from other departments of FTMC, photonics companies in Lithuania and abroad gaining new ideas for joint projects and applications. The year 2020 was extremally fruitful for the Department of Laser Technologies with new projects and scientific publications in high-ranked peer-review journals.

Fabrication of Mie-resonant metasurfaces via single-pulse laser interference

Single-pulse laser interference processing was used to convert a thin amorphous silicon film into a periodical array of Mie resonators – small dielectric particles that support electric and magnetic resonances. Metasurfaces, formed from Mie resonators, could be used in photonic devices for imaging, sensing, light harvesting, etc. Laser interference processing with sub-nanosecond duration laser pulses was used to convert thin amorphous silicon film, deposited on a glass substrate, into a 570 nm period array of hemispherical nanoparticles by inducing localised melting and dewetting of amorphous silicon. The obtained arrays of amorphous silicon particles exhibited a wavelength-dependent optical response with a strong electric dipole signature. Variation of the initial uniform amorphous silicon film thickness allowed tailoring of the resonances in the targeted visible and infrared spectral ranges. The proposed technique is a step to the economically more viable fabrication of Mie metasurfaces.

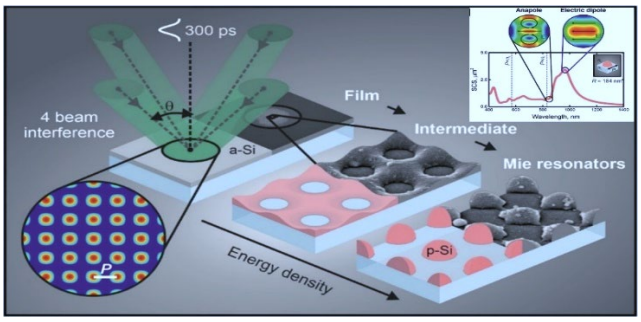

Fig. 1. Fabrication of Mie resonant metasurfaces by a single-pulse laser interference: an amorphous silicon (a-Si) film patterned by a 300 ps pulse and a four-beam interference setup. The inset on the top right corner shows scattering cross-section of a fabricated metasurface element (hemisphere radius 184 nm, the distance between hemispheres 570 nm) with highlighted electric dipole and anapole nature signatures.

simonas.indrisiunas@ftmc.lt

Control of optical resonances in dielectric nanostructures by laser-induced photo-thermal effects

An array of optically resonant dielectric nanostructures is usually fabricated using two-dimensional technologies (e. g. lithography), limiting the control over the shape of a fabricated structure. The possibility of controlling properties of the prefabricated dielectric nanostructure by photothermal effect induced by an ultrashort pulse laser irradiation was investigated. Two methods for control of the optical resonances of nanodisk arrays were explored: photothermal reshaping based on laser-induced melting, resulting in transition of the nanodisk to the shape with lower surface energy, and crystallisation of amorphous material followed by the change of the refractive index. Reshaping using tightly focused laser beam can be used for local control of nanostructure resulting in the formation of „pixels“ with different optical properties (colour) from the prefabricated template.

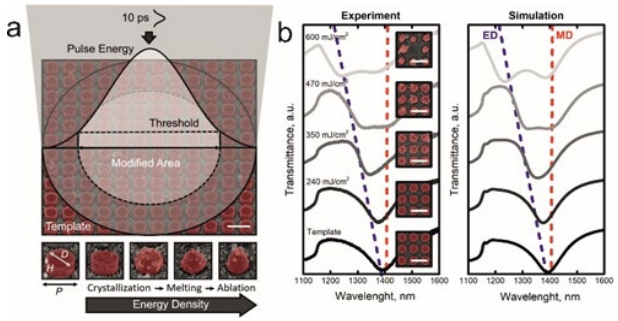

Fig. 2. Visualisation of photothermal effect on Si nanostructures (coloured red) on glass substrate using laser irradiation (a). Transmittance measurements (left) and simulations (right) of nanostructure array reshaped by increasing laser energy density (b). Insets show SEM images, scale bar – 1 µm.

simonas.indrisiunas@ftmc.lt

Laser-induced selective electroless plating on PC/ABS polymer: minimisation of thermal effects

The selective surface activation induced by laser (SSAIL) for electroless copper deposition on Polycarbonate/ Acrylonitrile Butadiene Styrene (PC/ABS) blend is a promising technique of electric circuit formation on free-shape dielectric surfaces. The limiting factor in increasing throughput of the technology is a laser activation step. Laser writing is performed by modern galvanometric scanners which reach the scanning speed of several meters per second. However, adverse thermal effects on PC/ABS polymer surface limit the high-speed laser writing. Investigations were conducted on how these thermal effects limit surface activation for selective metal deposition from the view of physics and chemistry. An advanced laser beam scanning technique of interlacing with a pulse-on-demand was applied to overcome mentioned fast laser writing problems. Experiments did not show a correlation between surface morphology and electroless plating on laser-treated areas. However, significant variation in the composition of the material was revealed depending on the surface activity for electroless plating.

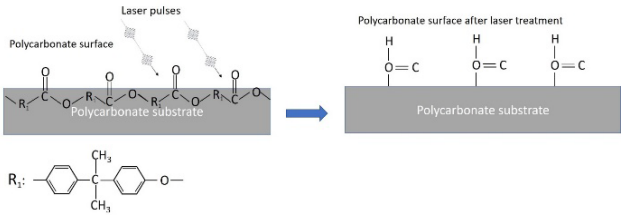

Fig. 3. Transformation of chemical groups on the PC surface after laser treatment leading to a formation of aldehyde.

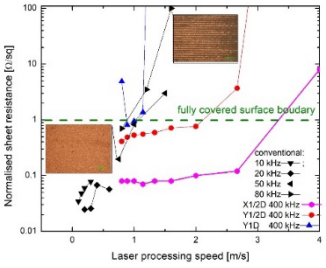

Fig. 4. Dependence of the copper layer sheet resistance on laser processing speed for various average laser power settings utilising the X1/2D, Y1/2D and Y1D laser writing techniques.

karolis.ratautas@ftmc.lt

Stress compensated backside coated chirped mirror deposited on a thin optical substrate

Chirped mirrors (CMs) are optical multilayer coatings designed for dispersion compensation in ultrashort laser systems. Chirped mirrors allow flexible dispersion properties of an optical system, but their bandgap is limited because of impedance mismatch between layer materials and the ambient medium. Backside coated chirped mirror (BASIC) is a CM designed and coated on the backside of the optical substrate which significantly reduces impedance mismatch. However, a thin optical substrate of the thickness of tenths of millimetres has to be used to minimise the dispersion impact caused by substrate material. This leads to mechanical stress induced by deposited coating to the optical substrate. As the optical substrate is relatively thin, stress can curve the final optical element and lead to mechanical failure caused by cracks or delamination of the coating. To minimise coating induced stress, careful stress reduction procedures were carried out for BASIC mirror production using ion beam sputtering technology. Such procedures include the choice of mixture material for low refractive index material layers as well as post-deposition annealing. In total, the flatness of 0.35 mm thick and 12.7 mm in diameter optical element was improved by more than 90 times from approximately 50λ to less than 0.5λ (λ=633 nm). BASIC mirror provided group delay dispersion value of −300 fs2 for 150 nm spectral bandwidth.

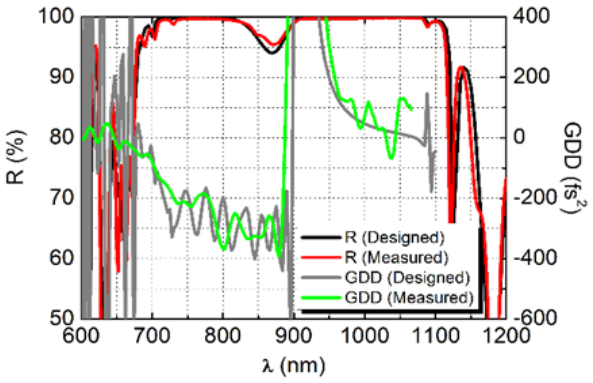

Fig. 5. Theoretical and measured reflection and GDD spectra of a BASIC mirror.

simonas.kicas@ftmc.lt

Enhancement of high reflectivity mirrors using sculptured thin films

The total generated output power in high-power laser systems is mainly limited by the laser-induced damage phenomena in coated optics. This research was conducted to develop advanced high reflectivity mirrors, capable of withstanding an extreme laser fluence and spectral stability at different ambient conditions. A concept of combination of ion beam sputtering and glancing angle deposition (GLAD) technologies was proposed and implemented to form a hybrid multilayer mirror for the 355 nm wavelength. The results show an improved reflectivity and optical resistance of consolidated coatings: the potential of laser induced damage threshold reaching 90 J/cm² for 355 nm wavelength (pulse duration 2.5 ns) while maintaining the reflectivity value higher than 99.5%. Such an element opens up new possibilities in the further development of extreme light sources.

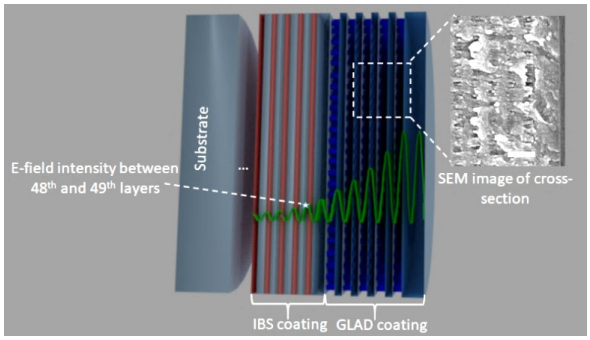

Fig. 6. Principal representation of the design and electric field distribution in hybrid high reflectivity coating. SEM image of GLAD coating cross-section is shown in the legend (the bar is set at 200 nm).

tomas.tolenis@ftmc.lt

Efficient two-stage transient stimulated Raman chirped pulse amplification in KGW

Increasing the wavelength of femtosecond laser pulses makes it possible to generate higher photon energy attosecond X-ray and higher efficiency THz pulses, and confine more energy in a single filament. The Transient Stimulated Raman Chirped Pulse Amplification method provides an alternative to the Optical Parametric Chirped-Pulse Amplifier (OPCPA) for generating intense SWIR pulses, eliminating phase matching limitations, far exceeding OPCPA efficiency, and providing an unprecedented temporal contrast. Efficient amplification of chirped supercontinuum pulses was achieved in a two-stage stimulated Raman amplifier based on KGd(WO4)2 crystals pumped with 1.2 ps pulses @ 1030 nm. The second stage demonstrated a conversion efficiency of 55% with an output pulse energy of 0.6 mJ @ 1135 nm. The amplified Stokes bandwidth was 10 times the pump bandwidth providing 145 fs pulses after compression.

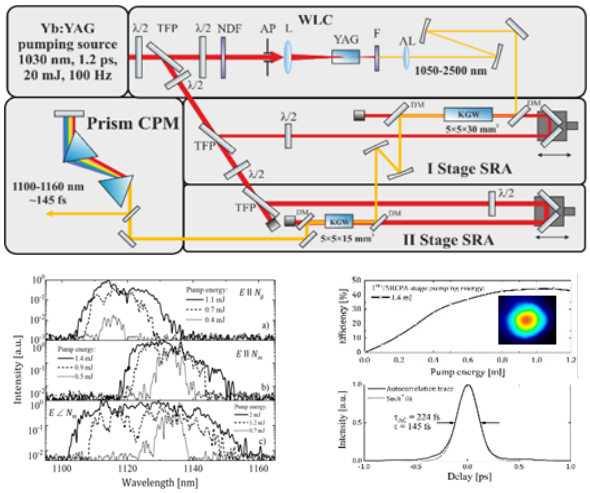

Fig. 7. The layout of an alternative method for generating intense SWIR pulses (top), transient SRS spectra broadening (bottom left), efficiency, amplified beam profile and compressed pulse (bottom right).

aleksej.rodin@ftmc.lt

TW-class laser for pumping THz and X-ray sources

A cost-effective and compact TW-class laser, developed in the Solid State Laser laboratory, provides a choice of output pulses: >20 mJ, 1 ps with M^2 < 1.1 at 1030 nm and >2.5 mJ, <20 fs with M^2~ 1.2 at 790 nm, as well as supercontinuum (SC) at 600 –2500 nm. The laser is based on fibre laser front-end, two-stage double-pass Yb:YAG chirped-pulse amplifier, grating compressor, SC generation, two cascades of second harmonic generation, three stages of the noncollinear optical parametric chirped-pulse amplifier (OPCPA), and chirped mirrors compressor. The same pump source for OPCPA and SC provides inherent synchronisation. Energy conversion efficiency has been improved by reusing depleted pump pulses and maintaining the wide OPCPA bandwidth by temporarily shaping them. The resulting ultrashort high-energy laser pulses are perfect for highly efficient THz and coherent X-ray sources.

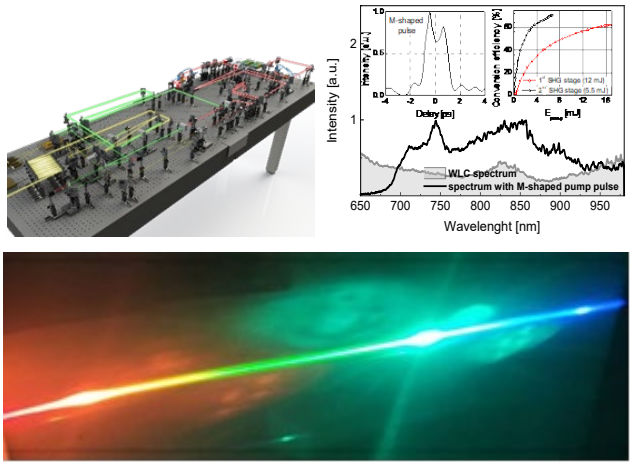

Fig. 8. The developed TW-class laser system (top left), the studied OPCPA bandwidth control principle (top right) and filamentation of intense laser pulses in a gas medium (bottom).

aleksej.rodin@ftmc.lt

In-depth comparison of conventional glass cutting technologies with laser-based methods

Conventional glass processing methods are widely used offering high throughput at low operating costs. As various laser-based methods are an appealing alternative, they need to be carefully validated before entering the industry. Three conventional technologies (mechanical scribing and breaking, diamond saw and waterjet cutting) were compared with volumetric scribing using laser Bessel beam and rear-side machining. The surface quality, side-wall roughness, residual stresses and flexural strength of cut parts were investigated under the same protocol. The elliptical shape of the Bessel beam induced directional transverse cracks, which enhanced the scribing and cleaving processes. The large non-diffractive length allowed to process 1 mm-thick substrate by a single pass. In the second approach, nanosecond laser pulses were used to fracture material into small parts, which were ejected through the rear-side. Such an approach ensures high material removal efficiency over 0.1 mm^3/J. Although the highest strength was measured for mechanical dicing and diamond saw cutting, the Bessel beam scribing provided the lowest surface chipping. The rear-side machining, which allows cutting and milling of complex 2.5D structures, overcame the waterjet technique.

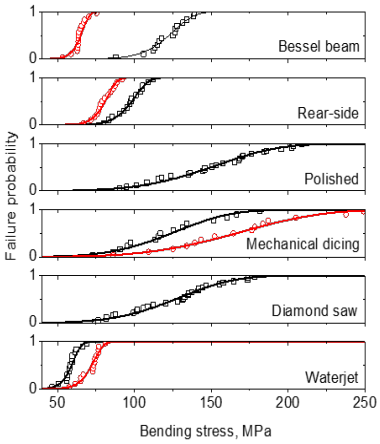

Fig. 9. The failure probability of samples, cut using different techniques and broken by the four-point bending setup. Black squares and red circles indicate the tension on the front and rear side of the samples, respectively.

juozas.dudutis@ftmc.lt

Influence of nonlinear- and saturable-absorption on laser lift-off threshold of oxide/metal structure

The pulsed laser ablation threshold, laser-induced damage threshold (LIDT), and lift-off threshold fluences are used to describe the minimum laser energy per unit area required to remove (ablate) material from the surface. However, among the theoretical models found in the literature, no one can fully explain the variation of the ablation threshold of metal/oxide structure with varying beam sizes and related peak intensities. A new model of the effective lift-off threshold of oxide/metal target is presented. The influence of nonlinear processes in the oxide layer on removing the metallic samples using a picosecond laser was investigated. Nonlinear and saturable absorption in the layer was included into modelling to predict a change in the effective laser lift-off threshold fluence with varying peak intensities in the *z*-scan type experiment. The results obtained using the new model demonstrate a good agreement with the experimental data.

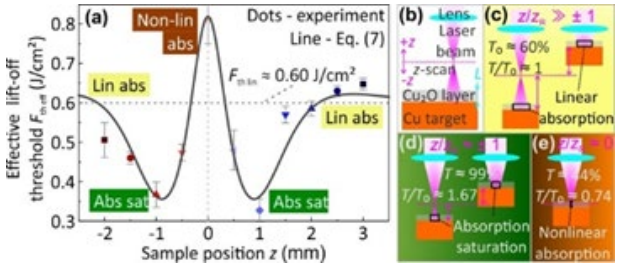

Fig. 10. (a) Effective lift-off threshold $F_{th\,eff}$ of oxide/copper dependence on sample *z* position. Dots represent the effective lift-off threshold; the solid grey line is the fit of experimental data points by the model. Pulse duration τ = 10 ps, wavelength λ = 1064 nm, and the number of pulses per spot N = 1. (b) Principal visual scheme of the proposed model with semi-transparent Cu_2O layer on top of Cu sample partially attenuating the focused picosecond laser beam in *z*-scan type laser ablation experiment. The different Cu_2O layer transmission cases are indicated depending on peak pulse intensities: (c) out of focus with sample positions $z/z_R \gg \pm 1$ and low intensities; (d) sample position $z/z_R \approx \pm 1$ in the saturable absorption intensity region; (e) sample position $z/z_R \approx 0$ in the focus of the beam and high peak intensities.

mindaugas.gedvilas@ftmc.lt

Controlling the wettability of stainless steel, from highly-hydrophilic to super-hydrophobic, by femtosecond laser-induced ripples and nanospikes

Ultrafast laser irradiation was utilised for manipulation of the wetting properties of stainless steel alloy surface. The wide range of water droplet contact angles, from highly-hydrophilic to super-hydrophobic, was achieved by generating laser-induced periodic surface structures (LIPSS) and nanospikes. In particular, the wetting state was controlled by accumulated laser fluence which determines the carbon/oxygen content and nano-texture type of the surface after laser treatment. The super-hydrophobic water-repelling surface was generated. The simple, single-step laser processing technology, was demonstrated as a promising tool for the large-scale industrial production of self-cleaning stainless steel.

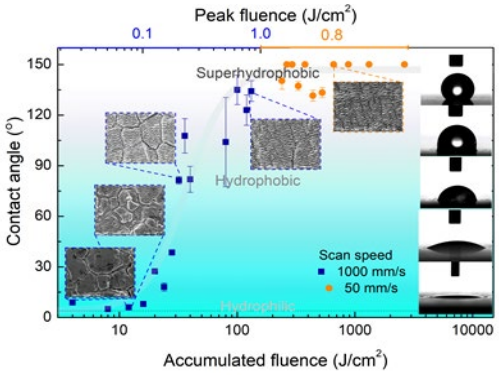

Fig. 11. Water droplet contact angle with laser-textured stainless steel surface versus the accumulated laser fluence. SEM and CCD camera pictures show the evolution of ripple formation with increased accumulated fluence and corresponding water droplet with ascending contact angle (from bottom to top).

andrius.zemaitis@ftmc.lt

Strong coupling effect in hybrid plasmonic modes for graphene study and advanced optical biosensors

Recent studies have shown that the strong coupling between the Tamm plasmon polariton (TPP) and surface plasmon polariton (SPP) components in the hybrid plasmonic mode is sensitive to the graphene monolayer. The decrease of the TPP and SPP dip components can be explained by changes in the conductivity of the silver layer due to the presence of this additional graphene/PMMA structure. The modified positions of the TPP and SPP components in the wavelength spectra indicates a strong coupling regime. Design of the hybrid plasmonic/graphene-based nanostructures could be used for advanced optical sensors and integrated optical circuit technologies. The optical sensing technology was applied for the sensitivity enhancement of the hybrid TPP-SPP mode. The SPP component of the hybrid TPP-SPP mode was about 6.4 times more sensitive than the single SPP for the BSA protein layer on a gold film. The sensitivity of the hybrid plasmonic mode could be controlled by using the strong coupling effect between the TPP and SPP components. That reduces absorption and scattering losses of

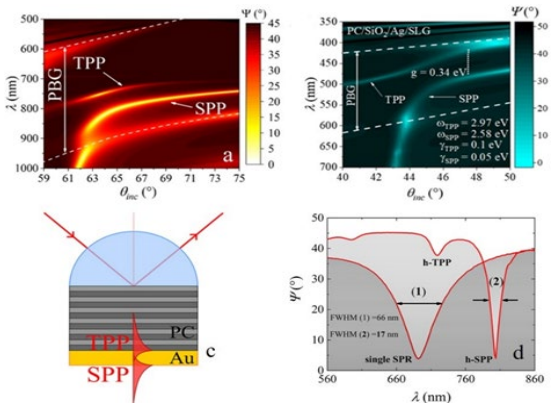

Fig. 12. The dispersion relations of a hybrid TPP-SPP mode (a) and PC/SiO_2/Ag/Graphene structure (b). (c) The principal experiment scheme for excitation of hybrid TP-SPP mode. (d) The difference of plasmonic resonance width between conventional plasmon resonance and hybrid plasmonic modes.

the metal for the SPP component in the hybrid TPP-SPP mode and, as a result, narrows the plasmonic resonance.

zigmas.balevicius@ftmc.lt

Damage-free patterning of thermally sensitive CIGS thin-film solar cells: Can nanosecond pulses outperform ultrashort laser pulses?

Nanosecond pulses are usually considered as an unsuitable tool for low-damage P3 scribing of heat-sensitive CIGS cells. Long pulse duration leads to high thermal effects and significant melt formation severely shunting the device and leading to a loss of power conversion efficiency. Instead, ultrashort lasers are chosen as the primary source for scribing of CIGS cells. Fortunately, this our study revealed that it is possible to minimise the conductivity of scribes performed with nanosecond pulses by properly selecting the wavelength of the laser radiation. As a results, the nanosecond pulses working at a wavelength close to the mid-infrared region could outperform ultrashort lasers in the 355 – 1342 nm wavelength range. The nanosecond pulses yielded

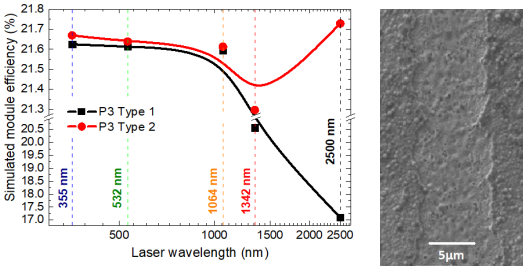

Fig. 13. (Left) Simulated CIGS module efficiency based on the conductivity of P3 scribes ablated at different laser wavelengths. The cases of a direct ablation (black curve) and a lift-off TCO removal (red curve) were simulated. The picosecond pulses were used in the 355 – 1342 nm range, while the nanosecond pulses at 2500 nm only. (Right) The P3 scribe with an exposed CIGS layer using the TCO lift-off.

the highest power conversion efficiency in mini-module simulations. A high absorption in the transparent conductive oxide (TCO) efficiently shielded the underlying CIGS, thus minimising the thermal damage.

edgaras.markauskas@ftmc.lt

Laser wakefield accelerated electron beams and betatron radiation from multijet gas targets

Laser Plasma Wakefield Accelerated (LWFA) electron beams and efficiency of betatron X-ray sources were studied using laser micromachined supersonic gas jet nozzle arrays. The nozzles were manufactured from fused silica implementing the hybrid laser nanosecond rear side machining and Femtosecond Laser-Induced Chemical Etching (FLICE) technique. Separate sections of the nozzle array enabled the formation of plasma targets used for the injection, acceleration and enhancement of electron oscillation. The experiment was performed using the 40 TW, 35 fs laser at the Lund Laser Centre, Sweden. The electron energies of 30-150 MeV and 1.0×10^8-5.5×10^8 photons per shot of betatron radiation with the critical synchrotron energy of 2.2-2.6 keV have been measured. The implementation of the betatron source with a nozzle array in wiggler geometry raised the efficiency of the X-ray generation. It increased the number of photons per shot by a factor of 2-3 relative to a single-jet gas target.

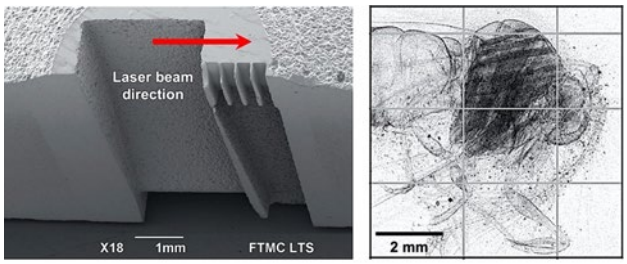

Fig. 14. (Left) The SEM image of the cross-section of a nozzle array in wiggler geometry cut-in-half. The array consists of a converging-diverging 1.5 mm slit nozzle and four capillary nozzles with the fixed channel dimensions of 200 µm × 200 µm. The red arrow indicates the orientation of the nozzle arrays relative to the incoming laser beam. (Right) The betatron X-ray transmission image of a moth averaged over 10 shots.

vidmantas.tomkus@ftmc.lt

Demonstration of a stable long-term operation of a kilohertz laser-plasma accelerator

Tiny 100 µm micronozzles, manufactured at the FTMC, enabled electron injection in a Laser Wakefield Plasma Accelerator driven by few-cycle kilohertz laser pulses for 5 hours of continuous operation. In collaboration with the Laboratoire d'Optique Appliquée of Institut Polytechnique de Paris, France, the electron bunches with 2.6 pC charge and 2.5 MeV peak energy were generated via trapping electrons in a downward plasma density ramp of the newly designed asymmetrically shocked gas nozzles. The results showed that the reproducibility and stability of the laser-plasma accelerator were greatly enhanced. The fused-silica nozzles demonstrated a high resilience to damage and provided reliable and reproducible results after using it for about $3\text{-}5\times10^7$ laser shots.

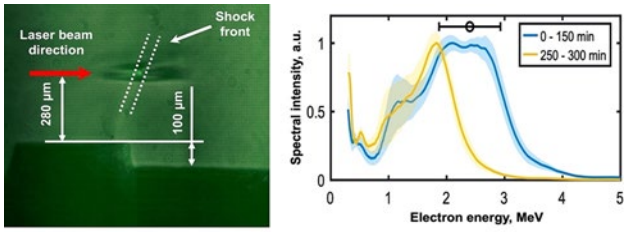

Fig. 15. (Left) The shadowgram of a laser beam propagating in the plasma of ionised nitrogen gas. White dotted lines indicate the shock front in the gas jet produced by the one-sided shock nozzle. (Right) Electron spectra measured continuously for 306 minutes. Each spectrum was averaged over 100 shots. Shaded areas show the standard deviation. The black error bar indicates the spectrometer resolution at 2.4 MeV.

vidmantas.tomkus@ftmc.lt

Characterisation of CoCrMo powder for additive manufacturing

Additive manufacturing (AM) cover various manufacturing techniques where the material has added a layer upon layer to produce a 3D object. AM could create geometrically complex parts from various materials. The materials shall possess specific properties to achieve predictable characteristics and high quality of 3D-printed objects. Properties of a Co-Cr-Mo-based superalloy powder were studied using various techniques: the scanning electron microscopy (SEM) with an energy-dispersive X-ray spectrometer (EDS), X-ray diffraction (XRD), X-ray photoelectron spectroscopy (XPS), Auger electron spectroscopy (AES) and particle-induced X-ray emission (PIXE). The results revealed dispersion of main components (Co, Cr, Mo), an attenuating of Co0.64Cr0.32Mo0.04 and Co0.9Mo0.1 phases, and differences in size, shape, surface roughness, structure and content of S, C, Mn and Si among individual particles. Depending on the particle surface structure, differences in the oxidation of particles have been found. The smallest particles had a low concentration of Co and Cr oxides, while the smooth ones had a higher metal oxide content. These findings could be used to predict the behaviour of particles during the additive manufacturing process.

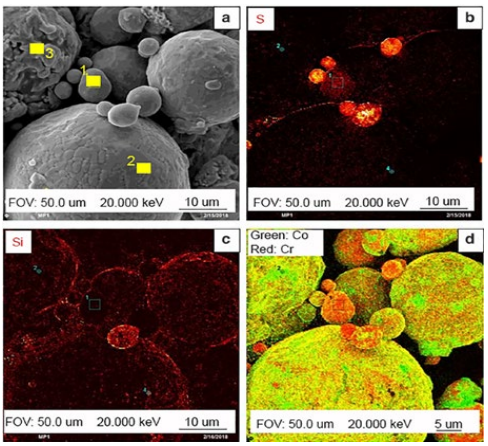

Fig. 16. (a) SEM image of 4 areas selected for AES analysis; (b) AES map (Thermal Pseudocolour Image) for S; (c) AESmap for Si; (d) Auger colour overlay: green - Co, red - Cr.

genrik.mordas@ftmc.lt

OPTOELECTRONICS

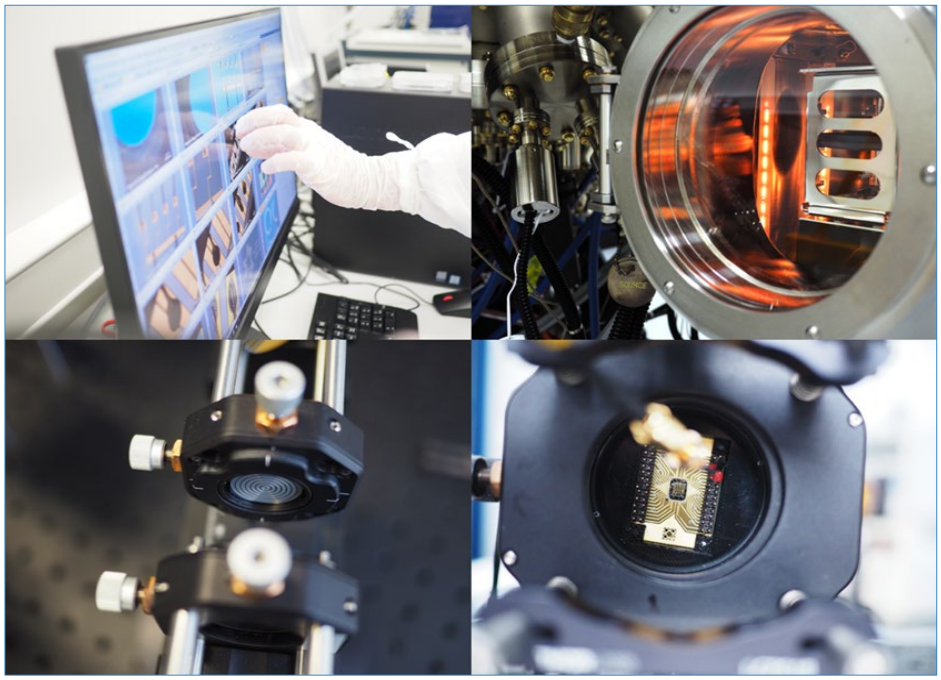

(Top, left) Inspection of InGaAs THz detectors processing.

(Top, right) Molecular Beam Epitaxy (MBE) apparatus.

(Bottom, left) Silicon based Bessel zone plate placed in an optical mount.

(Bottom, right) The array of AlGaN/GaN-based THz sensors.

Terahertz and infrared technologies: from materials engineering up to novel optoelectronic devices

Department of Optoelectronics keeps a tradition to further elaborate a complete and entire chain of scientific activities starting from materials design, comprehensive scientific research and development of prototypes of optoelectronic devices. The activities are possible, on the one hand, because of the ambitious team combining enthusiasm of young researchers and knowledge of experienced staff, on the other hand, due to the modern epitaxial growth facilities and advanced scientific equipment available in the laboratories of the Department. The Department structure experienced no changes within the last year, it consists of five scientific laboratories: Ultrafast Optoelectronics, Optoelectronics Technology, Semiconductor Optics, Terahertz Photonics, and Optoelectronics Systems Characterization. The staff amounts to 50 researchers: 33 doctors of sciences, 10 PhD students, and 9 engineers. The Department activities cover both fundamental and applied research dedicated to material physics of semiconductors and semiconductor technology, terahertz (THz) physics and spectroscopy, development of novel optoelectronic devices for THz and infrared ranges, as well as their applications. Among the dominating scientific topics one can underline design and investigation of quantum wells of GaAs/AlGasBi and GaInAsBi compounds, development of infrared LEDs based on these structures, and THz generation in van der Waals crystals. The year 2020 was quite successful in further development of antenna-coupled titanium-based microbolometers and their linear arrays, innovations in THz imaging systems for their use in discrimination of packaged low-absorbing objects and time-domain THz spectroscopy of two-dimensional plasmons in AlGaN/GaN heterostructures. Pandemic limitations of the year of 2020 had no essential effect on further evolution of the THz photonics and technology Cluster, the interlaboratory unit of the Department concentrating and coordinating all modern THz experimental facilities for development of THz technology and THz photonics-related components. The scientific equipment including various THz techniques, femtosecond lasers-based THz spectrometers as well as different continuous wave based THz set-ups for imaging, is enriched by a set of standard optical characterization techniques equipped with low-temperature facilities and possibilities to apply short-pulse electric fields. It makes the Cluster an attractive place to perform versatile experimental THz and optical investigations for foreign scientists, other Lithuanian research groups and high-tech companies. Researchers from UK, Belarus, Finland, Ukraine, Poland, Russia, China, and Estonia are employed in the laboratories of our Department or closely collaborate with us in order to extend the ongoing cooperation.

AlGaN/GaN devices on SiC substrate

Recent research was devoted to development of AlGaN/GaN devices on SiC substrate suitable for high voltage, low noise, and high frequency applications. We explored the GaN–SiC hybrid material without a thick GaN buffer. The unterminated and unpassivated Schottky barrier diodes (SBDs) were fabricated on this material demonstrating very high breakdown voltages and critical breakdown fields reaching the values up to 1 MV/cm. Moreover, developed transistor, so-called Thin High Electron Mobility Transistor (T-HEMT), demonstrated the acceptable current density and transconductance values with a negligible reduction in the performance under input power levels up to 3 W/mm for a channel width of 0.4 mm. The systematic low-frequency noise measurements revealed that the effective trap density is below the level of 10^{19} cm^{-3} eV^{-1}, which is similar to or even smaller than previously reported trap densities in HEMT structures with thick GaN:C buffers. The figure of merit for high-frequency T-HEMT performance, defined as the product of unity current gain cut-off frequency and gate length, was found to be up to 7 GHz µm. Our results confirm the potential of a GaN–SiC hybrid material for the development of HEMTs and SBDs for high-frequency and high-power applications with improved thermal stability.

justinas.jorudas@ftmc.lt

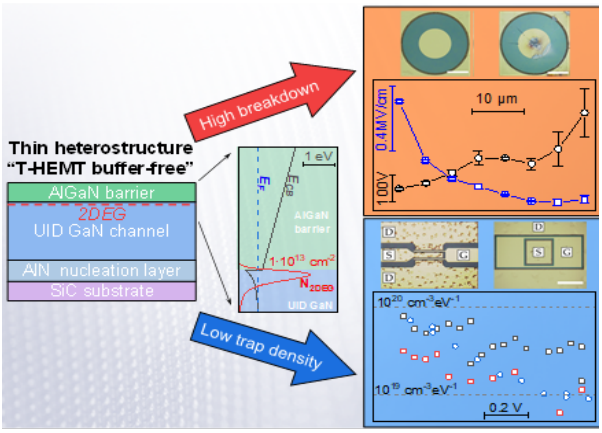

Fig. 1. (Left) Schematic cross section of the T-HEMT structure. (Midle) Calculated band diagram and 2DEG density distribution in the heterostructure. (Right, top) Breakdown voltage and critical electric field dependences of the distance between ohmic and Schottky contacts in the SBDs. (Right, bottom) Effective trap density as a function of the gate voltage swing for the RF T-HEMTs and DC T-HEMTs.

THz spectroscopy of two-dimensional plasmons

High density and electron mobility of a two-dimensional electron gas (2DEG) and electrical robustness make AlGaN/GaN hetero-structures an excellent candidate for the development of various electronic and plasmonic devices for the THz frequency range. The 2D plasmons in grating-coupled AlGaN/GaN structures were investigated by THz time domain spectroscopy (TDS) at a temperature of 90 K. Gratings of different periods (600, 800, and 1000 nm) and filling factors (50 and 80%) were developed to measure the plasmon dispersion and the coupling efficiency with THz radiation. The distinctive minima and inflection points were observed experimentally in a transmission amplitude and phase spectra, respectively. Comparative analysis of plasmon features in both spectra revealed that the phase signals are less sensitive to the defects in the grating-coupler. Moreover, the resonant features in the amplitude spectrum were found to be related to those in the phase spectrum by a simple integral relation. Our study revealed that the phase spectroscopy is a preferable tool for research of plasmon-related phenomena in the fields of THz physics and engineering.

irmantas.kasalynas@ftmc.lt

$$f_{pn} = \sqrt{\frac{e^2 N_{2DEG} k_n}{m^* \varepsilon_0 [\varepsilon_{sub} + \varepsilon_b \coth(k_n d_{2DEG})]}} \qquad \Phi(f') = C_1 + \int_0^{f'} \varphi_2(f) df$$

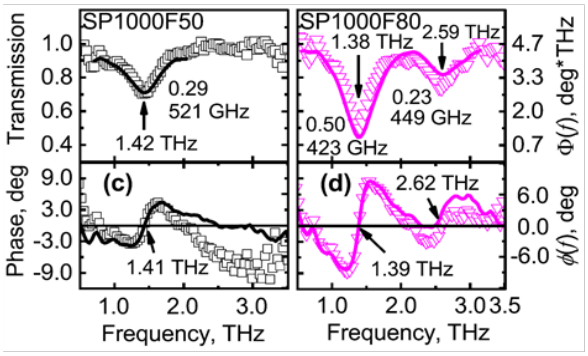

Fig. 2. Transmission amplitude (symbols, top) and phase (symbols, bottom) spectra of the plasmonic samples with a gating period of 1 µm and filling factor of 50 % (left) and 80 % (right). Confirmation of the relation between amplitude spectrum and the phase integral Φ(f) function (lines, top) and the phase spectrum via a Kramers–Kronig analysis (lines, bottom). Two numbers indicate amplitude and full width maximum values. Arrows indicate a position f_{pn} of each 2D plasmon resonance.

Electron effective mass in AlGaN/GaN structures

AlGaN/GaN high electron mobility transistors (HEMTs) are the most developed and promising structures among various III-nitride-based electronic devices. Despite intense material investigation and many practical applications, the problem arises of the electron effective mass in this material, especially at room temperature. We investigated the resonant behavior of the 2D plasmons in a wide range of temperature. Using the integral phase method, developed in our group, we found the temperature dependent effective mass in AlGaN/GaN heterostructures. The 2D plasmons experienced the red-shift in transmission power and phase spectra of all samples. The phenomenon was explained by renormalization of the effective mass, which started distinctly to deviate at 134 K increasing at 295 K up to 55% of its nominal value. Moreover, high quality plasmonic structures caused the excitation of the 2D plasmon resonant features at record high temperature (300 K). The results demonstrate a potential for grating-gated AlGaN/GaN heterostructures for the development of tunable THz emitters, phase modulators and other types of plasmonic devices.

irmantas.kasalynas@ftmc.lt

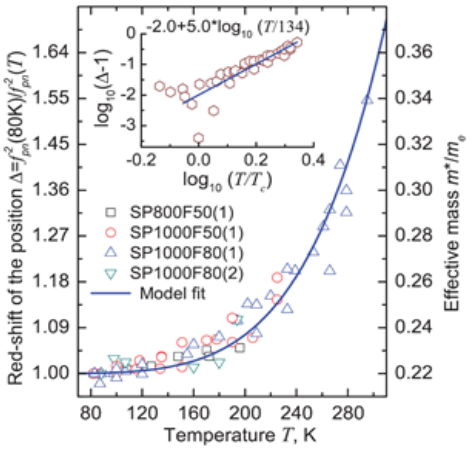

Fig. 3. Measured T-dependences of the red-shift of fundamental (1) and second order (2) resonant modes in different plasmonic samples and of the electron effective mass recalculated using an analytical dispersion characteristic of 2D plasmons. Inset: results in a log–log scale. Experimental data (points) are fitted to the following function (line): $m^*(T)/m0^* = 1 + 0.01\,(T/134)^5$.

Coherent thermal radiation of n-GaN grating

Micro- and nano-structures on the surface of semiconductors or metals offer the possibility to realize a strong light-matter interaction via polariton excitation. A polarized reflection and emission spectroscopy techniques were developed to study the coherent behavior of the surface plasmon phonon polaritons (SPPhPs) of the shallow n-type gallium nitride (GaN) grating. The coherence of polaritons was observed measuring the reduction of the linewidth and red-shift of the resonance in both reflection and emission spectra increasing the incident angle from 0 up to 45 degrees. Maximum coherence conditions were found numerically at a frequency of 562 cm^{-1} and observation angle of 37 degrees, demonstrating the coherence length value up to 724 μm (41 λ) for the 11 μm period surface relief grating. Good agreement between the experiment and theory was achieved, paving the way for the development of coherent thermal sources and components with desired spectral features in the THz and IR spectrum range.

vytautas.janonis@ftmc.lt

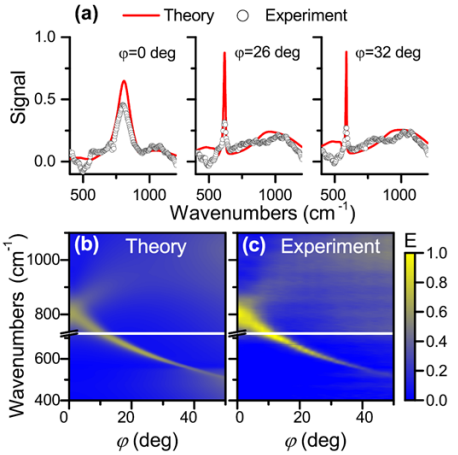

Fig. 4. (a) Measured emission (black symbols) and calculated emissivity (solid red line) differential spectra (TM-TE) of the n-GaN grating at various incident angles as indicated. (b) Calculated and (c) measured dispersion characteristics of SPPhPs of the shalow n-GaN grating with a period of 11 μm.

Terahertz generation in van der Waals crystals

Many semiconductors illuminated with femtosecond optical pulses generate short electromagnetic radiation bursts in the frequency range of up to 10 THz. This phenomenon is known as a simple and universal method of sourcing THz frequency signals, and is also used to investigate the intrinsic parameters of semiconductors. We applied this methodology to the novel semiconductor group: the hexagonal symmetry wurtzite and van der Waals type crystals. In all studied materials (wurtzite InAs nanowires, multilayer transition metal dichalcogenides (TMDs), as well as GaSe) the THz emission has been observed. The intensity and polarity of this emission strongly depends on the polarity and wavelength of exciting femtosecond pulse. The obtained results allowed us to estimate the energy levels of electronic bands of these materials. In addition, a new THz generating mechanism, the electric dipole originating from accumulation of dark excitons, has been discovered in the chalcogenide materials.

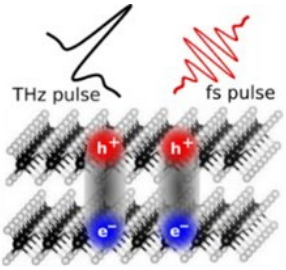

Fig. 5. The illustration of a THz radiation generation mechanism from multilayer TMDs.

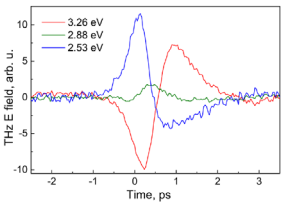

Fig. 6. The pulses of THz frequencies generated from GaSe crystal at various quanta energies.

ricardas.norkus@ftmc.lt, ignas.nevinskas@ftmc.lt

Infrared LEDs from quaternary bismide layers

Optical gas sensors require semiconducting light sources that radiate at the wavelength range from 2 to 4 µm. Until now, these type of sources have been grown on rather expensive GaSb substrates. A breakthrough has been achieved when the new system of semiconducting materials, the dilute bismides, has been discovered. These materials are being grown with a narrow band gap on more technologically accessible GaAs and InP substrates. Our latest research involved the fabrication of infrared LEDs based on the quaternary GaInAsBi compound quantum wells grown on InP. At first, the terahertz excitation at various wavelengths has been studied to estimate the electronic band offsets in heterojunctions between GaInAsBi and other semiconductors to be used as quantum well barriers. In other set of investigations, these quantum wells have been employed in light emitting diodes. The GaInAsBi LEDs with 4% of Bi emitted light of 2.5 µm wavelength. Taking into account that it is possible to achieve 6 µm emission wavelength in lattice-matched quaternary compounds on InP, these our results pave the way for fabrication of novel and efficient infrared sources.

vaidas.pacebutas@ftmc.lt

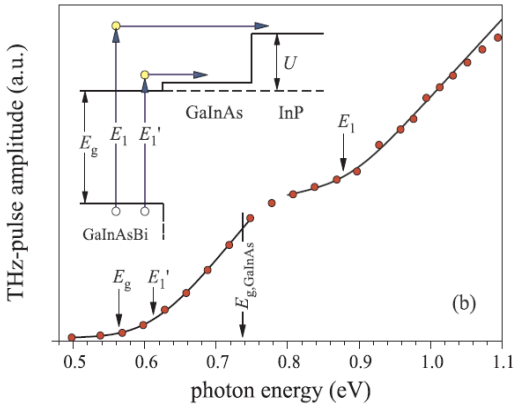

Fig. 7. THz radiation excitation spectra from a heterojunction with GaInAsBi layer, and their marked characteristic energies used to determine the band-offsets.

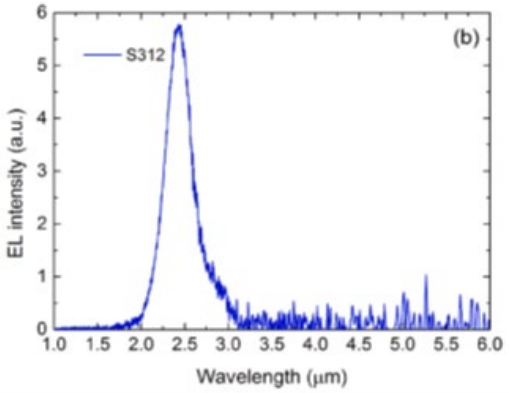

Fig. 8. Electroluminescence spectrum of the LED with a single GaInAsBi quantum well.

Terahertz imaging using spatial filtering methods

Spatial filtering methods are well-known techniques in visible and infrared microscopy. In particular, they are important in biology when there is a need to resolve and discriminate low absorbing or even transparent objects for the illumination. We have introduced phase-contrast and dark-field methods in room temperature THz imaging aiming to demonstrate suitability to resolve low-absorbing objects in THz frequency range. Special type of sample was constructed and investigated using direct (with no filtering), phase-contrast and dark-field THz imaging techniques at 0.3 THz range. Comparative results are presented in Fig. 9. Moreover, suitability of the different antenna-coupled titanium-based microbolometers for the spatial filtering THz imaging was demonstrated and their usage in control of a spatial mode profile in various weak power THz sources was revealed. The features of the microbolometers within 0.15–0.6 THz range were exposed and discussed, and their ability to detect spatial mode profiles beyond the antennas resonances, up to 2.52 THz, were explored in detail.

linas.minkevicius@ftmc.lt

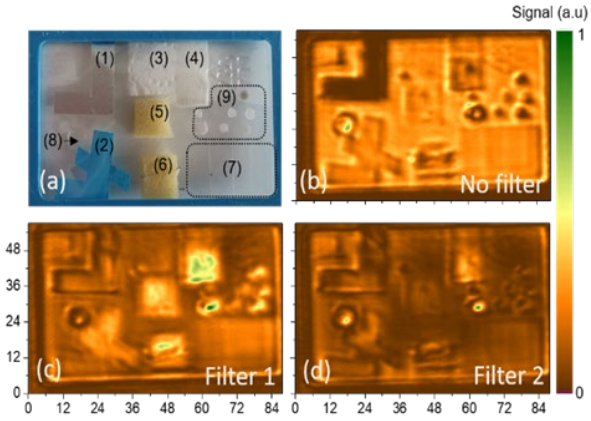

Fig. 9. (a) Photo of an investigated sample with a plastic substrate film: (1) – metal, (2) – rubber, (3) – paper towel, (4) – napkin, (5) – sponge, (6) – sponge with metal wire inside, (7) – plastic (from 1 to 4 layers), (8) – aperture (diameter: 4 mm), (9) – dots, made of silicone, acrylic and wax. (b) Direct raster scan image of the sample at 0.3 THz. Phase contrast images obtained using filter 1 (c) and filter 2 (d). THz image pixel size: 0.3 mm × 0.3 mm; images consist of 292 × 190 pixels. Filter 1: 2 mm circle shaped four paper sheets. Filter 2: 2 mm circle shaped aluminium foil.

MOLECULAR PHYSICS

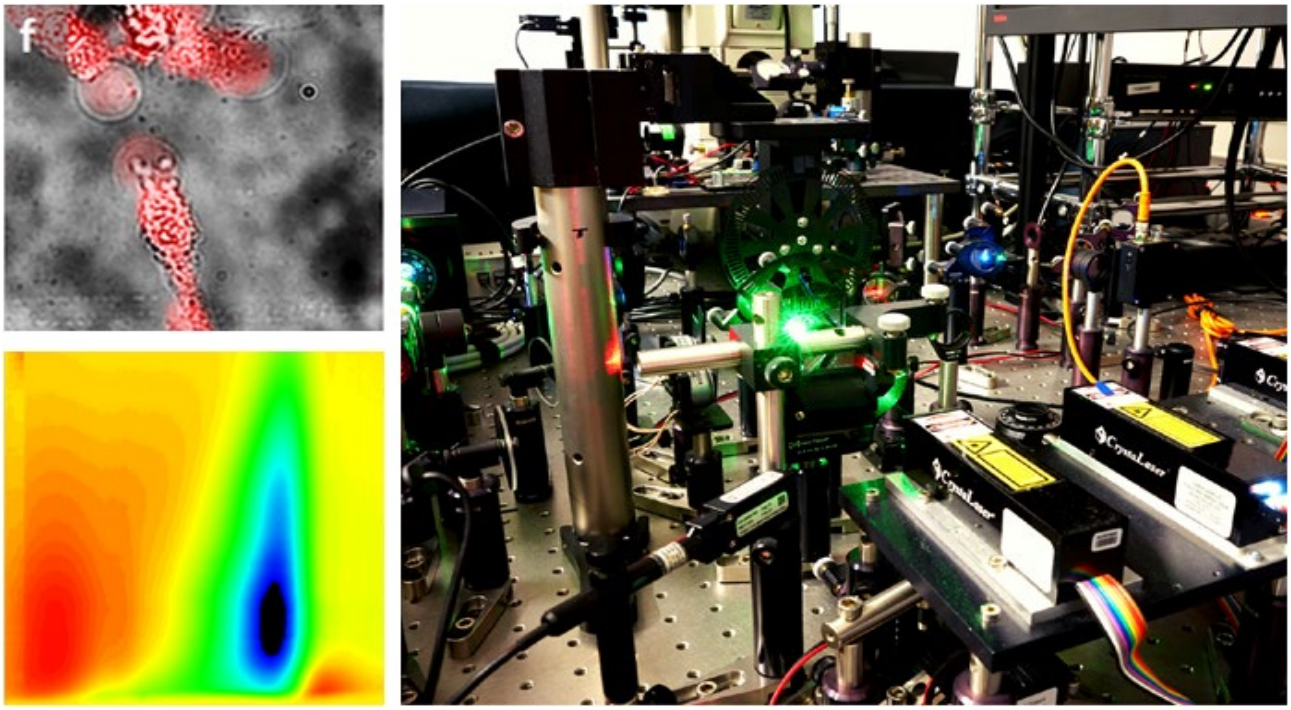

Photophysics of molecular systems

The activity of the Department of Molecular Compounds Physics is related to molecular photonics ranging from the investigation of natural and artificial molecular systems utilizing optical techniques to the development of molecular and hybrid devices. We seek a better understanding of photoinduced processes in biological and artificial molecular systems, optimization of the material properties and photoinitiated processes in photonic devices. Advanced experimental techniques such as ultrafast spectroscopy, nonlinear and single molecule microscopy, optoelectrical methods are used together with theoretical calculations to address complex excited-state dynamics and progressions of electronic events in optically excited molecular and hybrid systems. Objects of our investigation range from biological photosynthetic and protein-DNA complexes, molecular viscosity sensors, to organic and perovskite solar cells among others. This interdisciplinary research field requires expertise in physics, chemistry, biology as well as material and device engineering. Since it is difficult or even impossible to be excellent in all these research disciplines, our research is often based on collaboration with researchers form other Lithuanian and foreign academic and other high-tech institutions. Although sometimes we lose a privilege to perform the developments from the beginning to the end, it helps us to be a part of the international research.

Review on non-photochemical quenching in plants

Photosynthetic productivity usually saturates far below the maximum solar light intensity, meaning that in these conditions many absorbed photons and the resulting electronic excitations of the pigment molecules can no longer be utilized for photo-synthesis. To avoid photodamage, various protection mechanisms are induced that dissipate excess excitations, which otherwise could lead to the formation of harmful molecular species like singlet oxygen. This non-photochemical quenching (NPQ) of excitations can be monitored via a decrease of the chlorophyll fluorescence. In mini-review we describe the current level of knowledge of this process, discuss recent experiments performed in Wageningen and analyzed in our lab in Vilnius, and consider their implications to the biomass production.

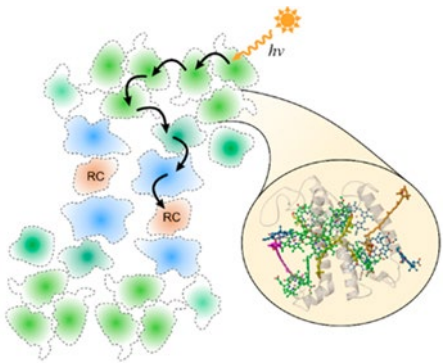

Fig. 1. Schematic illustration of the light-induced excitation energy transfer within the photosynthetic antenna, where each subunit comprise chlorophyll and carotenoid pigments bound to the protein scaffold.

jevgenij.chmeliov@ftmc.lt

Macro-, micro- and nano-roughness of carbon-based interface with the living cells: towards a versatile bio-sensing platform

Integration of living cells with nonbiological surfaces (substrates) of sensors, scaffolds, and implants implies severe restrictions on the interface quality and properties, which broadly cover all elements of the interaction between the living and artificial systems (materials, surface modifications, drug-eluting coatings, etc.). Substrate materials must support cellular viability, preserve sterility, and at the same time allow real-time analysis and control of cellular activity. We have compared new substrates based on graphene and pyrolytic carbon (PyC) for the cultivation of living cells. The structure, morphology, and interface properties of these substrates are analyzed in terms of their biocompatibility.

lena.golubewa@ftmc.lt;
renata.karpicz@ftmc.lt

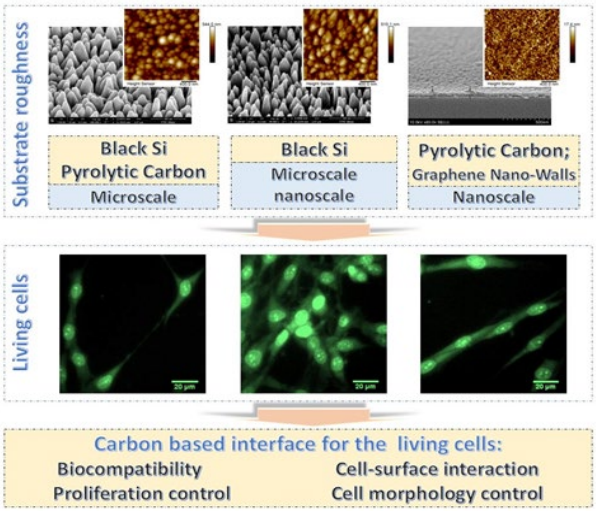

Fig. 2. (Top) Typical two-dimensional AFM and SEM surface images of PyC of 20 nm and 40 nm thickness on SiO_2, bSi. (Bottom) Typical fluorescent images of glioma cells grown on substrates with different roughnesses.

Time-resolved photophysics of non-fullerene organic solar cells

Organic photovoltaics has been persistently developed for over three decades as one of the alternative solar energy-harvesting technologies. During the last few years, a rapid power conversion efficiency increase was achieved by employing small low bandgap molecules as a substitute to fullerene type acceptors. One of their advantages is a small energy offset between donor and acceptor HOMO levels. Here we use several advanced transient investigation techniques, covering timescale from sub-ps to µs, to address all sequence of processes starting from photoexcitation of donor or acceptor to carrier extraction in several NFOPV devices. We show that, though small offset results in increased open-circuit voltage, at the same time, it limits cell performance because of inefficient hole transfer from excited acceptor to donor and enhanced geminate recombination.

rokas.jasiunas@ftmc.lt

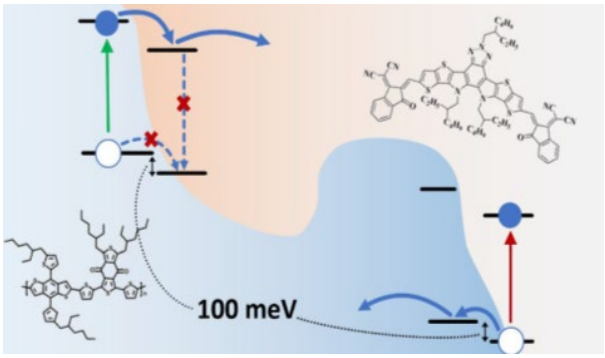

Fig. 3. Schematic representation of charge separation after donor (top, left) and acceptor (bottom, right) excitation. After investigating several systems with different HOMO level offsets, we showed that at least 100 meV offset is needed to prevent hole transfer from excited donor to acceptor, at the same time to enhance the hole transfer from excited acceptor to donor. They both reduce geminate recombination losses.

Characterization of thymine microcrystals by CARS and SHG microscopy

Orientation-dependent CARS/SHG imaging of the glass-deposited thymine crystals and quantum chemical calculations can clarify the arrangement of the thymine molecules in the crystal. Regular thymine structures exhibit the crystal polymorphism with very similar X-ray diffraction, IR, and Raman spectroscopic charac-teristics. Separate analysis of CARS or SHG data is not sufficient for unambiguous interpretation of crystal configuration. At the same time, a combination of the CARS and SHG techniques supported by quantum chemical calculations of Raman spectra and the dipole moment of thymine allowed us to conclude that in the thymine crystal the most probable are thymine-thymine inverse and thymine-thymine symmetric molecular configurations.

andrej.dementjev@ftmc.com

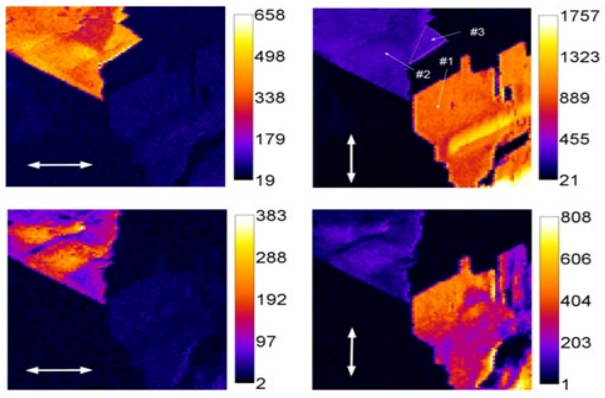

Fig. 4. The CARS (top) and SHG (bottom) images of thymine with two perpendicular linear polarizations of the incoming light indicated with white arrows. The areas #1 and #2 appear in the image at different polarization orientations of the incoming light. The region #3 is noteworthy for its lack of the SHG. The size of the images is 20x20 µm. CARS and SHG images obtained at the same height of sample. Lateral resolution was 0.9 µm.

Energy barriers restrict charge carrier motion in MAPI perovskite films

Hybrid perovskites are successfully used in such optoelectronic devices as highly efficient solar cells, bright tunable LEDs, fast and sensitive photodetectors. To further improve these devices, it is crucial to understand their charge carrier transport. In this work, by combining transient photocurrent, transient photoluminescence and time-delayed collection field experimental techniques, we monitored charge carrier motion at different temperatures. Our results indicate that charge carrier mobility at low temperatures is mainly determined by energy barriers, rather than charge carrier traps, most likely formed by imperfect intergrain connections. Suggested concept of the energy barriers moves beyond the conventional understanding of carrier mobility diffusion and recombination processes in hybrid perovskites, being of great importance for devices produced in lateral configurations, such as field-effect transistors, lateral photodiodes, photodetectors, and recently suggested lateral solar cells.

rokas.gegevicius@ftmc.lt

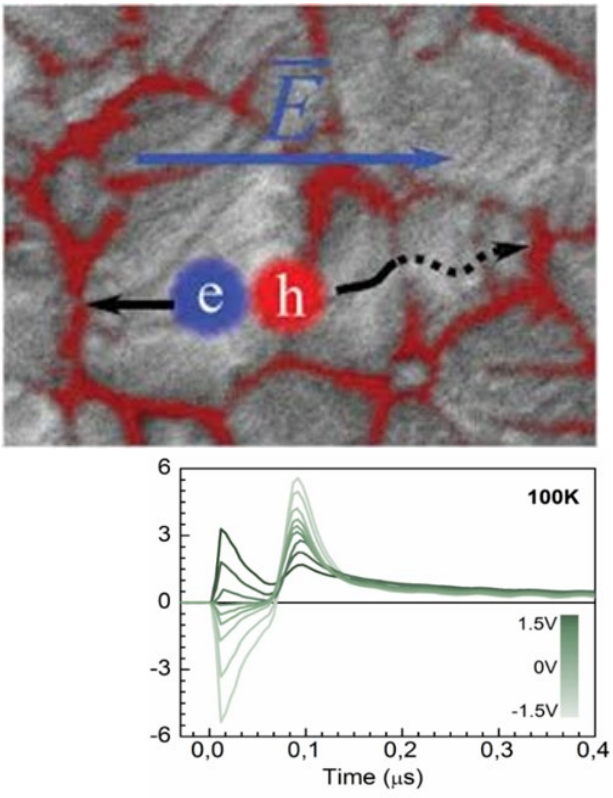

Fig. 5. Time-delayed collection field photocurrent kinetics indicates the existence of the energy barriers in hybrid perovskite materials.

Equilibrium state of open molecular system

Calculation of the equilibrium state of an open molecular quantum system interacting with a bath remains a challenge to this day, mostly due to a huge number of bath degrees of freedom. Here, we present an analytical expression for the reduced density operator in terms of an effective Hamiltonian for a high temperature case. Comparing with numerically exact results, we show that our theory is accurate for slow baths and up to intermediate system–bath coupling strengths. The key quantity in our theory is the effective coupling between the states, which depends exponentially on the ratio of the reorganization energy to temperature and, thus, has opposite temperature dependence than could be expected from the small polaron transformation. Our result should be useful for simulations of relaxed fluorescence spectra of molecular aggregates.

leonas.valkunas@ftmc.lt

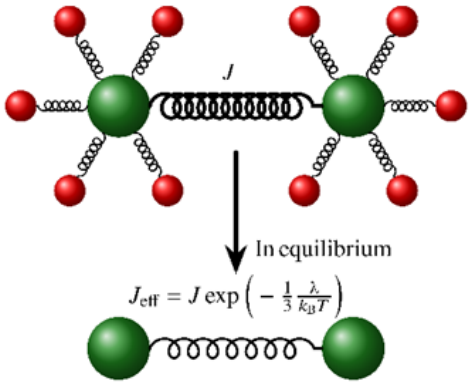

Fig. 6. Illustration of the effective resonance coupling. In open molecular systems the electronic states (green balls) interact with each other with resonance coupling J and also with vibrational degrees of freedom (red balls). We show that in equilibrium such system can be described as purely electronic system with smaller effective resonance coupling Jeff, that depends exponentially on the reorganization energy λ and the thermal energy kBT.

NANOENGINEERING

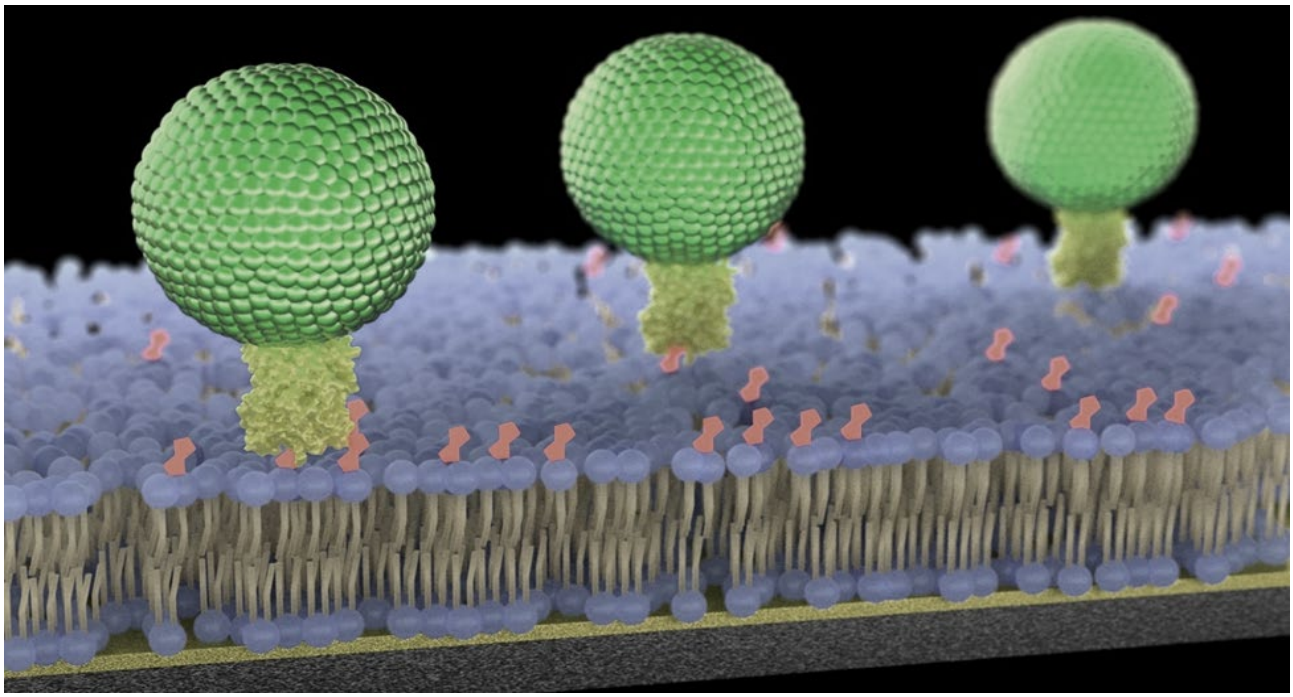

Department of Nanoengineering focuses on new tools and processes for fabrication of functional nanoarchitectures for broad applications: from photonics to life sciences and medicine. One of our long-term interests is the development of reliable miniaturised platforms for biophysical studies at different levels: proteins, single cells and tissues. Also, we aim at establishing cost-effective and easy nanofabrication platforms, suitable for patterning and functionalisation of new nano- and biomaterials. Among our achievements of the past decade we can name high-speed atomic force microscopy and nanolithography, new supramolecular architectures and cell membrane-mimetic assemblies, nanobiochips for single-cell analysis, electrochemical and optical devices for biosensing, micro and nanopatterned hydrogels for tissue engineering.

Refined experimental approach for direct determination of the mechanical properties of model lipid bilayers

We applied our expertise in surface chemistry and scanning probe microscopy to investigate and refine the experimental methodology of measuring the mechanical properties of soft giant unilamellar vesicles (GUVs). We demonstrated that decorating the surface with self-assembled monolayers of optimal composition permits to reduce the mobility of the GUVs, which is essential for the atomic force microscopy (AFM) investigation, while not modifying their mechanical properties to a significant degree. Also, by preparing the AFM probes with carefully controlled indenter geometry (Fig. 1), we showed the importance of proper selection of the mechanical model for the processing of the data and the probe geometry. This study provides an example of the power of the combination of techniques, such as control of the surface chemistry and precision mechanical investigation by the AFM, applied to a challenging problem of soft matter physics.

arturas.ulcinas@ftmc.lt

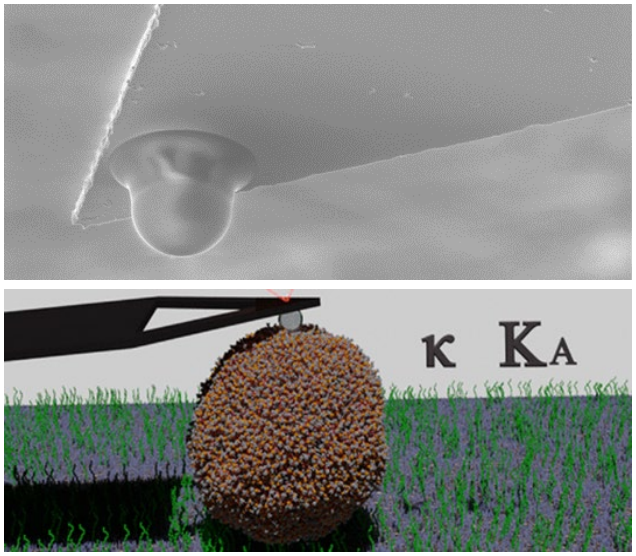

Fig. 1. (Top) SEM micrograph of a home-made cantilever probe for the AFM indentation technique. (Bottom) A cartoon explaining the in situ determination of the mechanical properties of the surface-anchored giant unilamellar lipid vesicles.

PEG hydrogel coatings on glass - a reliable substrate for functional modifications and biochip fabrication

We have developed an efficient protocol for controlled and stable photochemical synthesis of polyethylene glycol (PEG) hydrogel coatings on glass substrates. In this way, we have overcome a range of inherent issues related to the functional modification of industrial scale-made glass, such as impurities and batch-to-batch variation of the surface composition. Our protocol is based on UV-controlled self-initiated photografting and photopolymerization (SIPGP) performed in registry with surface chemical modifications of the regular microscopy glass (coverslip) substrates. Namely, we have observed an interesting effect of initiator-free photografting at the liquid-solid interfaces involving specific surface chemical groups. By performing atomic force microscopy (AFM) analysis in the quantitative imaging (QI) mode, we were able to compare the nanoscale morphology and swelling behavior of the hydrogel coatings in native uncompressed and compressed states, respectively. The glass-supported hydrogel layers performed as reliable substrates for microfabrication of covalently-bound protein patterns achieving a sub-200 nm resolution. We made fibronectin patterns consisting of densely packed protein molecules, which maintained the structural integrity upon hydrogel swelling. Beside the remarkable stability of the hydrogel coatings in buffer and in cell culture, they showed good antifouling characteristics. Therefore, they proved well suitable for producing cell-adhesive patterns for individual analysis as well as for spatially controlled cell culture. Most importantly, the hydrogel-based architectures on glass were non-toxic, and they showed no indications of disintegration/ chemical degradation even under prolonged cell culture conditions.

ramunas.valiokas@ftmc.lt

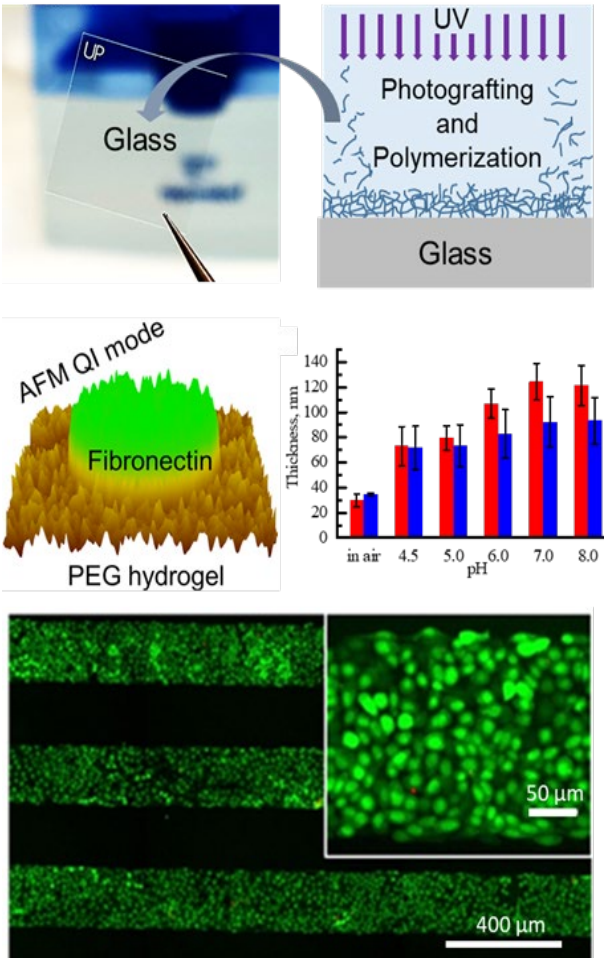

Fig. 2. (Top) Photograph of a glass-made chip substrate and a schematic explanation of the PEG hydrogel-synthesis process. (Middle) The in situ AFM characterization and swelling behavior determination of the PEG hydrogel coating. (Bottom) Fluorescence microscopy images of 96 h-long immortalized human cell line culture.

SPECTROELECTROCHEMISTRY

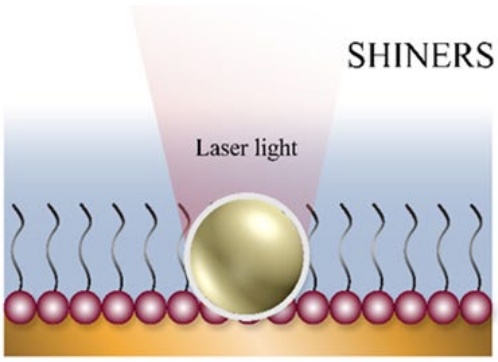

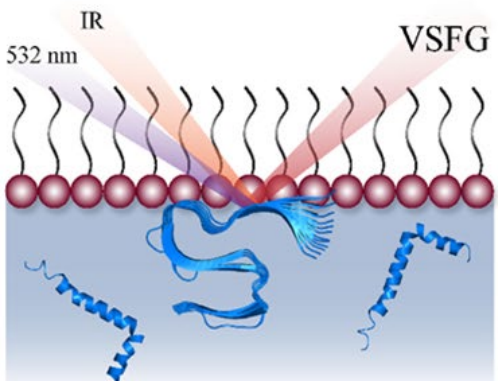

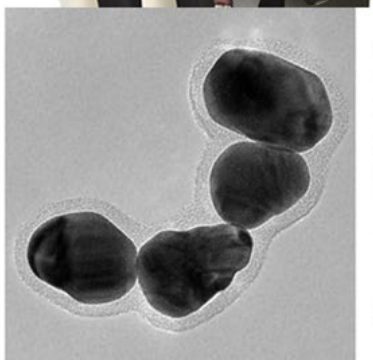

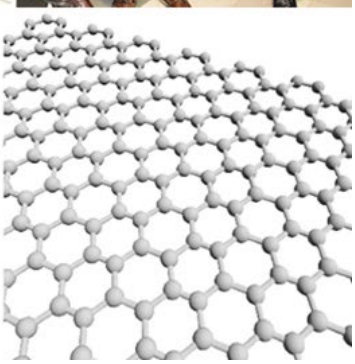

Spectroscopy of adsorption and biochemical processes at surfaces and interfaces, chromatography of bio-active secondary metabolites in herbal material

Electron transfer reactions, electrocatalysis, functioning of biomolecules, self-assembly, and various biochemical processes take place predominantly at the surfaces and interfaces. To predict and control the way those processes will proceed, a molecular level of understanding is required. Our group employs and develops novel spectroscopic techniques that enable to probe complex liquid and solid interfaces that are difficult to study with most common spectroscopic techniques. Shell-isolated nanoparticle enhanced spectroscopy (SHINERS) is the most promising vibrational surface-enhanced Raman technique. It was developed in order to overcome the limitations of a substrate use in surface enhanced Raman spectroscopy (Tian et al. 2010). Recently, our group used SHINERS to study potential-induced changes in the molecular structure of self-assembled molecules. We also successfully characterized the surface of functionalized graphene and a biological system of yeast cells using SHINERS. Multiwavelength Raman spectroscopy was employed to get insights into the electrochemical redox transitions of polyaniline in solutions of different acidities. We have used chromatography methods to extract information on bio-active secondary metabolites in herbal material. Vibrational sum-frequency generation spectroscopy (VSFG) is a unique technique with an intrinsic surface specificity. It enables to record the vibrational spectrum explicitly of the surface without any interference with a signal from the bulk material. It is a very versatile technique that can be used to study many different surfaces and interfaces such as solid/air, solid/liquid, liquid/air. We applied VSFG to study the structure of hen egg-white lysozyme aggregates adsorbed to DOPG/D2O and air/D2O interfaces. The greatest potential of VSFG lies in its ability to measure liquid surfaces with a sensitivity of a few molecular layers. Currently, we are studying the aggregation of proteins at the surface of model lipid membranes by using VSFG. The aim of our study is to answer one of the most important questions in biology and chemistry: what is the role of protein-membrane interaction in protein aggregation process?

Differential multiwavelength Raman study of electrochemical redox transitions of polyaniline in solutions of different acidities

Specific Raman features were disclosed by the differential Raman spectroscopy for redox transformations of polyaniline (PANI) from its oxidized to semioxidized, and to reduced forms within a broad range of solution pH from 1 to 9. Raman spectra were excited by using different laser lines ranging from UV (325 nm) through blue (442 nm) and green (532 nm) up to the red (633 nm) spectral regions. The observed spectra features were shown to depend drastically on the spectra excitation wavelength. For excitation at 325 nm, the features of the reduced form are observed, resulting in negative difference Raman bands (Ox-Red) within the entire pH range studied. At a blue excitation at 442 nm, both positive and negative difference bands for Ox-Red spectra are observed that are dependent on solution pH, whereas an inversion from negative to positive difference bands for Semiox-Red difference spectra was observed at higher pH values, indicating a possible resonance with an intermediate half-oxidized form of PANI (Fig. 1). At a red excitation (633 nm), characteristic features for polarons were observed for Semiox-Red difference spectra that are absent in the corresponding Ox-Red spectra.

albertas.malinauskas@ftmc.lt

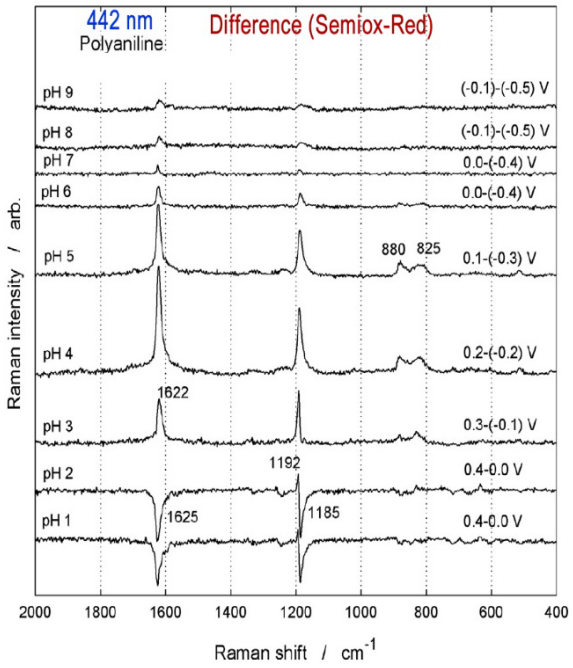

Fig. 1. Difference Raman spectra showing pH-dependent intercom-versions of different redox forms of polyaniline upon electrochemical oxidation and reduction. Positive-going features at intermediate pH values show resonance enhancement of Raman bands of intermediate half-oxidized form.

Structure determination of Hen Egg-White Lysozyme aggregates adsorbed to lipid/water and air/water interfaces

Protein misfolding and aggregation is related to many neurodegenerative diseases, including Alzheimer's and Parkinson's. Thus, the knowledge of adsorption process of aggregates at different interfaces is required for understanding the mechanism of diseases. In this work, vibrational sum-frequency generation (VSFG) spectroscopy was used to study the structure of hen egg-white lysozyme (HEWL) aggregates adsorbed to DOPG/D_2O and air/D_2O interfaces. We find that aggregates with a parallel and antiparallel β-sheet structure, together with smaller unordered aggregates and a denaturated protein, are adsorbed to both interfaces. Our study identified hydrophobicity as the main driving force for adsorption to the air/D_2O interface. Adsorption to the DOPG/D_2O interface is also influenced by the hydrophobic interaction. However, the electrostatic interaction between the charged groups of protein and the headgroups the lipid has the most significant effect on the adsorption. We find that the intensity of VSFG spectrum at the DOPG/D_2O interface is strongly enhanced by varying the pH of the solution.

simona.strazdaite@ftmc.lt

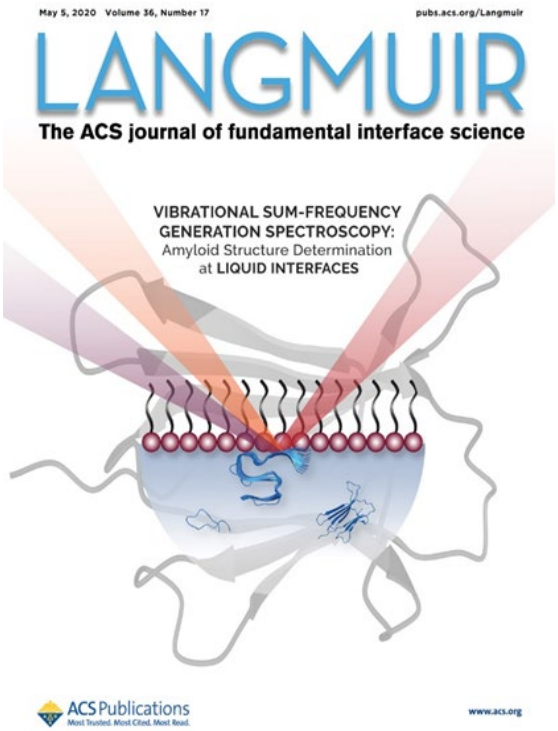

Fig. 2. The cover of Langmuir journal with a drawing from our paper.

Investigation of toxic, radical scavenging and antifungal activity of marsh rosemary essential oils

The object of our research is bio-active secondary metabolites of marsh rosemary *Rhododendron tomentosum* growing in Lithuania. The chemical composition of essential oils (EOs) was investigated by gas chromatography, mass spectrometry and flame ionization detector, and up to 70 constituents were identified. Toxic activity *in vivo* of marsh rosemary EOs was evaluated using a brine shrimp (*Artemia* sp.) bioassay. The LC_{50} values (11.23–20.50µg/mL) showed that the oils are notably toxic. The shoot EO gathered during seed-ripening and containing appreciable amounts of palustrol (26.0%), ledol (21.5%) and ascaridol (7.0%) demonstrated the highest toxicity. Radical scavenging activity of marsh rosemary EOs was evaluated, and it was found depending on the plant vegetation stage. The highest activity (48.19 and 19.89 mmol/L TROLOX equivalent obtained by $ABTS^{\bullet+}$ and $DPPH^{\bullet}$ assays, respectively) was evaluated for young shoot EOs. Agar disc diffusion assay against pathogenic yeast *Candida parapsilosis* revealed the potential antifungal activity of marsh rosemary EOs. An alternative investigation of antifungal activity employed mediated amperometry at yeast *Saccharomyces cerevisiae*-modified electrodes. The subjection of yeast cells to vapors of march rosemary EOs resulted in a significant increase of electrode response due to disruption of yeast cell membranes.

asta.judzentiene@ftmc.lt

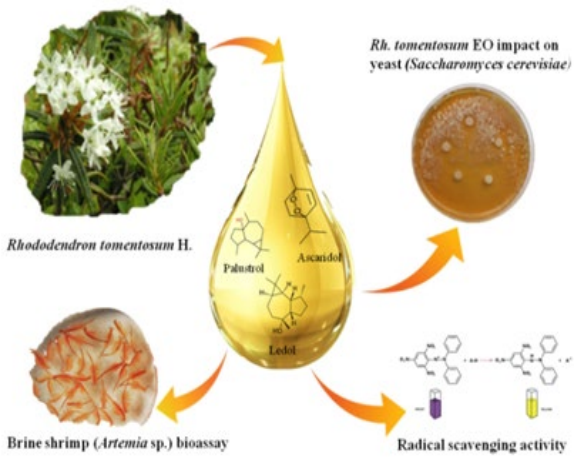

Fig. 3. Graphical illustration of experimental works.

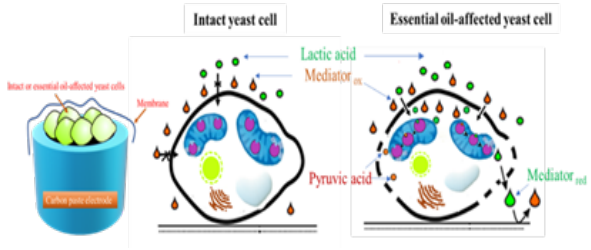

Fig. 4. Schematic image of amperometric measurements. Effect of EO on the yeast membrane permeability was monitored by measuring $K_3[Fe(CN)_6]$-mediated current response to a lactic acid at yeast-modified electrodes treated with vapors of marsh rosemary EO.

FUNCTIONAL MATERIALS AND ELECTRONICS

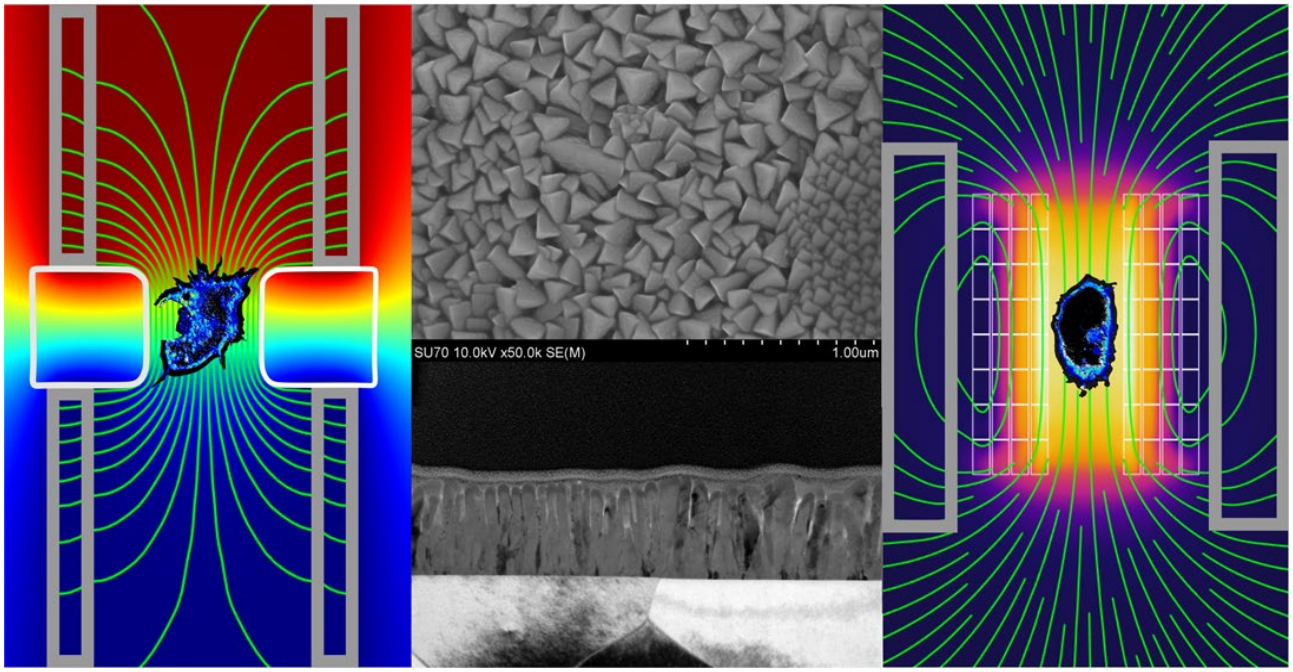

(Left) Electric field distribution in cross-flow treatment chamber during cell electroporation. (Right) Magnetic field distribution in pulsed coil magnet. (Middle) Electron scanning microscopy and transmission electron microscopy images of magnetoresistive La-Sr-Mn-O nanostructured film.

Advanced functional materials for magnetic, chemical and bio-sensors, microwave absorbers and bioelectric applications

In the last decade the increasing demand of various sensors and sensor systems has resulted in the development of novel technologies for fabrication of advanced functional materials, thin films and nanostructures. The department of Functional materials and electronics is developing growth technologies of advanced materials and thin films with special properties which might be used in various areas of applications. The physical, chemical and biological properties of such materials are investigated and used in developed components and systems. The numerical calculations as well as experimental investigations of prepared structures and biological cells are performed using various computational tools and experimental techniques, and responses of these materials to external stimuli (electrical, magnetic, light, microwaves, etc.) are studied for wide range of applications.

Towards colourless-to-green electrochromic smart glass based on a redox active polymeric semiconductor containing carbazole moiety

Smart windows containing electrochromic materials can practically be applied for greenhouses. For this application, maximum transmission in a visible (400 – 700 nm) range is required. In addition, these windows should modulate near-infrared (NIR) and block ultraviolet (UV) light without any significant impact to the light of visible range in order to control consistent temperature, which is required for the most optimal growth of plants. We found that the polymer with carbazole and thiiran electro-active groups exhibited colourless in neutral, saturated green in the radical cation and green-blue in dicationic states demonstrating favourable optical contrast and satisfactory coloration efficiency. Applied theoretical and electrochemical methods suggest that this newly created electroactive polymer could be a promising candidate as a neutral green electrochromic material.

gintautas.bagdziunas@ftmc.lt

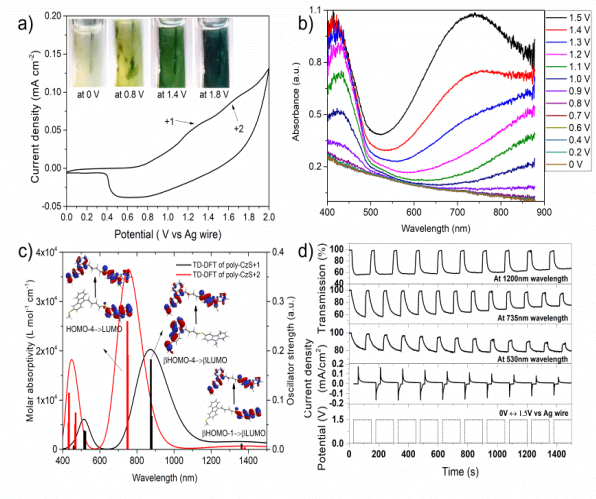

Fig. 1. The evaluation of spectroelectrochemical and electrochromic properties of used polymer: (a) cyclic voltammogram of the polymer on ITO electrode and colour changes, (b) UV-VIS-NIR spectra at various applied potentials, (c) TD-DFT computed UV-VIS-NIR spectra, (d) optical switching at potentials.

Evaluation of affinity sensor response kinetics towards dimeric ligands linked with spacers of different rigidity

We have investigated the binding kinetics of several genetically designed granulocyte colony-stimulating factor (GCSF) models, which like the antibody, have two binding sites. Three different ligands based on GCSF homo-dimeric derivatives, linked by differed linkers of different length and flexibility, were studied using antibody-like receptor (GCSF-R) based on two GCSF-receptor sites immobilized to Fc domains. To design the affinity sensor, the GCSF-R was immobilized on a thin gold layer via self-assembled monolayer conjugated with Protein-G. Binding kinetics between immobilized GCSF-R and all three different recombinant GCSF-based homo-dimeric derivatives were studied by total internal reflection ellipsometry. Binding rate constants were determined using three-step model. It was observed that both (i) affinity and (ii) binding kinetics depend on the length and flexibility of the linker that connects both domains of a GCSF-based ligand. The fastest

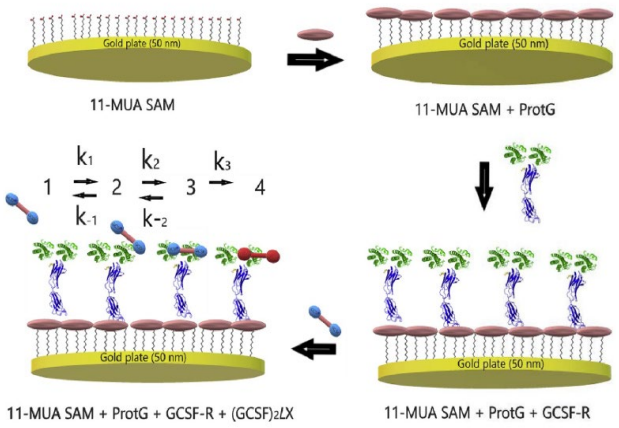

Fig. 2. Schematic representation of surface modification using various GCSF dimeric proteins.

association between immobilized GCSF-R and GCSF-based ligands was observed for ligands with the GCSF domains interconnected by the longest and the most flexible linker. Present research enables to predict the optimal linker structure for the design of GCSF-based medications.

ieva.plikusiene@ftmc.lt

Compact square-wave pulse electroporator with controlled electroporation efficiency and cell viability

A commercially available, compact, programmable device for high-voltage, square-wave electric pulse generation used for biological cell electroporation has been proposed, designed, and tested. The device has a variable energy storage capacitor bank enabling to avoid the accumulation of high amounts of energy. The main advantage of such a device is the increased range of possible pulse durations and amplitudes as compared to commercially available electroporators. The device can generate a single electrical pulse or a sequence of single pulses with widths from 3 µs to 10 ms and amplitudes up to 3.5 kV. The design of the generator using a crowbar circuit enabled to ensure the rise and fall time of the pulses less than 0.1 µs independent on the load impedance. The device is equipped with the LCD screen for the monitoring of the input parameters and an additional LCD screen for the display of the pulse waveform during the experiments. The latter screen significantly improved the quality of the investigation by providing more precise control of the current pulse shape and preferable conditions of the experiment (e.g., no sparking or heating of the cell suspension). This electroporator was successfully tested on suspensions of Saccharomyces cerevisiae yeast cells. It was demonstrated that the application of square-wave pulses ensured better control of the electroporation efficiency and cell viability after pulsed electric field treatment.

arunas.stirke@ftmc.lt

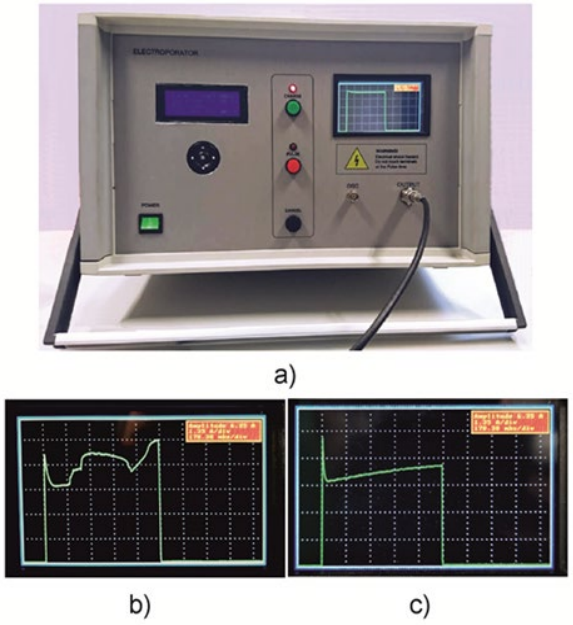

Fig. 3. (a) Compact square-wave generator for electroporation of biological cells. Display shots demonstrate the sparking in a cuvette (b) and current increase during the pulse due to heating of the substance in a cuvette (c).

New perspective method for investigation of electroporation

Effects induced in a membrane and intracellular structures depend on a cell type, pulse and media parameters. In order to achieve desired outcomes, membranes should be permeabilized in a controlled manner, and thus the efficiency of electroporation should be investigated in advance. Recently, by using mediated amperometry we developed a new method for the investigation of electroporation and its effects on cellular machinery. Single mediator systems comprised of hydrophilic (L-lactic acid) or lipophilic (menadione) mediators were successfully employed to investigate membrane permeability as well as cellular responses. The exposure of yeast cells to a single electric field pulse (τ = 300 µs, E = 16 kV/cm) resulted in up to tenfold increase of current strength mediated by hydrophilic mediators. Exposure to pulsed electric field (PEF) resulted in decrease of menadione mediated current strength (from 138 to 32 (±15) nA) which could be completely compensated by supplementing the electrolyte with NADH.

arunas.stirke@ftmc.lt

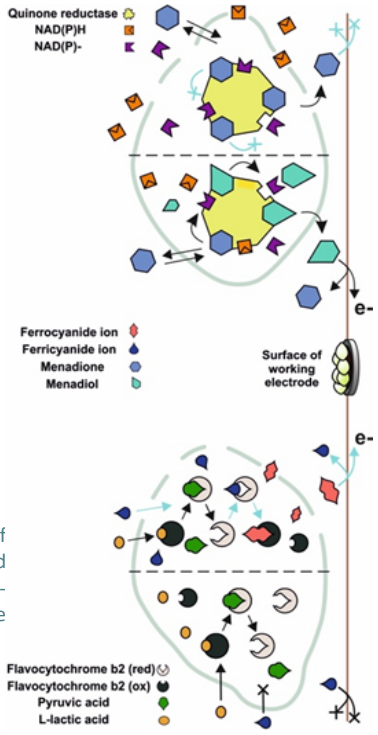

Fig. 4. Schematic overview of the developed new method for investigation of permeabilization of the cell membrane after the PEF treatment.

Gated bow-tie diode for microwave to sub-terahertz detection

We propose a new design microwave radiation sensor based on selectively doped semiconductor asymmetrically shaped structure (bow-tie diode). The novelty of the design comes down to gating of the active layer of the diode above different regions of the two-dimensional electron channel. The gate influences sensing properties of the bow-tie diode depending on the nature of voltage detected across the ungated diode, as well as on the location of the gate in regard to the diode contacts. When the gate is located by a wide contact (Fig. 5a), the voltage sensitivity increases ten times as compared to the case of the ungated diode, and the detected voltage holds the same polarity of thermoelectric electromotive force of hot electrons as in an asymmetrically shaped n-n+ junction. Another remarkable effect of a wide contact gate is a weak dependence of the detected voltage on frequency that makes such microwave diode a proper candidate for detection of electro-magnetic radiation in microwave and sub-terahertz frequency range (Fig. 5 c). The gate located beside a narrow contact of the bow-tie diode (Fig.5 b) increases the voltage sensitivity by two orders of magnitude, but changes the polarity of the detected voltage into the opposite.

steponas.asmontas@ftmc.lt

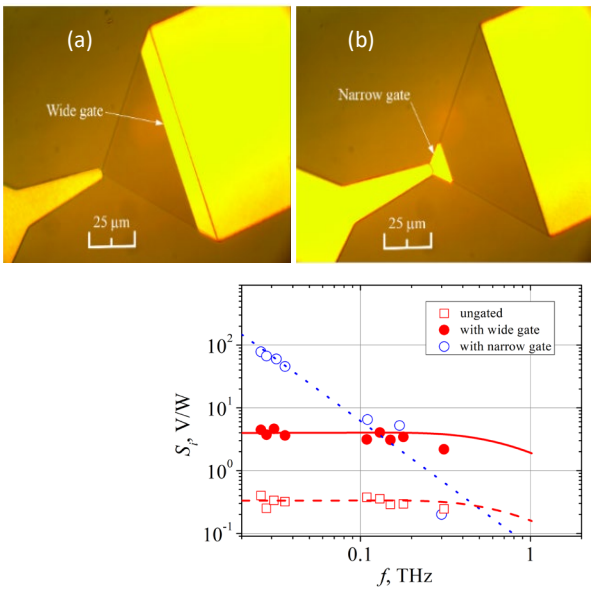

Fig. 5. (Top) The microphotographs of the bow–tie diodes with a narrow gate beside the neck of the diode (a) and with the gate near the wide metallic contact (b). (Bottom) Frequency dependence of the voltage sensitivity of the bow-tie diodes: ungated (open red squares), with wide gate (solid red circles), and with a narrow gate (open blue circles). Lines mark calculated frequency dependences.

Novel non-destructive method for monitoring of the magnetic pulse welding quality

The measurement of the magnetic field dynamics in the gap between the magnetic field shaper and the movable welded workpiece (flyer) was proposed for non-destructive magnetic pulse welding (MPW) evaluation. The created probe with CMR-B-scalar sensor made of thin manganite films together with the measurement module allows to measure locally the magnetic field in the narrow gap with high time resolution. The analysis of magnetic field dynamics provides a valuable information about the phenomena occurring at MPW. The experimental results show that the maximum magnetic field in the gap between the field shaper and the flyer is achieved much earlier than the maximum of the current pulse of the coil, and the first half-wave pulse of the magnetic field has two peaks. The time instant of the minimum between these peaks depends on the charging energy of the capacitors and is associated with the collision of the flyer with the parent. Along with the first peak maximum and its time-position, this feature could serve as an indication of the welding quality. This method can be applied in future for simulation and monitoring of the welding process of known materials, as well as for evaluation of the welding quality.

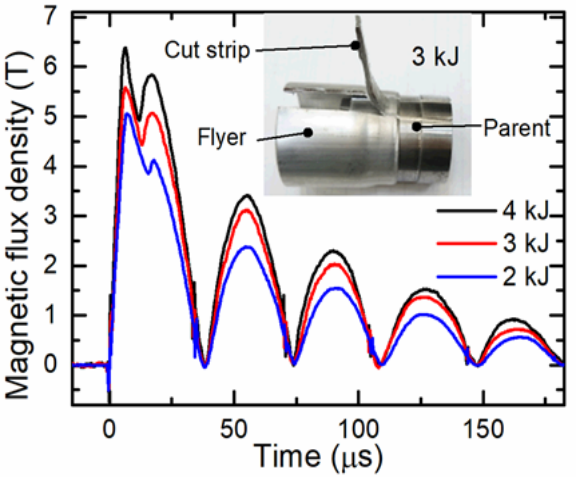

Fig. 6. Magnetic field between the field shaper and aluminum flyer tube during its welding with steel parent at different charging energies of magnetic pulse generator.

voitech.stankevic@ftmc.lt

NANOSTRUCTURES FOR APPLICATIONS

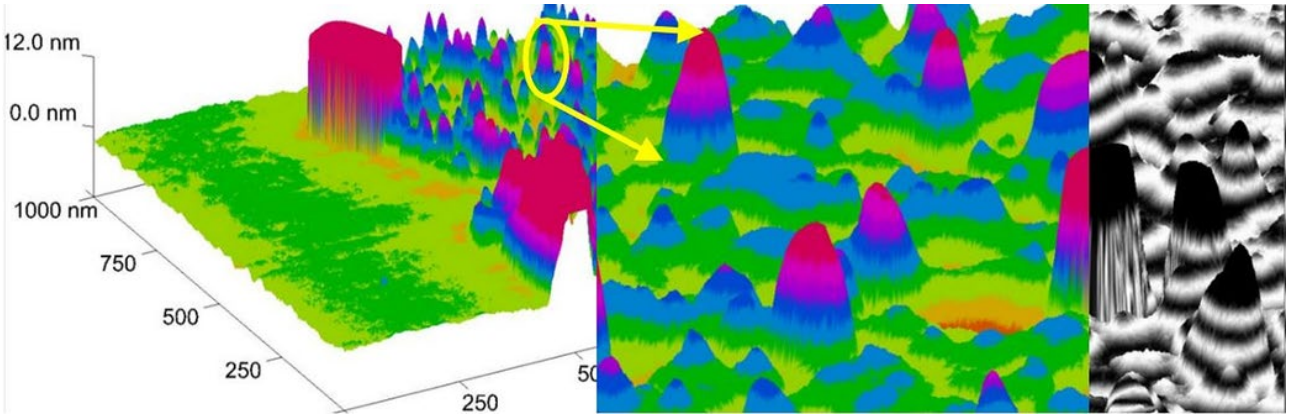

Hybrid 2D/3D systems for intelligent receptors

The guiding objectives of our applied research and technology studies are to develop the working prototypes of the systems based on photonic methods, optoelectronic devices and intelligent analysis of the system output information. The key function of the systems is a conversion of the physical / chemical characteristics of selected targets, including processes, things, persons and etc., into a digital stream representing the individual features of the targets. So, the systems are expected to function as photonic receptors providing specific information about the targets required for the decision making in the large networks known as the internet of things (IoT) and Internet of Everything (IoE). Our research and development (R&D) projects aim to create the techniques that are compatible with the semiconductor technology and allow to combine the usual three dimensional (3D) material thin films with the two-dimensional (2D) material layers in a single device. We are absolutely sure that the 2D/3D hybrid structures can lead to the highly innovative models of the photonic devices and the novel approaches in the integration of diverse functional elements within the compact autonomous systems. We plan to include semiconductor lasers, detectors, PV-based powers sources, and an output signal circuit in these compact systems. Three deeply related parts are considered being the core fields in this our work.

First, the synthesis and investigation of the functional materials and related structures. Our investigations and technology studies create the basis for the strictly controlled deposition technologies of the 2D materials adaptable to the bottom-up approach in the device fabrication. At this stage of studies, we mainly use two classes of the 2D materials, namely graphene and molybdenum disulphide (2D-MoS_2) as the typical transient metal dichalcogenide. Understanding of a relationship between the growth conditions and the properties of the 2D-materials is the primary challenge in our studies of the methods acceptable to modify the functional parts of the photonic systems. We found it crucial to control the defects that have to be visualised and characterised with sufficient accuracy. A sample planar structure with micro-crystalline graphene is illustrated in the headline figure by the topography images of a scanning probe microscope. Description of the defects detection in 2D-MoS_2 and development of practical devices can be found below in this report.

Second, the testing of the novel ideas in the working models of the devices. Our experimental and digital modelling results are acceptable to propose the approaches for modification of electrical and optical (from the visual to the far infrared waves) properties for the large area devices. An exciting way to control the interaction between the electromagnetic waves and the metamaterials is described in the highlight about the Fano resonance. There are two primary targets in our scientific and technology studies, namely (i) relationship between the optical – electrical parameters and the core characteristics of the layers and (ii) relationship between the technology conditions and the device parameters. We use the results for development of the IR laser based systems in the joint R&D projects.

Third, the development and testing of the prototypes of the devices and integrated systems for the intelligent data collection and analysis in practical applications. The primary target of this part of the work is finding the solutions of the problems that address the needs of potential producers and end-users. Therefore, the R&D projects typically involve the partners capable of making the right choices of the essential characteristics for the expected commercial products.

In the present stage, we almost reached the critical mass of the technology infrastructures required for the high technology level manufacturing of the key parts of the prototypes of the semiconducting photonic systems that can be called the photonic receptor systems. The combined self-powered systems based on the 2D- and 3D-materials are almost in the proof of the concept stage. We think that the most fascinating property of our 2D/3D hybrid systems is a compatibility with flexible and transparent substrates. Thus, our hybrid modules can be easily integrated into small volume devices, small robots, gadgets and even used as the smart dust or the intelligent photonic receptors.

Single variable defined technology control of the optical properties in MoS_2 films with controlled number of 2D-layers

For the first time we introduced the method to control the properties of the atomic thin MoS_2 layers by the fused calibration diagram that describes a fixed relationship between the thickness of metallic Mo precursor coating and the properties of 2D-MoS_2 film. The atomic thin MoS_2 films were grown on a large area substrate with an initially metallic Mo precursor by chemical sulphur vapour deposition. It was demonstrated that, under fixed conditions of the PVD Mo formation, the number of the 2D-analogous MoS_2 layers is directly related to the deposition time of metallic Mo by magnetron sputtering (Fig. 1). The relationship was confirmed by the experimental results obtained from the Raman and optical spectroscopies. The arrangement of the layers was determined by the optical absorption coefficient spectra of the polarisation of the incident light parallel to the surface of the samples (Fig. 2). The analysis of the optical absorption spectra below the fundamental absorption edge proved the multi-component nature of the optical transitions related to the band structure of the MoS_2 films with a limited number of the 2D-layers. The method can be transferred and adapted to the technology control of an entire family of the 2D-layers of transient metal dichalcogenides grown by the CVD method from a metallic precursor films on large areas of various substrates.

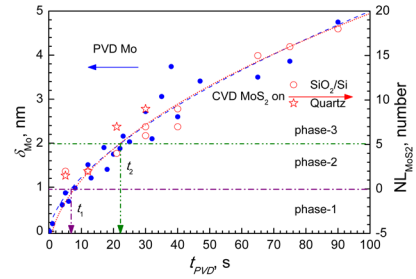

Fig. 1. Fused calibration diagram combining the dependence of Mo film thickness, δ_{Mo}, and number of 2D-MoS_2 film layers.

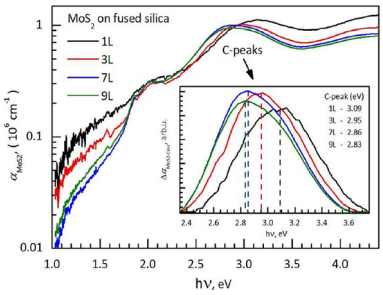

Fig. 2. Absorption coefficient spectra of MoS_2 films with individual thickness described by the number of 2D-layers: 1L, 3L, 7L and 9L. Inset: the C-exciton peak described as a difference between the absorption coefficient and the baseline extrapolated from the corresponding spectrum.

arunas.setkus@ftmc.lt

Photovoltaic effect-driven IR response of heterojunctions obtained by direct CVD synthesis of MoS_2 nanolayers on crystalline silicon

Development of technologies of hybrid combined 3D and 2D materials is recognised as highly attractive opportunity to create new optoelectronic devices with unique properties originating from the atomic thin structure. Here, a direct synthesis of MoS_2 2D-layers on p-Si was demonstrated to be acceptable to fabricate a photovoltaic effect–driven photodetector based on a hybrid 2D/3D heterojunction. It was experimentally shown that the heterojunction with the top and bottom contacts was highly sensitive to the illumination between 650 and 1200 nm. The response to light originated by the photovoltaic effect in the sample devices without an external power supply. The maximum sensitivity of the 2D/3D heterostructures to the optical power of the illumination was up to 210 V/W, being nearly independent of the wavelength (see Fig. 3). The analysis of the experimental I-V, C-V characteristics, Raman spectra and AFM surface images allowed us to construct a flat band model of the hybrid 2D/3D n-p-heterojunction that explained the electrical properties of the n-MoS_2/p-Si photodetectors.

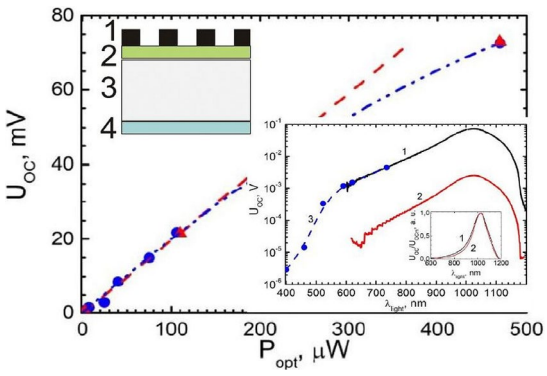

Fig. 3. The response of the n-MoS_2/p-Si heterojunction detector to the light: the UOC response versus the optical power for the response maximum at λ=1024 nm. Inset (top, left): sketch of the device construction, 1 – front side contact strips, 2 – top MoS_2 film, 3 – p-Si substrate (250 μm thick), 4 – back side contact. Inset (bottom, right): the spectra of the open circuit voltage U_{OC} response to the light with the optical power 470 μW (1, 3) and 2.5 μW (2). The light source was monochromator (1, 2) and the LEDs (3) (points are the experimental data, line is an eye guide). Second level inset: a version of the same spectra recalculated as the ratio of the response signal to the maximum response signal at λ=1024 nm.

The photovoltaic effect-driven light detectors offer highly promising ways in development of the autonomous photonic systems.

arunas.setkus@ftmc.lt

ASTROPHYSICS

We study complex systems, from star clusters to galaxies, by employing ground- and space-based observations, as well as numerical simulations.

Evolution of dwarf galaxy observables

The growth of dwarf galaxies over the lifetime of the Universe can be efficiently tracked with semi-analytical models. We present such a model of isolated dwarf galaxy evolution and use it to study the build-up of observed correlations between dwarf galaxy stellar mass, gas mass, metallicity and star formation rate. We analyse the evolution by running a large number of models with different merger histories in order to determine the importance of stochasticity on the present-day properties of dwarf galaxies. Redshift evolution shows that even isolated galaxies change significantly over the Hubble time and that "fossil dwarf galaxies" with properties equivalent to those of high-redshift analogues should be extremely rare, or non-existent, in the local Universe. A break in most galaxy property correlations develops over time, at a stellar mass $\sim 10^7$ $M_\odot$. It is caused predominantly by the ionizing background radiation and can therefore in principle be used to constrain the properties of reionization. The difference between galaxies quenched during reionization and those continuing to form stars at later times (see Fig. 1) is maintained in stochastic models compared with an averaged one, but becomes less clear.

kastytis.zubovas@ftmc.lt

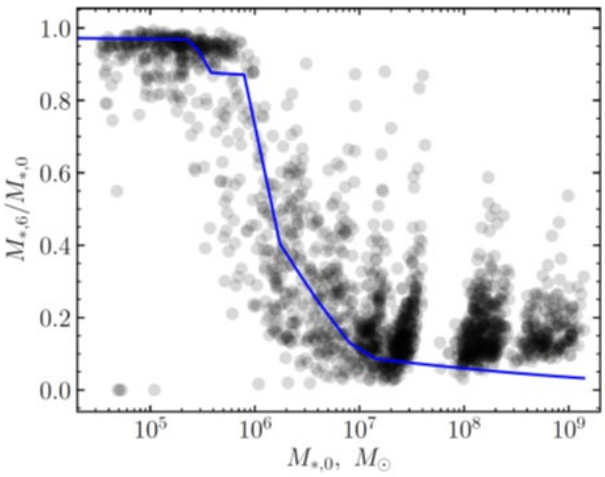

Fig. 1. Fraction of stars formed before the end of cosmic reionization (~1 billion years after the Big Bang) as a function of present-day stellar mass in model dwarf galaxies. Blue line represents model with averaged growth of dark matter halo, while grey circles represent individual galaxies with stochastically different halo growth histories. Low-mass galaxies are efficiently quenched during reionization and form few stars later, while more massive galaxies keep forming stars throughout the age of the Universe.

Red giant stars in the dwarf galaxy Leo A

Leo A is a gas-rich dwarf irregular galaxy of low stellar mass located at the outskirts of the Local Group. It has an extended star formation history with stellar populations spanning a wide age range (~0.01-10 Gyr). As Leo A is a well-isolated dwarf galaxy, it is a perfect target to study a galactic structure formed entirely by processes of self-induced star formation. We analysed populations of the brightest asymptotic giant branch (AGB) stars and red giant branch (RGB) stars over the entire extent of the Leo A galaxy using multicolour photometry data obtained with the Subaru Suprime-Cam (*B*, *V*, *R*, *I*, H_α) and HST ACS (*F475W* & *F814W*) cameras. We found a previously unknown sequence of 26 peculiar RGB stars which probably have a strong CN-band in their spectra (~380-390 nm). By splitting the RGB sequence into blue and red parts, we revealed different spatial distributions of the two subsets, with the former being more centrally concentrated than the latter. Cross-identification with spectroscopic data available in the literature suggests that the bulk of blue and red RGB stars are, on average, similar in metallicity; however, the red RGB stars have a wider range of metallicity. We also found that the distributions of luminous AGB and blue RGB stars have nearly equal scale-lengths (0′.87 ± 0′.06 and 0′.89 ± 0′.09, respectively), indicating that they could belong to the same generation. The distribution of red RGB stars has a larger scale-length of 1′.39 ± 0′.06 and shows prominent breaks in the surface number density radial profile at ~4′ and ~6′ along the major axis of Leo A. We also present a catalogue of 32 luminous AGB stars and 3 candidate cAGB stars.

rima.stonkute@ftmc.lt
vladas.vansevicius@ftmc.lt

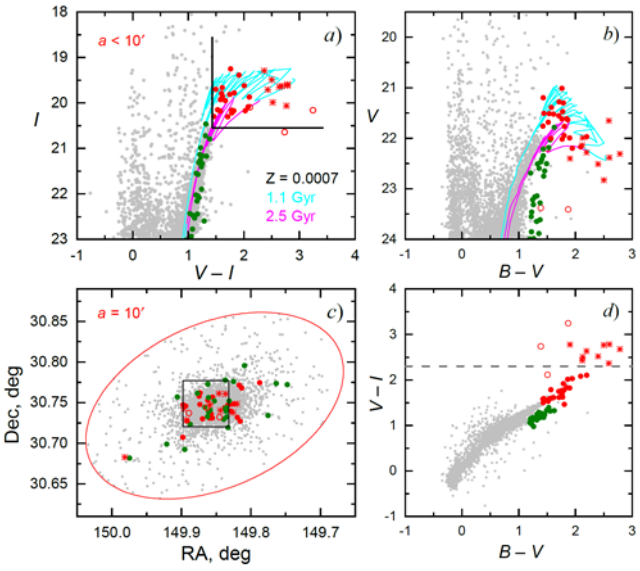

Fig. 2. Subaru Suprime-Cam photometry data. (a) *I* vs. *V* – *I* diagram. Red symbols depict: dots – AGB stars; asterisks – AGB stars with dusty envelopes; open circles – cAGB stars. Green dots mark peculiar RGB stars. Grey dots are the remaining objects in the catalogue. Symbols and colours correspond to the same objects in all panels. (b) *V* vs. *B* – *V* diagram. Isochrones of 1.1 Gyr (cyan) and 2.5 Gyr (magenta) ages and of Z=0.0007 metallicity are overlaid in panels (a) and (b). The isochrones are shifted in magnitude and colour, adopting a true distance modulus of 24.58 and foreground MW extinction. (c) spatial distribution of objects within the a=10′ ellipse (b/a=0.6) centered on the Leo A galaxy. A black square shows the area of NIR observations. (d) two-colour diagram, *V* – *I* vs. *B* – *V*. A horizontal dashed line marks the lower limit (*V* – *I* = 2.3) of the region occupied by luminous AGB and cAGB stars with dusty envelopes.

MODELING

Dynamics of singlet oxygen molecule trapped in silica glass: density functional theory calculation

The two lowest electronic excited states of free or matrix-isolated oxygen molecule O_2 are the metastable singlets ($^1\Delta_g$ and $^1\Sigma_g^+$), located at 0.97 and 1.62 eV above the triplet ground state ($^3\Sigma_g^-$), respectively. O_2 molecules in the lowest excited singlet state are often referred as "singlet oxygen". This form of oxygen is of immense importance in such fields as photobiology, photodynamic cancer therapy, and photocatalysis. Optical transition from the lowest-energy singlet to the ground-state triplet is forbidden by spin and symmetry selection rules. The interaction of O_2 with the environment can relax these strict selection rules. As a result, optical lifetimes are highly environment-dependent. In this work we studied the luminescence polarization anisotropy of O_2 in silica to understand the nature of oxygen - silica interaction. We found that oxygen interacts very weakly with SiO_2, resulting in luminescence lifetimes of about 1s, the longest lifetimes of singlet oxygen in any condensed medium. Regardless, the rotation of oxygen molecules in silica voids is highly constrained, yielding a finite luminescence anisotropy. These conclusions were confirmed by our first-principles calculations of O_2 in silica.

audrius.alkauskas@ftmc.lt

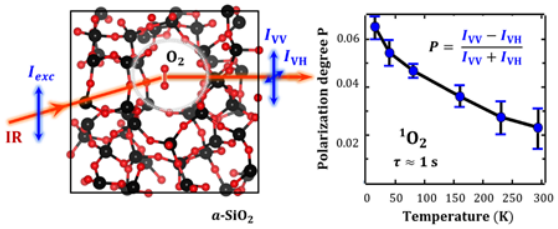

Fig. 1. Left: measurement of luminescence polarization anisotropy of singlet oxygen trapped in a silica glass. Right: polarization degree as a function of temperature.

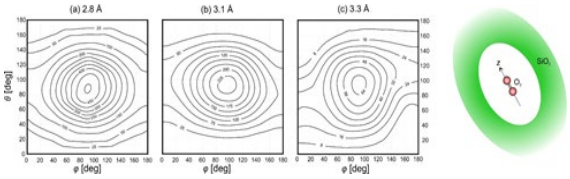

Fig. 2. Rotational potential energy surfaces of oxygen in silica voids of different size, as calculated by density functional theory.

Modeling of ribbon and oblique structures of benzene-1,3,5-triyl-tribenzoic acid

We proposed two models to describe the occurrence of two self-assembled molecular structures (ribbon (R) and oblique (O)) formed of intact and deprotonated benzene-1,3,5-triyl-tribenzoic acid (BTB) molecules (Fig. 3). To determine the intermolecular interaction potentials for the R and O phases, the density functional theory calculation for clusters of BTB molecules was performed. The Monte Carlo (MC) simulations for the R phase demonstrated how the interactions between singly deprotonated BTB molecules lead to formation of 2D ribbons separated by the inter-ribbon gap (Fig. 4, right). The O phase can be formed of intact and singly deprotonated molecules (Fig 4, center). The ground state and MC modeling for the O and honeycomb (HON) structures demonstrated that for intact molecules (deprotonation level, DPL=0) the energy of the HON structure is always lower than that of the O phase. With increase of DPL, the difference of energies of these two structures decreases and for DPL=1 the O phase has higher probability to exist in comparison to the HON phase.

evaldas.tornau@ftmc.lt

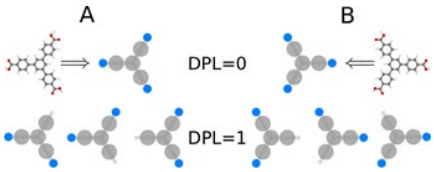

Fig. 3. BTB molecule and its states in our model. Top row: two states of intact molecule (DPL = 0). Bottom row: six states of singly deprotonated molecule (DPL = 1). Vertex with a proton (−COOH) is indicated by a blue-filled circle.

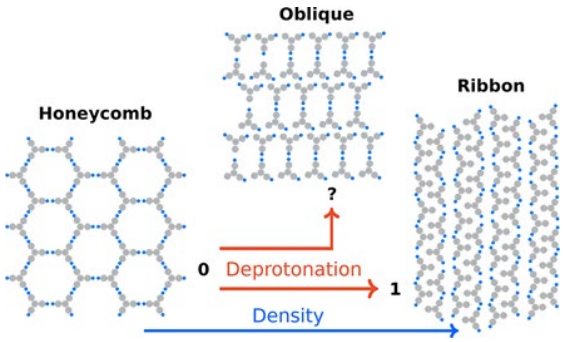

Fig. 4. Snapshots of Monte Carlo calculations demonstrating the BTB structures occurring with increasing molecular density: honeycomb at DPL= 0 (left), oblique at DPL < 1 (center) and ribbon at DPL = 1 (right).

Pinning control of unstable equilibrium in arrays of coupled FitzHugh–Nagumo oscillators

Equilibrium of a single nonlinear oscillator can be stabilized by means of well-known methods, e.g. proportional, tracking filter, and time-delayed feedback techniques. However, in arrays of oscillators it is impractical and even impossible to control each unit. To get around the problem the so-called 'pinning control' can be used. The repulsive feedback, either '*–qu*' or ''*–q*<*x*> is applied to a single randomly chosen (accidentally accessed) oscillator or to a small fraction of the oscillators. If the coupling of the units and the feedback force are sufficiently strong, then the stability of the equilibrium of the entire array is achieved. We have applied the pinning technique to the array of neuronal type, the FitzHugh–Nagumo (FHN), oscillators.

arunas.tamasevicius@ftmc.lt

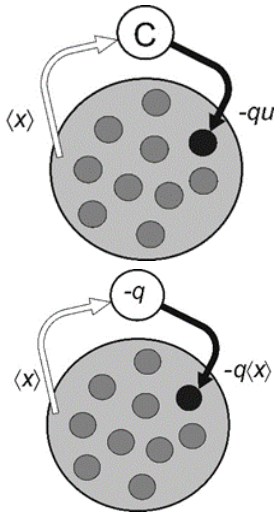

Fig. 5. Arrays of mean-field coupled FHN oscillators. (Top) Control via an auxiliary oscillator; the 'C' is a copy of the FHN unit. (Bottom) Control via inverted mean field; the '–q' is an inverting amplifier. Large light gray circles represent the mean-field medium, small dark gray circles symbolize the individual oscillators, black circles denote the pinned oscillators, the open circles in the feedback loops are the controllers.

Comparison of models of photoconductive terahertz antennas based on ordinary differential equation and Monte Carlo method

Numerical models of complex physical systems are often simplified, taking into account only the most important processes. Such simplifications sometimes can become the threshold for further development of the technology. In the case of photoconductive terahertz antennas, we have investigated full-wave numerical models that describe the dynamics of photoexcited carriers and related electrodynamic process. Two different complexity models for photocurrent have been used: ordinary differential equations (ODE) and Monte Carlo (MC) simulation. We demonstrated that a simple ODE model, where the photocurrent is supposed to be proportional to the concentration of photoexcited electrons, can be useful when the duration of photoexcitation is relatively long (FWHM ≥ 250 fs). At shorter laser pulse lengths, the transient dynamics of electron drift velocity at sub-picosecond time scale makes a significant impact on the growth of photocurrent speed. This leads to the overestimation of electric field amplitude in the high-frequency range of the ODE model. The MC simulation procedure has higher computational costs and is more difficult for implementation, but it provides the correct results for any length of the laser pulse.

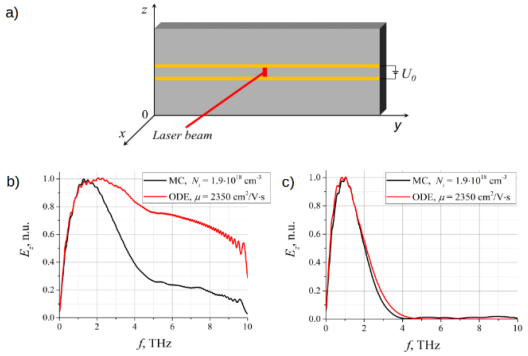

Fig. 6. (a) A view of the photoconductive antenna. THz pulse spectra generated by (b) 25 ps laser pulse and (c) 250 ps laser pulse. Black line shows MC, red – ODE results. The concentration of ionized impurities and electron mobility are taken 1.9 10^{18} cm^{-3} (MC) and 2350 cm^2/Vs (ODE), respectively.

zilvinas.kancleris@ftmc.lt

Generalized Lorenz-Mie theory for photonic wheels and their interaction with nanoparticles

Plane light waves can carry angular momentum which is usually longitudinal. In confined (focused) light waves it can be oriented transversely. Such electromagnetic fields therefore are called 'photonic wheels'. We create photonic wheels with an aplanatic system and expand them into vector spherical harmonics. This decomposition is applied to create a generalized Lorenz-Mie theory of photonic wheels. We study the interaction of these beams with gold and silicon spheres and reveal an appearance of localized longitudinal angular momentum in the scattered field. Lastly, we employ the multiple scattering method and simulate a chiral cluster of nanoparticles in the focal plane of a photonic wheel.

sergejus.orlovas@ftmc.lt

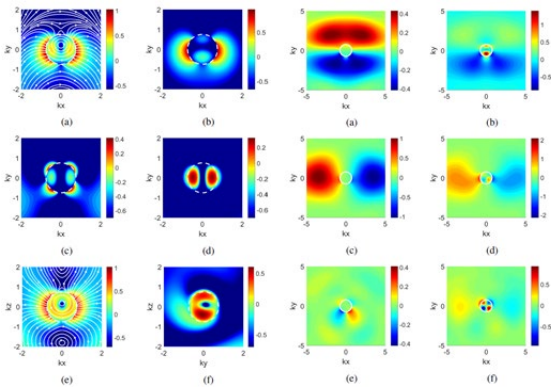

Fig. 7. (Left) Distribution of normalized electric field intensities for the photonic wheel interacting with a silicon nanoparticle in the xy-plane (a-d), xz-plane (e) and yz-plane (f). (Right) The distribution of angular momentum density of the photonic wheel beam interaction with spherical silicon (b,d,f) and gold (a,c,e) nanoparticles.

Tomographic reconstruction of highly focused azimuthally and radially polarized vector beams

The knife-edge method is an established technique for tomographic profiling of even tightly focused light beams. However, the straightforward implementation of this method fails if the materials and geometry of the knife-edges are not chosen carefully or, in particular, if knife-edges used are made of pure materials. Artifacts are introduced in these cases in the shape and position of the reconstructed beam profile due to the interaction of the light beam with the knife. Hence, the corrections to the standard knife-edge evaluation method are required. We have investigated the knife-edge method for highly focused radially and azimuthally polarized beams and their linearly polarized constituents. We have introduced relative shifts for those constituents and report on the consistency with the case of a linearly polarized fundamental Gaussian beam. An adapted knife-edge profiling technique was presented and proof-of-concept tests are shown demonstrating the tomographic reconstruction of beam profiles.

sergejus.orlovas@ftmc.lt

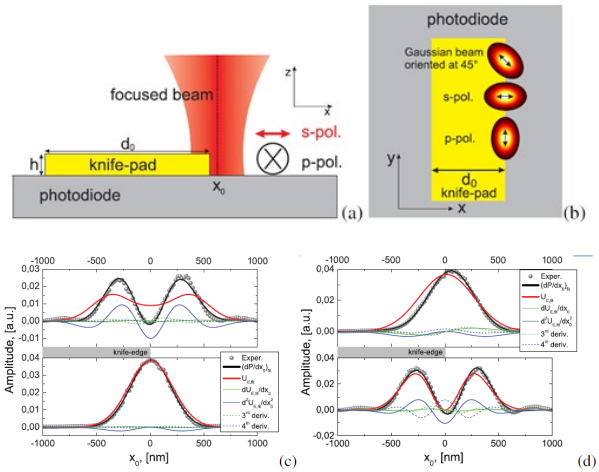

Fig. 8. Schematic depiction of the knife-edge method: (a) xz-plane and (b) xy-plane. Depiction of the adapted knife-edge method for linear constituents of tightly focused radially (c) and azimuthally (d) polarized beams. The derivatives of the experimentally measured photocurrents (gray circles) and the fitted curve (black) with the beam profile (red) and its first four derivatives are shown for λ= 700 nm.

Generation of high-energy vector Bessel beam for void and micro-crack generation in transparent materials

Efficient generation of a high-quality and high-energy vector Bessel beam is possible using an S-wave plate (radial/azimuth polarization converter) together with an ordinary glass axicon. We have examined laser-induced modifications in glass using such beams with different pulse durations. We have achieved material cracking and have observed dominant crack propagation directions caused by the intensity asymmetry of the generated beam. By translating the beam, we have demonstrated a potential application of the vector Bessel beams and their transverse polarization components for micro-processing of transparent materials using ultra-short pulses.

sergejus.orlovas@ftmc.lt

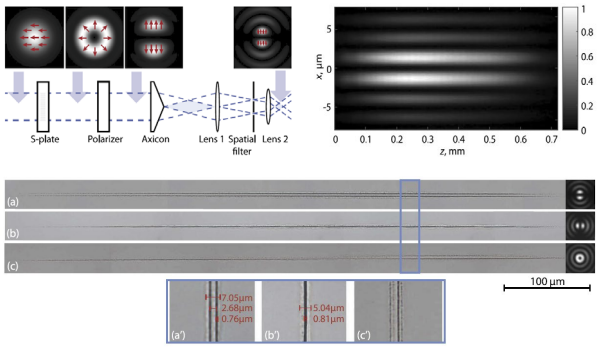

Fig. 9. (Top, left) Setup for single transverse intensity component of radially polarized vector Bessel beam generation. Red arrows indicate polarization vectors. (Top, right) Beam intensity profile in the xz plane of the experimentally generated radially polarized vector Bessel beam. (Bottom) Transmission microscopy images of modifications in fused silica sample with radially polarized vector Bessel beam and its orthogonal polarization components.

Complex source vortices and their interaction with chiral cluster of nano-particles

Vectorial complex source vortex beams accurately and properly describe highly focused vertical beams. Such beams are widely used as optical tweezers, spanners and optical traps. In order to describe the micromanipulation of objects properly, we analytically represent these beams in the basis of electromagnetic multipoles. In particular, three different polarizations of optical vector vortex beams were studied in detail. We have utilized the representation of the studied beams in vector spherical harmonics to investigate their interaction with a chiral cluster of gold nanoparticles.

sergejus.orlovas@ftmc.lt

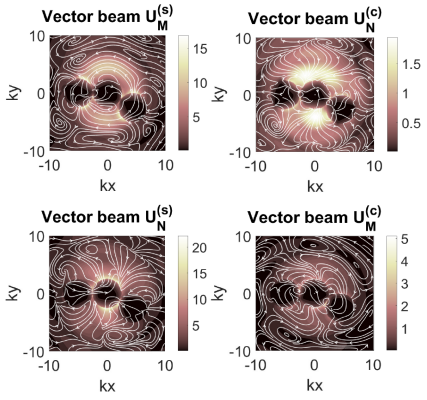

Fig. 10. Modulus of the total electric field for transverse electric (first row) and transverse magnetic (second row) vector vortices scattered of the cluster of three gold spheres. Optical vortices are spherically (left row) and cylindrically (right row) polarized.

NONLINEAR DYNAMICS AND CHAOS

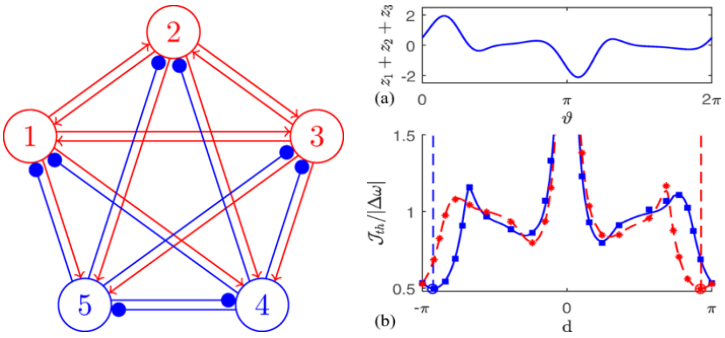

Fig. 1. (Left) Schematic diagram of a network of synaptically coupled five FitzHugh-Nagumo (FHN) neurons. Red circles with numbers 1, 2, and 3 are excitatory neurons and blue circles with numbers 4 and 5 are inhibitory neurons. (Right) Testing the minimum-charge control theory in the case of stimulation of excitatory neurons. (a) Effective phase response curve used to build the optimal waveform. (b) The threshold of the mean absolute value of the current J_{th} normalized to the frequency detuning $\Delta\omega$ as a function of the distance d between the positive and negative pulse of a trial waveform. The blue and red curves obtained according to the phase reduction theory correspond to the positive and negative $\Delta\omega$, respectively. Symbols are obtained by solving original nonlinear differential equations.

Entrainment of a network of interacting neurons with minimum stimulating charge

Periodic pulse train stimulation is generically used to study the function of the nervous system and to counteract disease-related neuronal activity, e.g., collective periodic neuronal oscillations. The efficient control of neuronal dynamics without harming brain tissue is key to research and clinical purposes. We developed the minimum charge control theory for a network of interacting neurons exhibiting collective periodic oscillations. The aim of the minimum charge control strategy is to minimize the integral charge transferred to the neurons in both directions during the stimulation period. This optimization is clinically relevant because it aims to reduce damage to nerve tissue during stimulation. We derived a general expression for the optimal waveform, which provides an entrainment of a connected neural network to the frequency of stimulation with the minimum mean absolute value of the current injected into neurons. The optimal waveform is of bang-off-bang type, and its parameters are determined by the parameters of the effective phase response curve (PRC) of the entire network. To build the optimal waveform, only limited information on the PRC is required. The optimal waveform represents periodically repeated positive and negative rectangular pulses. The pulse sequence depends on the sign of the frequency detuning, $\Delta\omega$. For $\Delta\omega > 0$, this sequence is such that the positive pulse hits the network at the timing of the maximum of PRC while the negative pulse hits the network at the timing of the minimum of PRC. As a result, the maximum phase advancement occurs in the network during one period of the forcing. Areas under the positive and negative pulses are equal to each other, so that a clinically mandatory condition of charge-balance is satisfied. Examples of application of the minimum-charge control theory for a small-scale network of synaptically coupled FHN neurons and a large-scale network of synaptically coupled quadratic integrate-and-fire (QIF) neurons are presented in Figs. 1 and 2, respectively.

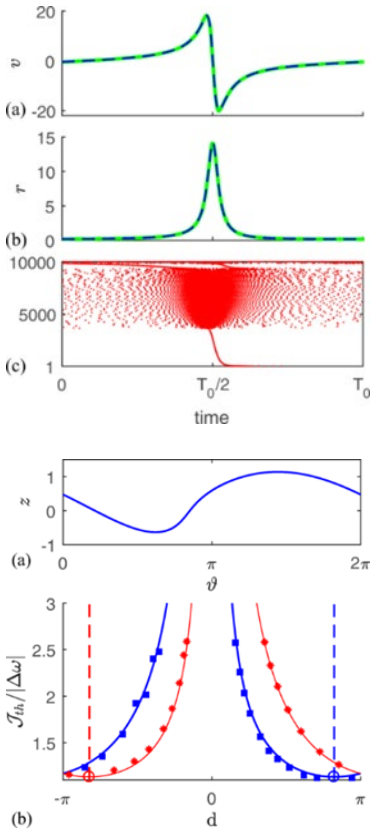

Fig. 2. (Top) Dynamics of a network of 104 synaptically coupled QIF neurons in the absence of stimulation. (a) The evolution of the mean membrane potential v(t) and (b) the spiking rate r(t). (c) The raster plot. Here the dots show the spike moments for each neuron, where the vertical axis indicates neuron numbers.

(Bottom) Testing the minimum-charge control theory for the QIF network. The designations are the same as in Fig. 1 in the right column.

kestutis.pyragas@ftmc.lt

ELECTROCHEMICAL MATERIAL SCIENCE

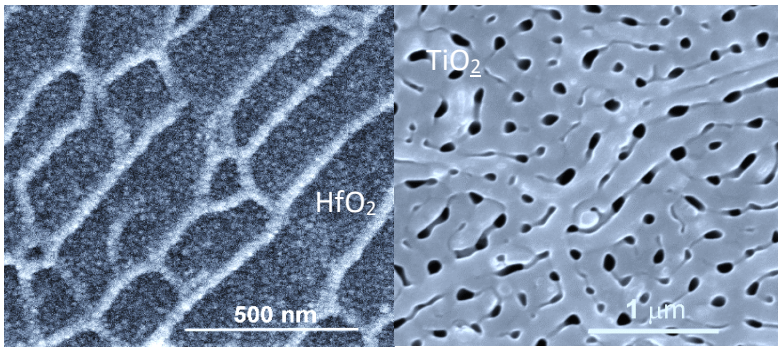

Atomic layer deposition (ALD) of ultra-thin oxide films

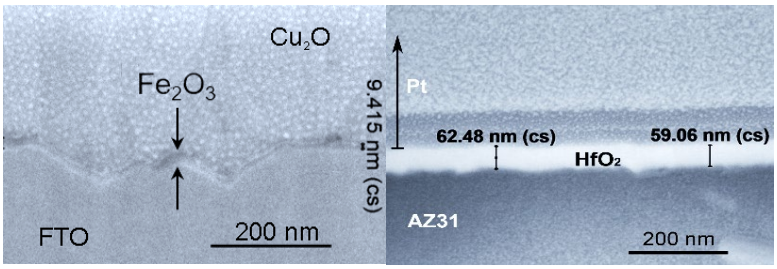

Technologies for electrochemical energy conversion and storage, solar-driven electrochemistry, smart anticorrosive and wear resistant coatings

Electrochemical energy conversion and storage technologies offer attractive solutions to many contemporary renewable energy-related issues. The R&D activities in this area in Department of Electrochemical Material Science and Department of Chemical Engineering and Technologies are focused on the development and profound understanding of materials, processes and devices for aqueous Na-ion batteries, (photo)electrochemical production of hydrogen or other value-added chemicals, electrochemical synthesis of silicon nanostructures and other materials, including superparamagnetic and luminescent nanoparticles with possible applications in photovoltaics, nanomedicine, etc. Electrochemical, chemical as well as physical methods (electrodeposition, atomic layer deposition, magnetron sputtering) are applied for the surface modification and production of smart materials with exceptional electrocatalytic, anticorrosive, magnetic, mechanical or other properties. The integral part of the process of new materials development is a thorough characterization of their structure, morphology and chemical composition. Environmental friendliness is an imperative for all newly developed technologies. Corrosion, tribological, physical and electrochemical studies of the interaction of metal surfaces with biofuels (ethanol, biodiesel, biolubricants) are carried out as well. Electrochemical oxidation appeared beneficial to tribological research. Anodic coatings with exceptional resistance to friction and wear were developed in the FTMC Tribology laboratory. The prototypes were scaled up in the FTMC Anodization pilot plant. Tribotesting was expanded to derivatized biobased compounds and secondary raw materials, eventually leading to promising lubricant formulations for hydraulic systems in recently completed project COSMOS (H2020-635405). These investigations also included plasticizers and adhesives, the latter being the main focus of a new project TERMINUS (H2020-814400), which involves several large corporations and top European universities. The FTMC Tribology laboratory is in charge of adhesive development for recyclable multilayer packaging in this consortium. Smart coatings with active corrosion protection ability for metals in aggressive environments are developed. Corrosion tests are carried out in the FTMC Accredited Corrosion Research Laboratory which performs characterization and evaluation of the corrosion-caused changes in metals, alloys, composite coatings, paints and lacquers in natural and artificial atmospheres, and can also assess the microbially induced corrosion of materials in ambient atmosphere or model media.

Anticorrosion protection of lightweight alloys by ultrathin hafnium oxide films

Magnesium alloys, due to their lightness and superior mechanical properties, are promising materials in many fields. However, their high susceptibility to corrosion is an issue. While Mg corrosion is mostly considered as a detrimental factor, the activity could be regarded as a valuable property in biomedical applications. Corrosion enables harmless dissolution of Mg-based implants in-vivo and eliminates the need for secondary surgery. Examples are temporary implants for osteosynthesis, cardiovascular stents or tissue scaffolds. A toxic dose of the corrosion product Mg^{2+} is unknown, the cytotoxic activity of these ions on osteoblast cells was not determined, and they promoted bone growth in damaged locus. Our group applied ultrathin hafnium oxide films to tailor the corrosion rate enabling to release in vivo just trace amounts of hafnium. We used atomic layer deposition (ALD) technique to form hafnia films. The films, due to chemical stability, optical transparency, wide band gap, photoluminescence and high dielectric constant, has potential to be applied in various fields: organic solar cells, capacitors, switching memories, field effect transistors, heat mirrors, as well as in production of chemical sensors.

eimutis.juzeliunas@ftmc.lt

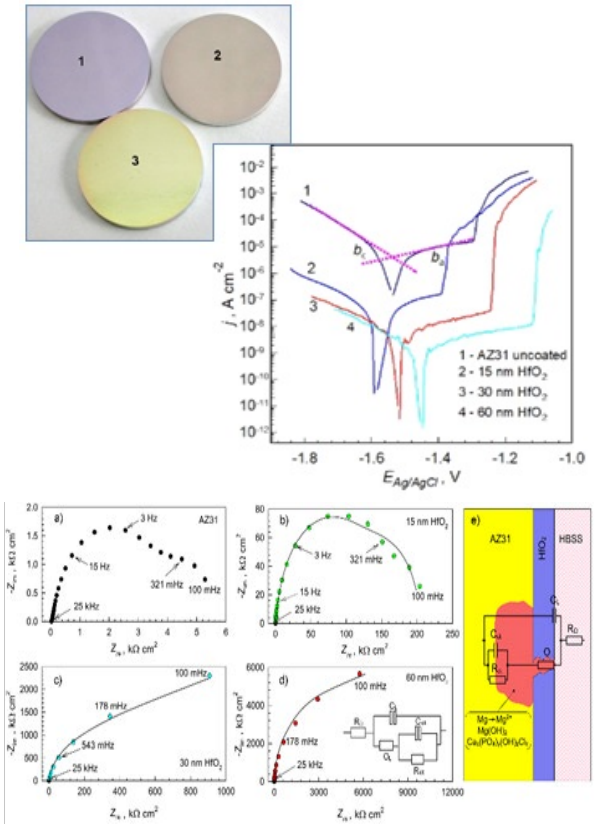

Fig. 1. (Top) ALD HfO_2 coated magnesium alloy samples and their Tafel plots. (Bottom) electrochemical impedance spectra.

Substrate impact on the structure and electrocatalytic properties of molybdenum disulfide for HER from water

It is expected that utilization of molybdenum disulfide (MoS2)-based nanostructured electrocatalysts might replace Pt-group electrodes most effectively when applied for hydrogen evolution reaction (HER) from water. In this study, the hydrothermal synthesis at the Mo, Ti, Al, anodized Ti and hydrothermally designed titanium suboxide substrates was performed. The electrodes obtained were characterized and the HER activity was tested. In this way, MoS_2-based HER catalyst possessing a surprising stability and a low Tafel slope was designed via attachment of nanoplatelet-shaped MoS_2 species to the nanotube-shaped anatase-TiO_2 surface.

arunas.jagminas@ftmc.lt

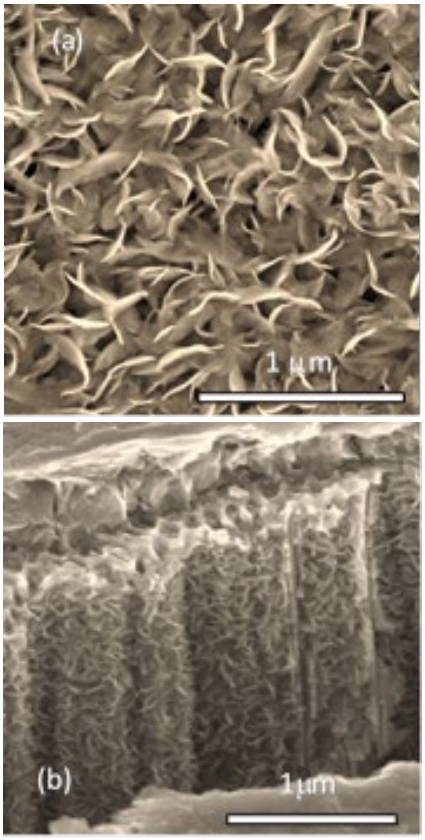

Fig. 2. SEM images of nanostructured MoS_2 nanoplatelets on the Ti/TiO_2 substrate.

Effect of secondary phases removal and dissolution of by-product on photoelectrochemical response of Cu_2ZnSnS_4 film

An influence of surface treatment of as-synthesized Cu_2ZnSnS_4 (CZTS) thin films on photoelectrochemical response in $Eu(NO_3)_3$ water solution was studied. We have shown that dissolution of copper sulfide in KCN solution and subsequent dissolution of ZnS in HCl solution is insufficient to achieve maximal photoelectrochemical response. The additional treatment in the KCN solution for only 10 s results in the highest photocurrent density of 1.6 mA/cm^2 at cathodic potential of -0.324 V vs. saturated hydrogen electrode (SHE) under 100 mW/cm^2 illumination (λ=505 nm). Photoelectrochemical and Mott-Schottky measurements (Fig. 3) reveal the layer with negative charge captured on the CZTS surface during removal of the ZnS secondary phase from the CZTS surface in HCl solution. The XRD, SEM and XPS measurements demonstrated the dissolution of copper sulfide in KCN solution, zinc sulfide in HCl solution and removal of thin layer of copper chloride during a short (10 s) additional treatment in KCN solution. The CZTS thin film has been synthesized on Mo foil by an electrochemical co-deposition of CuSn layer and next Zn layer followed by a sulphurization at temperature of 580 °C.

putinas.kalinauskas@ftmc.lt

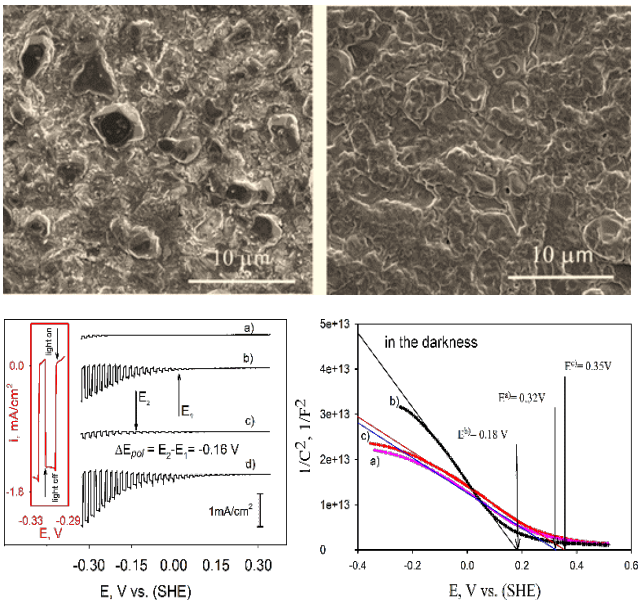

Fig. 3. (Top) SEM images. Cathodic photocurrent (bottom, left) and Mott-Schottky plots (bottom, right) of Cu_2ZnSnS_4 film.

Nanocrystalline WO_3 films for photoelectrochemical generation of reactive chlorine species

Conventional chlor-alkali method used for production of chlorine gas and chlorine-based disinfectants is among the most energy-intensive processes in chemical industry, therefore, more sustainable alternatives with lower carbon footprint are sought. Photoelectrochemical (PEC) generation of reactive chlorine species (Cl_2, HClO, ClO^-) is a promising technology in the area of water disinfection, as it combines the advantages of (i) using the renewable solar energy, (ii) possibility to produce disinfectants on-site and on-demand and (iii) eliminates the need for sophisticated infrastructure for storage and handling of hazardous chlorine species. In this study nanocrystalline WO_3 layers were formed using simple sol-gel synthesis and polyethylene glycol as a structure-directing agent. Faradaic efficiency of photoelectronchemical hypochlorite formation was ~30 %, and antimicrobial effect of PEC chlorination was demonstrated on Gram-positive *Bacillus sp.* and Gram-negative *E. coli* C41(DE3) bacteria. High bacteria-killing power of the investigated system was attributed to generation of highly reactive chlorine radicals as intermediates.

jurga.juodkazyte@ftmc.lt

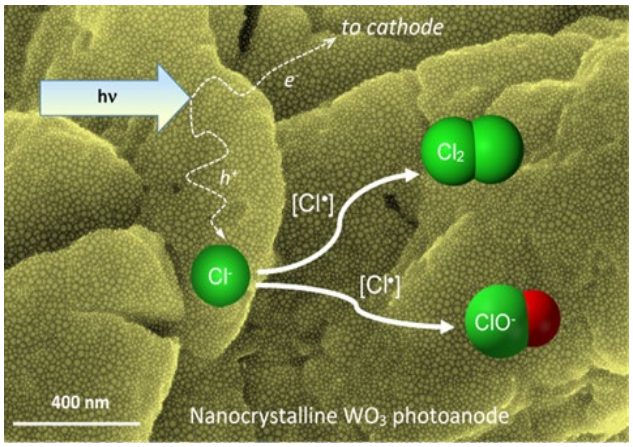

Fig. 4. Schematic representation of PEC formation of reactive chlorine species on nanocrystalline WO_3 photoanode.

Computational investigation of NASICON-structured $Na_xTi_2(PO_4)_3$ (x=1 – 4) compounds

Na Super Ionic Conductors (NASICON) phosphate framework compounds are a very attractive class of materials for their use as Na-ion battery electrodes. A series of NASICON-structured $Na_xTi_2(PO_4)_3$ (N_xTP) compounds corresponding to varying degrees of sodiation (x = 1–4) have been investigated using high-level hybrid density functional theory calculations and group theoretical symmetry considerations. The existence of mixed titanium oxidation states for x = 4 (Ti^{2+}/Ti^{3+}) and x =2 (Ti^{3+}/Ti^{4+}) and a single oxidation state for x = 1 (Ti^{4+}) and x = 3 (Ti^{3+}) has been shown. The results show a necessary set of symmetry reductions taking place due to the highest possible Na/VNa and Ti charge ordering with changing x. In addition, the existence of large differences between the origin and the size of the band gap was shown. The band gap changes from 4.05 eV 2p–3d gap in $Na_1Ti_2(PO_4)_3$ to 0.59 eV 3d–3d gap in $Na_4Ti_2(PO_4)_3$ with extra states due to mixed Ti valence. These results serve as an important electronic structure benchmark for further studies of such polyanion materials and help to explain some important properties of these systems relevant to battery applications.

linas.vilciauskas@ftmc.lt

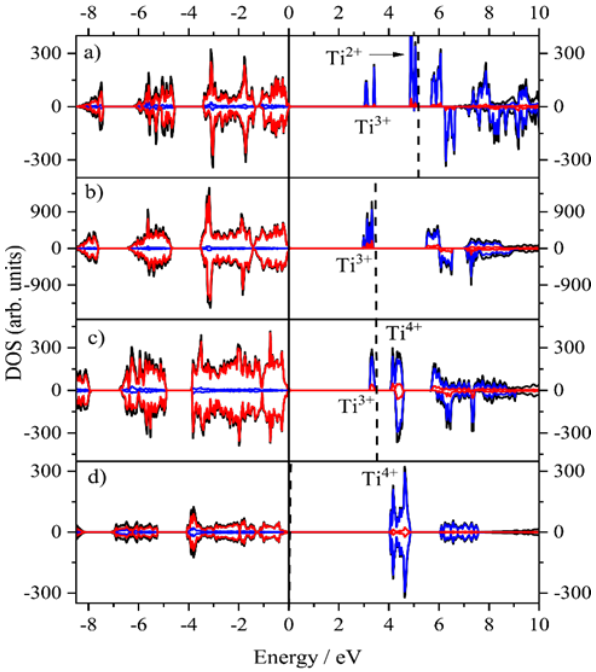

Fig. 5. Electronic Density of states (DOS) calculated with the B1WC functional for (a) N4TP, (b) N3TP, (c) N2TP, (d) N1TP. The top of O 2p band is taken as zero. Negative values represent spin-down electrons. Dash line shows the position of Fermi energy (black line: total DOS, red line: O, blue line: Ti).

Friction reduction using nanothin titanium layers on anodized aluminum as potential bioceramic material

Effective friction reduction by nanothin titanium layers on anodic coatings was revealed. The layers of Ti or TiO_2 were deposited at various thickness on anodized alumina using atomic layer deposition or sputtering. Under dry friction conditions, the nanolayers of 100 nm thickness assured low coefficient of friction on anodized alumina during early stages of mechanical contact. Tribological performance of nanothin layers was much better than that of thicker coatings or plain Ti alloys. The deposition with Ti made the surfaces biocompatible with periodontal ligament stem cells suggesting a variety of biomedical applications.

tadas.matijosius@ftmc.lt

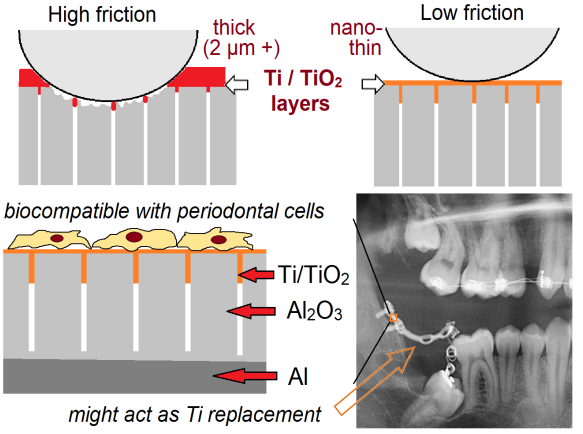

Fig. 6. Capability of nanothin layers of titanium or its oxides to dramatically reduce friction and impart biocompatibility to anodic coatings on aluminum.

MATERIALS FOR CATALYSIS

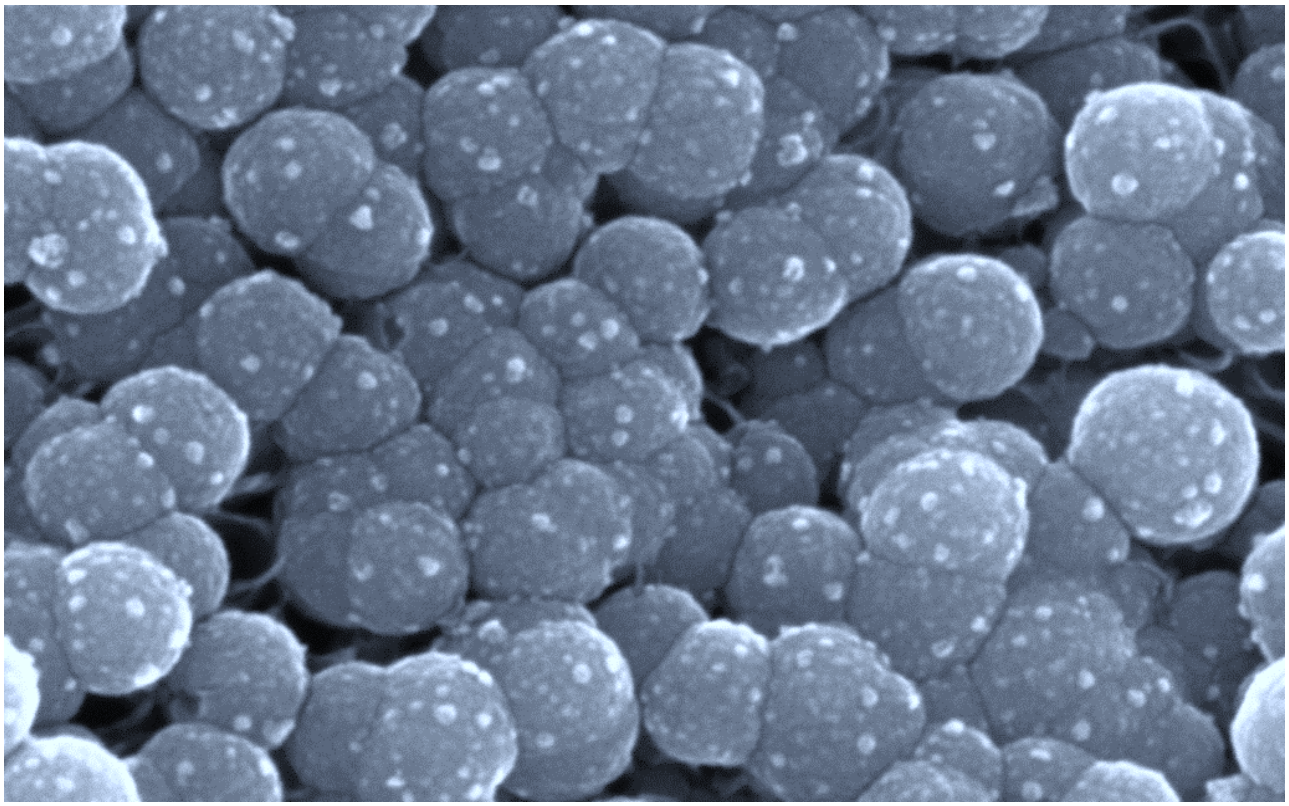

Electroless metal deposition: from fundamental research to application for microelectronics, fuel cells, and in other areas

Electroless metal plating is a well-known method for the deposition of metal coatings by a controlled chemical reduction and formation of small (nano-scale) metal particles. The autocatalytic metal ion reduction systems are widely used for decorative and functional purposes, i. e. for deposition of a conductive metal layer on dielectrics, semiconductors, or conductors with a complicated configuration without external current. The selection of suitable reducing agents and conditions of the reaction (temperature, concentration of the reacting substances, etc.) plays a very important role in creating stable solutions and obtaining coatings with required characteristics, such as purity and surface roughness. The use of conventional hydrogen-containing reducing agents is related to environmental and technological problems: (i) the plating bath cannot be recycled, i. e. the reducing agent oxidizes irreversibly; (ii) the plating rate and solution stability are not high enough. For these reasons, the search and investigations of the reducing agents of a new type, e. g. charge-transfer reducers, namely the different oxidation state metal-ion redox couples, are actual nowadays, and they are developed and applied in the Department of Catalysis. The main reducing agents used are Ti(III) and Co(II), which oxidize during the electroless plating processes to Ti(IV) and Co(III). An additional advantage of such systems, where no hydrogen is formed during the electroless plating process, is the possibility to reduce the oxidized form of the reducing agent to the initial state. The R&D activities of our Department in this area are focused on the development of new electroless metal plating processes as well as fundamental studies of reactions occurring in autocatalytic metal ions reduction systems employing electrochemical quartz crystal microgravimetry. The electroless metal plating method is also successively used for the fabrication of new catalytic materials for fuel cells. The non-noble metal and noble metal catalysts with a low amount of noble metal-supported titanium, titania nanotube arrayed surfaces, carbon, graphene powder, or other supports with enhanced activity towards the oxidation of various fuels, have been developed. The catalysts obtained are promising anode materials and can be used in the practical fuel cells.

Development of catalysts for hydrogen generation

With traditional energy resources decreasing, a search for alternative energy sources is becoming more and more active. As fuel cells are environmentally friendly energy sources, they are intensively investigated as generators of cleaner power compared to fossil fuel-based technologies. Consequently, fuel cells can successfully change the traditional energy resources. Hydrogen is considered an eco-friendly and alternative energy source able to replace all non-renewable energy sources. Herein, we use a simple method for the fabrication of efficient Co-based catalysts for the hydrolysis of sodium borohydride ($NaBH_4$). Effective Co/Cu, CoB/Cu, and CoBM/Cu (M = Mo, Zn, Fe) catalysts have been prepared by a simple electroless deposition method using a morpholine borane as a reducing agent in the glycine solution. The activity of the prepared catalysts has been investigated for hydrogen generation from an alkaline $NaBH_4$ solution. It was determined that these synthesized catalysts demonstrate the catalytic activity for the hydrolysis reaction of $NaBH_4$. The lowest obtained activation energy of the hydrolysis reaction of $NaBH_4$ was 27 kJ mol^{-1} for the CoBMo/Cu catalyst which forms the hierarchical cauliflower-shaped 3D structures and high roughness surface area (Fig. 1). Moreover, the CoBMo/Cu catalyst retains

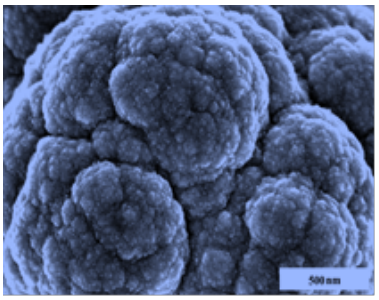

Fig. 1. SEM image of the CoBMo/Cu catalyst.

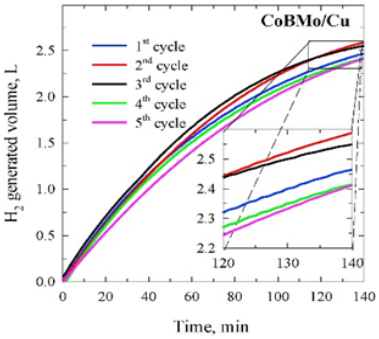

Fig. 2. Reusability tests of H_2 generation from 15ml 5 wt.% $NaBH_4$+0.4wt.% NaOH catalyzed by the CoBMo/Cu catalyst at 323 K over five runs.

98% of its initial catalytic activity in the hydrolysis of $NaBH_4$ in the fifth run, indicating excellent reusability (Fig. 2).

zita.sukackiene@ftmc.lt

Highly active wood-derived nitrogen-doped carbon catalyst for the oxygen reduction reaction

The number of studies dedicated to renewable energy conversion and storage devices, such as batteries, fuel cells, and photovoltaic systems has gained utmost importance as pollution levels, caused by large-scale consumption of fossil fuels, have continued to rise year by year. The interest has risen to develop the metal-free and cheap, biomass-derived electrocatalysts for oxygen reduction reaction (ORR). Herein, we report a facile strategy to synthesize a cheap and electrochemically active nanocarbon material from the renewable and biological resource, wood biomass. Carbonaceous materials have been obtained by thermochemical activation with NaOH followed by doping with nitrogen using dicyandiamide (DCDA). It was found that the wood-derived N-doped carbon exhibits an irregular granular structure: it consists of mostly amorphous carbon with a rough surface structure (Fig. 3a, c), but at the same time, some parts of the catalyst show the typical structure of nanoplatelets (Fig. 3b). TEM analysis shows that the material consists of graphitic lattice fringes (Fig. 4b) and areas of amorphous carbon with a porous structure (Fig. 4c, d). The thickness of the 10x layered catalyst particle is 3.55 nm, and the interlayer spacing between the two layers is ~0.35 nm. Likewise, the interlayer spacing of a few-layered graphene is also close to 0.35 nm, revealing that some parts of the catalyst possess a graphene-like structure. The activity of materials has been evaluated for ORR using the rotating disk electrode (RDE) (Fig. 5). Compared to the most commonly used commercial carbon XC 72R, the synthesized wood-derived N-doped carbon exhibits remarkably improved electrocatalytic ORR activity. It shows an onset potential of 0.92 V vs RHE and a half-wave potential of 0.85 V vs RHE in an alkaline

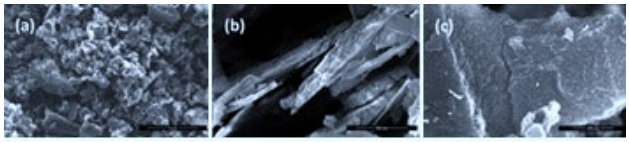

Fig. 3. (a–c) SEM images of wood-derived N-doped carbon.

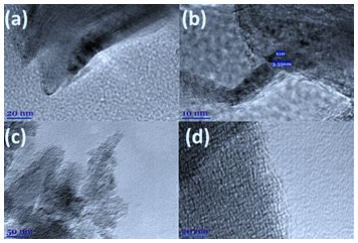

Fig. 4. (a–d) TEM images of wood-derived N-doped carbon.

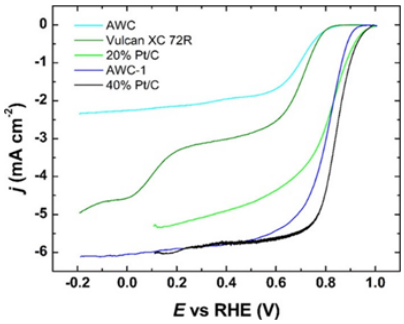

Fig. 5. RDE voltammetry curves for oxygen reduction on GC electrodes modified with different catalyst materials in O_2-saturated 0.1 M KOH. Here v = 10 mV s^{-1}, ω = 1900 rpm.

medium in addition to improved stability compared to commercial Pt/C. The results of this study demonstrate that nitrogen-doped activated carbons based on biomass are promising alternative materials to state-of-the-art precious-metal-based catalysts and may be an excellent catalyst carrier for many other applications.

loreta.tamasauskaite@ftmc.lt

ENVIRONMENT

Sustainable technologies for observation, simulation, prevention and mitigation of climate change and atmospheric pollution

Poor air quality and climate change are closely linked. Reducing air pollution from human activity sources helps to improve air quality and address climate change in a more integrated way. The European Green Deal is at the heart of European efforts to achieve sustainability. A modern environmental research relies on solutions that bring together recent achievements in technologies and sciences that underpin our understanding of the Nature to deliver a sustainable environmental future, economic growth and greater well-being. In the Department of Environmental Research the main focus is directed towards the investigations of impact of changing atmospheric composition on air quality, climate change and ecosystems. By conducting the fundamental and applied research, we are aiming to find long-term solutions, especially in experimental techniques, devoted to develop and apply the methods of mass and size spectrometry, spectroscopy, stable isotope analysis and chromatography which determine the dynamics, balance and sources of atmospheric compounds in environmental components. Objectives: To develop and improve principles, means and technologies of the environment quality evaluation and ensure the scientific competence in the fields of environmental physics and chemistry, by understanding the key factors influencing the climate change and air quality. Tasks: Development of technologies, modeling approaches and equipment for the environment protection quality control as well as methods and experimental basis for the investigation of micro impurities dynamics and balance in the environment components by evaluating the impact on climate change given by transformation, composition, formation, evolutionary processes of atmospheric chemical compounds. The Department is engaged in a police-making activity, the creation of the taxonomy, a world's first-ever classification system proposed by the EU Commission in accordance with the EU sustainability-related policy objectives. Also, the Department is working on preparation of the EU emission inventory report under the UNECE Convention on Long-range Transboundary Air Pollution (LRTAP) and GHG emissions under United Nations Climate Change Convention (UNFCCC).

Identification of wintertime carbonaceous fine particulate matter (PM2.5) sources in Kaunas, Lithuania using polycyclic aromatic hydrocarbons and stable carbon isotope analysis

The study aimed at demonstrating the application of polycyclic aromatic hydrocarbons (PAHs) and $\delta^{13}C$ measurements to resolve airborne carbonaceous particle sources in wintertime. Six residential dwellings (Fig. 1) were selected at urban and suburban locations to evaluate the indoor-outdoor characteristics of carbonaceous particulate matter (PM) in Kaunas, Lithuania during January and March 2013. Total carbon (TC) concentration was mostly higher in outdoor samples compared to the indoor ones: the TC concentrations in winter measurement campaign ranged from 8.6 to 78.5 μg/m^3 outdoors and from 1.5 to 40.9 μg/m^3 indoors.

Based on I/O ratios of $PM_{2.5}$ (TC) we conclude that in most cases indoor sources had a limited effect on indoor $PM_{2.5}$ (TC) concentration. On the other hand, I/O ratios of individual PAHs were found to be often >1, indicating contributions from indoor sources. Results of our investigation demonstrate that I/O ratios of PAHs are sensitive indicator for general indoor pollution sources.

The simultaneous stable carbon isotope ratio and PAHs diagnostic ratio analysis enabled to identify main anthropogenic sources (traffic, biomass burning and coal combustion) of $PM_{2.5}$. A comparison of the stable carbon isotope ratio and PAHs diagnostic ratios of $PM_{2.5}$ (TC) outdoors revealed significant contribution from solid fuel combustion (mainly biomass) and local traffic. The $\delta^{13}C$ ratio of TC was different in indoor and outdoor environment. The reason for the difference most likely was the presence of additional aerosol source (cooking or cleaning agents) indoors as it significantly altered the measured isotope ratios. Indoor aerosol particles were characterized by larger particles sizes (0.60–0.94 μm), than the outdoor (0.32–0.56 μm) (see Fig.2). Size segregated indoor aerosol particles were mostly depleted in 13C comparing to the outdoor PM. This finding supports the existence of distinct indoor TC sources. It is likely that the size-segregated TC in indoor air was produced by primary combustion processes (fireplace, wood-fired boilers and cooking) or originated from the secondary aerosol formation of volatile organic compounds emitted from the indoor activities (cooking, building materials, cleaning substances, etc).

inga.garbariene@ftmc.lt

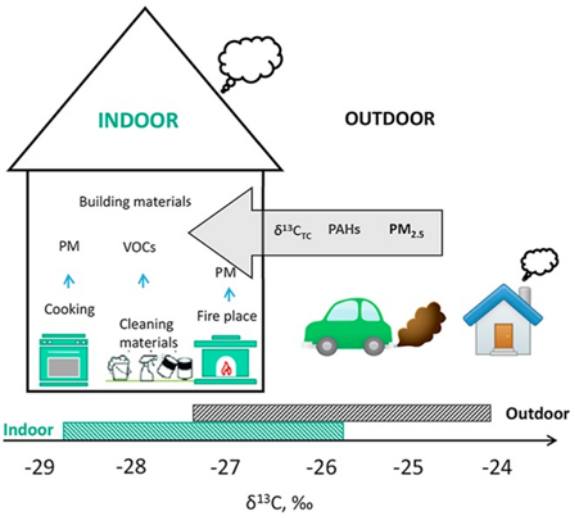

Fig. 1. Schematics of residential dwellings and $\delta^{13}C$%.

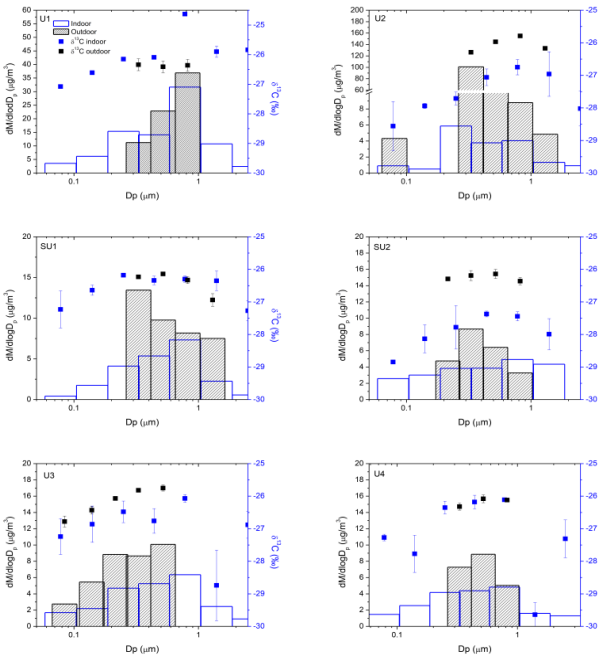

Fig. 2. Averaged outdoor/indoor TC mass size distribution and isotopic composition for each site.

NUCLEAR

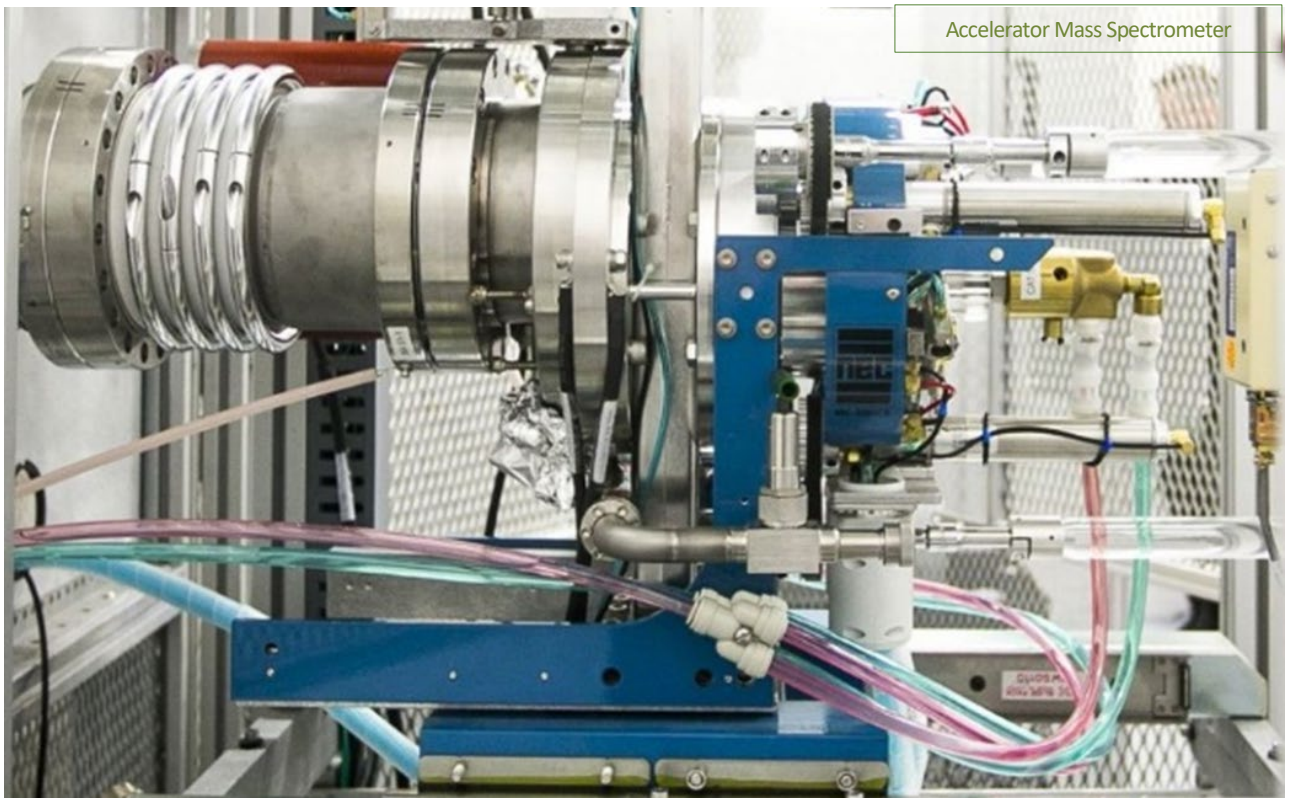

Accelerator Mass Spectrometer

Nuclear research for applications today and innovative technologies for future

The Department of Nuclear Research applies known and develops innovative technologies and methods in the fields of experimental nuclear spectroscopy, nuclear energy safety, radiation protection, radiochemistry, mass spectroscopy, Mössbauer spectroscopy, ion beam analysis and material modification. The pillars of the safety field are the safe operation assurance of nuclear facilities, the optimization of radioactive waste management, the assessment of shielding materials, and the comprehension of processes of radionuclides transport through engineering barriers to enable nuclear facility safety. These activities are implemented both in Lithuania for Ignalina NPP decommissioning/ waste management purposes, in the European Union participating in commercial tenders, and in HORIZON 2020 projects as European Joint Programme on Radioactive Waste Management (EURAD) and the Pre-Disposal Management of Radioactive Waste (PREDIS) devoted to obtain the know-how required to implement safe pre-disposal and long-term management of radioactive waste. Special attention in the department is paid to environmental impact assessment of energy generating facilities, elemental and isotopic analysis of groundwater, food fabrics and products and also industrial stocks, medical samples with sensitivity up to 1 ppq (for non-interfered isotopes). Application of stable isotope ratio analysis ($\delta^{13}C$, $\delta^{15}N$, $\delta^{18}O$ and $\delta^{34}S$) in environmental, biomedical and food samples stimulates new promising technologies. ^{14}C measurements open the potentially new field of activity related to carbon dating and analysis of triple carbon ratio for dedicated samples. The new innovative and intelligent pollution assessment methods and tools are being developed for the technological pollution reduction. Complementary information on material properties (magnetic properties, oxidation and corrosion of iron compounds) is determined by Mössbauer spectroscopy. Development of ion beam methods for material analysis and modification is important part of our activities having intersection both with semiconductor materials and applications for lasers. Investigation of organic scintillator films opens new possibilities for their application for detection and spectroscopy of ionizing radiation particles. The principles of the high energy electromagnetic radiation generation are investigated using ultrashort laser pulses, taking into account their practical application in future.

Environmental impact assessment of energy generating facilities by investigating vertical distribution of radiocarbon in the bottom sediment core of the cooling lake

The vertical distribution of radiocarbon ^{14}C was examined in the bottom sediment core, taken from Lake Drūkšiai, which has served for 26 years as a cooling pond since 1983 of the Ignalina Nuclear Power Plant (INPP) operation using two RBMK-1500 reactors. ^{14}C specific activity was measured in alkali-soluble and -insoluble fractions of the sediment layers. In addition, ^{14}C distribution was examined in the scales of pelagic fish caught between 1980 and 2012. Our measurements reveal that, during the period 1947–1999, the radiocarbon specific activity in both fractions exhibits a parallel course with a difference of 5 ± 1 pMC (percent of modern carbon) being higher in alkali-soluble fraction, although ^{14}C specific activity in both fractions increased by 11.4–13.6 pMC during the first 15 years of the plant operation. However, during the 2000–2009 period, other than previously seen, a dissolved inorganic carbon (DIC) → aquatic primary producers → sediments ^{14}C incorporation pattern occurred, as the radiocarbon specific activity difference between alkali-soluble and -insoluble fractions reached 94, 25, and 20 pMC in 2000, 2006, and 2008, respectively. Measurements in different sediment fractions allowed us to identify the unexpected organic nature of ^{14}C contained in liquid effluences from the INPP in 2000–2009. The discrepancy between ^{14}C specific activity in fish scales samples and DIC after 2000 also confirmed the possibility of organic ^{14}C contamination. Possible reasons for this phenomenon might be industrial processes introduced at the INPP, such as the start of operation of the cementation facility for spent ion exchange resins, decontamination procedures, and various maintenance activities of reactor aging systems and equipment.

ruta.bariseviciute@ftmc.lt

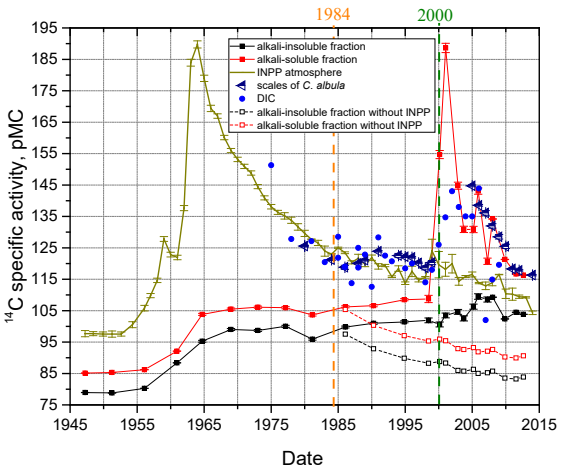

Fig. 1. ^{14}C specific activity in the alkali-soluble and -insoluble sediment fractions, in the planktivorous vendace (*C. albula*) scales in DIC, as well as radiocarbon specific activity that would have occurred without INPP impact.

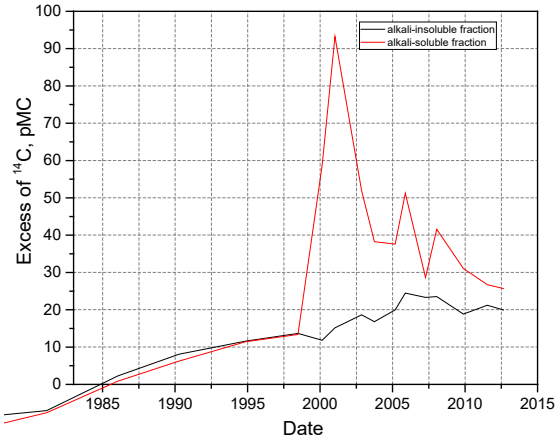

Fig. 2. Evaluated INPP impact in terms of excess of ^{14}C specific activity in the alkali-soluble and -insoluble sedimentary organic fractions.

Application of stable isotope ratio analysis: seasonal changes of sources and volatility of carbonaceous aerosol at urban, coastal and forest sites in Lithuania

The stable carbon isotopic composition of fine aerosol particles collected during summer and early fall at urban, coastal and forest sites in Lithuania is investigated to find out the seasonal changes of sources and volatility of carbonaceous aerosol. By studying $\delta^{13}C$ values in different volatility fractions of the organic aerosol, we gain insight into formation and aging mechanisms of the organic aerosol. Isotopic composition shows seasonal difference - aerosol is clearly enriched in ^{13}C in winter samples compared to summer samples. Organic carbon (OC) is mostly primary in winter (biomass burning) at the urban site, whereas in summer the photochemical processing is active, thus changing the OC properties at the urban scale.

agne.masalaite@ftmc.lt

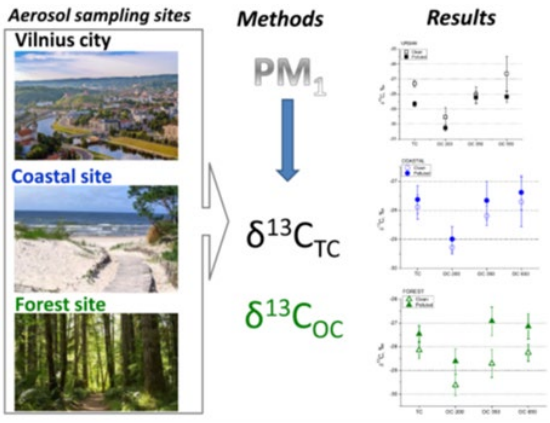

Fig. 3. Particulate matter of aerosol particles, PM1, were investigated in three locations using isotope ratio mass spectrometry.

Application of stable isotope ratio analysis: suppression of phase transitions and glass phase signatures in mixed cation halide perovskites

Cation engineering provides a route to control the structure and properties of hybrid halide perovskites, which has resulted in the highest performance solar cells based on mixtures of Cs, methylammonium, and formamidinium. A multi-technique experimental and theoretical study of structural phase transitions, structural phases and dipolar dynamics in the mixed methylammonium/dimethylammonium $MA_{1-x}DMA_xPbBr_3$ hybrid perovskites is presented. Results demonstrate a significant suppression of the structural phase transitions, enhanced disorder and stabilization of the cubic phase even for a small amount of DMA cations (Fig. 4). As the DMA concentration approaches the solubility limit in $MAPbBr_3$, we observe the disappearance of the structural phase transitions and indications of a glassy dipolar phase. The summary of experimental results is presented in Fig. 5. The bluish part of the phase diagram marks the glassy behavior of the electric dipoles.

andrius.garbaras@ftmc.lt

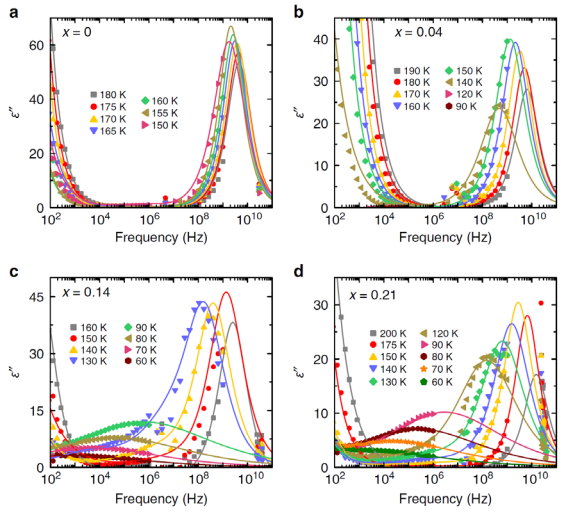

Fig. 4. Frequency dependent dielectric permittivity of mixed $MA_{1-x}DMA_xPbBr_3$ perovskites.

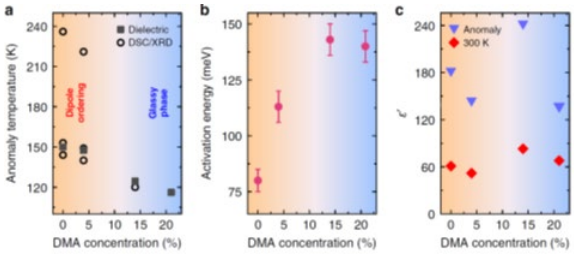

Fig. 5. DMA concentration dependence of (a) phase transition temperatures, (b) activation energy of molecular cation motion and (c) dielectric permittivity at the anomaly (129 Hz) and 300 K (1 MHz).

Application of stable isotope ratio analysis: long-term changes in trophic ecology of blue mussels in a rapidly changing ecosystem

By studying stable isotopes ($\delta^{13}C$, $\delta^{15}N$) it is possible to trace energy and nutrient flows in archived samples of blue mussel (*Mytilus edulis trossulus*) spanning 24 years (1993–2016). We found decreasing trends in $\delta^{13}C$ and $\delta^{15}N$ as well as in mean size and total biomass of mussels, but no unidirectional changes in their stoichiometry or condition index. Changes in isotope composition were best explained by nitrogen-fixing cyano-bacteria and increased terrestrial organic carbon from land runoff (reflecting precipitation). It was revealed that altered trophic relationships from climate-induced changes in the productivity base may strongly impact keystone species, with potential knock-on effects on ecosystem functions.

andrius.garbaras@ftmc.lt

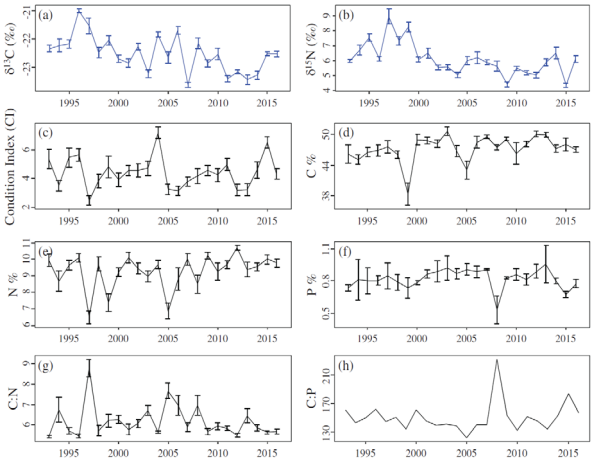

Fig. 6. Time series for *Mytilus* proxies (annual mean values and standard error). Here n = 15 to 20 individuals per year for (a) $\delta^{13}C$, (b) $\delta^{15}N$, (c) condition index (CI), (d) C%, (e) N% and (g) C : N ratios and (j) Bayesian standard ellipse area (i.e., trophic niche of population, SEA_B, plain line). n = 3 for (f) P% data and (h) related ratios C : P at Isskären (Baltic Sea).

Advanced technologies for graphite radioactive waste characterization

A method to identify neutron activation and surface contamination terms for the spent graphite waste was introduced by using RBMK-1500 graphite modeling and analysis of nuclear spectrometry results. The simplified model of the reactor core (SCALE 6.2 for 4×4 fragment of the core (Fig. 7) was used for simulation of neutron activation of graphite impurities in the RBMK-1500 reactor. Calculations were supplemented by the non-destructive measurements of gamma-ray emitting nuclides and destructive analysis of selected samples of the graphite stack of Ignalina NPP Unit 1 reactor. Analysis demonstrates that the partial contribution of different contamination sources can be identified by combining modeling and measurements. The scheme of the method includes three steps: calculation of neutron activation (including fission of actinides present as impurity in graphite); comparative analysis with measured activity values; evaluation of the excess activity in the graphite. The U impurity concentration is directly proportional to concentration of sum activity of ^{239}Pu and ^{240}Pu, which is measured by destructive alpha analysis. The experimental and simulated values of ^{137}Cs generated from U impurity in the graphite stack are provided in Fig.8. According to measured content of Cs isotopes (the proportion of Cs is estimated by the presence of actinide in the graphite), the contamination term caused by transport of volatile Cs could be determined in the graphite components.

rita.plukiene@ftmc.lt

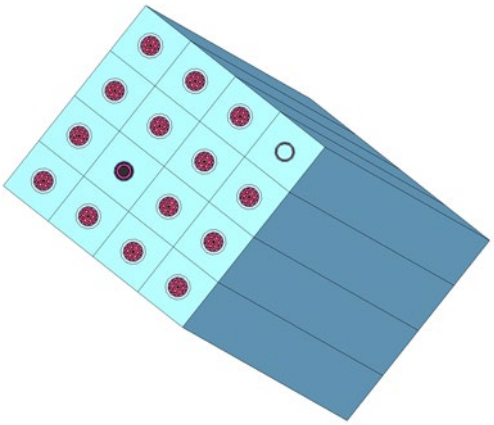

Fig. 7. The 3D model (SCALE6) of reactor 4×4 fragment.

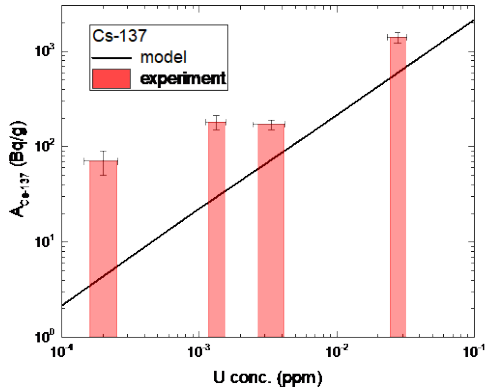

Fig. 8. Experimental and simulated values of fission product ^{137}Cs generated from U impurities in the graphite stack.

Mössbauer spectroscopy for investigation of inorganic material: synthesis, structural, magnetic, mechanical and biological properties of Fe and Zn co-substituted beta-tricalcium phosphate (β-TCP)

Calcium phosphates are significant inorganic part of bones and teeth. Doping with biologically active Fe and other elements improves their properties and modifies synthesis conditions. Beta-tricalcium phosphate bioceramics synthesized by wet co-precipitation method is suitable for application in medicine for regeneration of bone tissues. The XRD and EPR data has showed that Fe occupies the same crystalline positions. Mainly, the slow relaxation paramagnetic state of Fe was observed by Mössbauer spectroscopy indicating even distribution (large Fe-Fe distances) of iron in beta-tricalcium phosphate. Mössbauer spectroscopy allowed to determine the Fe state in detail which is impossible by other methods, especially at low Fe doping levels of ceramics. Magnetization data was also in accordance with the paramagnetic Fe state.

kestutis.mazeika@ftmc.lt

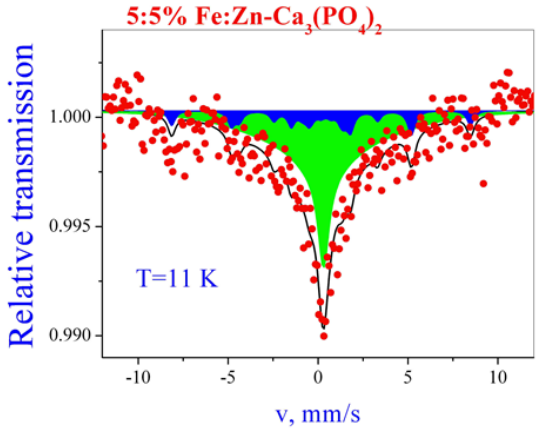

Fig. 9. Mössbauer spectrum of doped 5:5% Fe:Zn tricalcium phosphate at 11 K temperature showing slow paramagnetic relaxation of Fe spins resulting in splitted hyperfine structure of spectrum.

TEXTILE TECHNOLOGIES


photo Happeak & serge gandzumian

Green deal in textile

The activities of the FTMC Textile Departments in 2020 were strongly focused on the Green Deal Concept targeted to encourage the textile industry to adopt environmentally friendly practices. International project (EUREKA) *Eco Design Casual Garments from Biodegradable and Natural Fibers Based on the Principles of the Circular Economy* was launched in 2020. Our scientists develop fabrics from biodegradable, such as plant-derived thermoplastic polylactic acid, naturally organic wool, and hemp fibres which will be offered as an alternative to the currently widely used synthetics. Environmentally friendly organic chemicals are used for innovative finishing of the fabrics as well. Industry partners from Lithuania *MB Grata forma* and partners from The Netherlands take part in this project aimed to develop sustainable, eco-design fashion garments which, at the end of their life cycle, could be fully recycled or composted, thus contributing to a sustainable environment. Following Green Deal Strategy and moving further towards sustainable textile manufacturing processes, the FTMC as R&D partner joined the project initiated by JSC *Nova Fabrica* (program Experiment). More energy-efficient and environmentally friendly solutions for finishing processes in textile will be developed by investigating and adapting a linear non-thermal plasma source created by the industry partner. The development of a smart personal protective equipment and investigation of thermoregulation properties remain at the core of the research of the Textile Departments. The project *Strengthening of The Researcher's Interdisciplinary Competences Directing Them toward the Development of Smart Protective Textile Products* is ongoing, and prototype of a smart garment, protecting against ballistic impact with integrated active temperature control system and EMR shielding properties, is under the development. Three national industrial companies already showed their interest to use the results of this project. The ACAMSII project funded by European Defence Agency (EDA) is continued as well. Several active and passive adaptation mechanisms were integrated into a textile-based soldier camouflage system. Most of research studies of the FTMC Textile Departments are dedicated for industry needs. Even certification services because of Covid-19 pandemic have found its place in our activity range.

Experimental and theoretical investigation of thermal properties of spacer fabrics with phase changing material

To validate the obtained experimental results, we used the developed computational finite element (FE) model for transient heat transfer analysis in fabrics with environment-friendly phase changing material (PCM) butyl stearate. Its melting/heating absorption occurs at temperature range from 19°C to 34°C, and the solidification/heat release is visible at temperature range from 34°C to 19°C. The combined differential scanning calorimetry (DSC) and FE simulation-based analysis was used to study the validity of the material sample dimensions for effective heat capacity in temperature measurements. A similar computational procedure enabled to estimate the relationship between the effective latent specific heat and the PCM coating. For validation of the developed computational model, the infrared radiation (IR) heating-cooling experiments on fabrics with different deposits of the PCM were performed (Fig. 1). The internal space of the crucible in which the material sample is loaded was similar to a cylindrical cell as shown in Figs. 2(a) and (b). The noticeable influence of the PCM content on the transient thermal behavior during heating-cooling cycles was determined. The experimental results have been compared with the results of the FE model simulation. The values of the latent heat during melting and solidification were obtained as integrals, which correspond to hatched areas in Fig. 2(c). In Fig. 2(d) it is demonstrated that certain geometries and temperature change rates may appear inappropriate for the DSC measurements.

audrone.sankauskaite@ftmc.lt

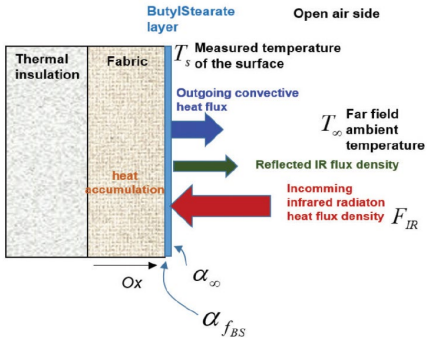

Fig. 1. Computational model for investigation of thermal properties of the fabric coated by the butyl stearate PCM layer in case of IR heating.

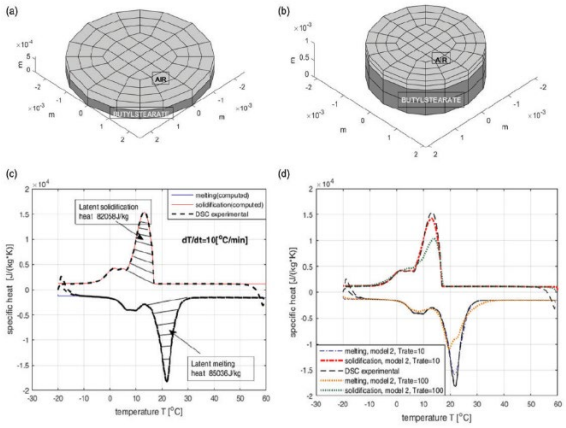

Fig. 2. Evaluated INPP impact in terms of excess of ^{14}C specific activity in the alkali-soluble and -insoluble sedimentary organic fractions.

Investigation of thermoregulation properties of various ceramic-containing knitted fabric structures

Thermophysiological comfort helps the body to retain heat balance while resting or at various levels of physical activities. To ensure the thermal comfort during high physical activity, the clothes must have good thermoregulation properties. Textile containing ceramic additives, which are able to absorb and emit back the thermal energy from the human body, can be used to improve the thermal properties of the fabric. The thermal efficiency of the manufactured knits was characterised by the dynamics of accumulated/released heat generated by IR rays and expressed as achieved steady-state surface temperature while and after the heating (Figs. 3 and 4). The dynamic thermal IR absorbing/releasing capabilities of knitted fabrics depend not only on the amount of bio-ceramic additives in the inner layer, contacting the skin directly, but also on the total quantity of ceramic additives in the fabric. Thermal resistance and liquid moisture management properties were investigated during the research as well. It was determined that heat accumulation is directly related to the calculated quantity of bio-ceramic additives in the knits. The obvious correlation between accumulated/released heat, thermal resistance, and the quantity of bio-ceramic additives in all investigated knitted structures was also investigated. Taking into account all the results of the thermoregulation properties, the optimal ceramic-containing knitted structure comfortable for wearing next to the skin in cold weather, was selected.

laimute.stygiene@ftmc.lt

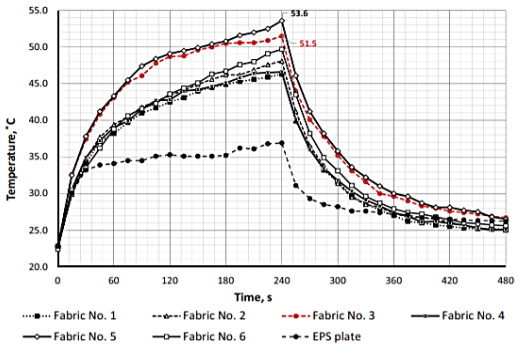

Fig. 3. Dynamic curves of accumulated/released heat in knitted fabrics (before and after IR irradiation by 250W IR lamp).

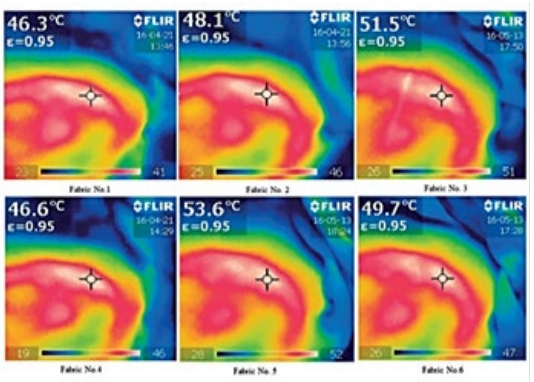

Fig. 4. Thermograms with measured temperatures of all investigated knitted fabrics, recorded using thermal imaging camera (IR exposure time 240s).

METROLOGY

National Metrology Institute of Lithuania

We can do anything we want with numbers and this is why metrology is here to add coherence and sense.

FTMC Metrology Department was authorized to perform and implement functions of the National Metrology Institute (NMI) since 1 July 2014. The year 2019 was historical for all metrology community and scientists all over the world - the new definitions of the *kilogram*, the *ampere*, the *kelvin* and the *mole*, the units of the International System of Units (SI) came into force on 20 May, as a decision of the 26th General Conference on Weights and Measures.

Lithuanian NMI was internationally recognized among associate and member countries of The Metre Convention (*Convention du Mètre*). Metrology Department has implemented and peer-reviewed QMS fulfilling the requirements of ISO/IEC 17025 standard which is recognized by EURAMET. This year Lithuanian NMI became one of seven NMIs of Nordic-Baltic countries which established European Metrology Network (EMN) *Smart Specialisation in Northern Europe*, strengthening a regional cooperation between the NMIs of the region and looking forward to a new *European Partnership on Metrology* - the program for research and innovation in metrology under the Horizon Europe 2021-2027.

FTMC Metrology Department maintains national standards in seven areas of measurements. **Time and Frequency Standard Laboratory (TFSL)** is reproducing the value of the unit of time, the second (*s*), and the unit of frequency, the hertz (*Hz*). The mission of TFSL is to represent Lithuanian Coordinated Universal Time UTC(LT), ensuring the traceability of the magnitudes reproduced to the International System of Units (SI), their dissemination to Lithuanian scientific establishments, personal and legal bodies by calibrating their working standards and measurement devices, dissemination of Lithuanian time scale, and other relevant means. The TFSL in cooperation with the *JSC BaltStamp* provides qualified time stamping services, which meet the eIDAS regulations and the ETSI standards. The time stamping service issues up to two million time stamps per month for Lithuanian government organisations and European users.

The mission of the **Electrical Standards Laboratory** is maintaining and developing the standards of unit of voltage, the volt (*V*), and unit of resistance, the ohm (*Ω*), ensuring their traceability to the SI system, calibrating working standards and measurement devices, pursuing research in the field of voltage, resistance and electrical current measurement.

The mission of the **Temperature Unit Standard Laboratory** is to realize the international temperature scale ITS-90 and the value of the unit of temperature, the kelvin (*K*), ensuring their traceability to SI system. Lithuanian National Standard of the temperature unit (in the range from -195°C to +961,78 °C) is of a primary level and the reference freezing point of Cu (+1084,62 °C) is of a secondary level.

The Government of the Republic of Lithuania transferred the **National Standards of Mass and Length** Laboratory (NSMLL) to FTMC in 2019. The mission of the national gauge blocks standard is maintaining and transferring length unit (in the range from 0,5 mm to 100 mm with 0,0001 mm uncertainty) ensuring its metrological traceability to the SI system. The mission of the national mass unit standard is maintaining and developing the standards of mass unit ensuring the traceability to the SI system in the range from 1 mg to 20 kg with uncertainty from 0,4 mg to 3,2 mg. Reference equipment of NSMLL can also measure the magnetic properties and density of weights.

Metrology is not restricted only to the standards of physical units. The reliable, traceable and accurate chemical measurements in different sectors of health care, safety and environment protection could be provided by the **Laboratory for Metrology in Chemistry (LMC)**. In 2020 LMC provided more than 350 different chemical measurements for the customers. This year LMC has started a new research project and finalized the ALCOREF Project *Certified forensic alcohol reference materials* in the frame of European Metrology Programme for Innovation and Research (EMPIR). The consortium of ten partner countries was formed with the coordination of Federal Institute for Materials Research and Testing in Germany. The main objective of the project is a development of a new regional metrological capacity for certification of certified reference material (CRM) for breath alcohol control.

The **Ionizing Radiation Metrology Laboratory (IRML)** participated in the interlaboratory comparisons *World-wide proficiency test on determination of anthropogenic and natural radionuclides in water, fish and simulated aerosol filter samples* organized by International Atomic Energy Agency. The calibrations, ensuring traceability to the National Standard of Ra-223, Tc-99m and I-131, were carried out for Lithuanian hospitals and other customers, Ignalina Nuclear Power Plant (under decommissioning now) in particular. In 2020 the IRML organized the intercomparison for local laboratories of gamma-ray emitters and low-activity measurement in water.

Radiological characterization of graphite from RBMK-1500 nuclear reactor

The radiological characterization of graphite from RBMK-1500 nuclear reactor was carried out by modeling and experimental methods. The activities of gamma-ray emitters (^{60}Co, ^{134}Cs, ^{137}Cs, ^{154}Eu) and pure beta-ray emitters (^{14}C, ^{36}Cl) were determined. Radionuclide activity measurements were traceable to national primary and secondary standards maintained by the FTMC Ionizing Radiation Metrology Laboratory.

arunas.gudelis@ftmc.lt

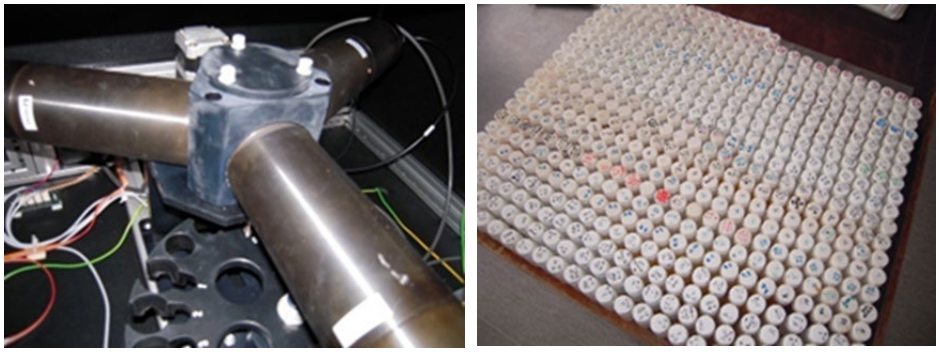

Fig. 1. (Left) The Triple-to-Double Coincidence Ratio system, a primary standard for pure beta- and electron-capture radionuclide stan-dardization. (Right The samples prepared for liquid scintillation counting.

OPEN ACCESS FACILITIES

Electron microscopy, X-ray spectroscopy and XRD open-access center (OAC)


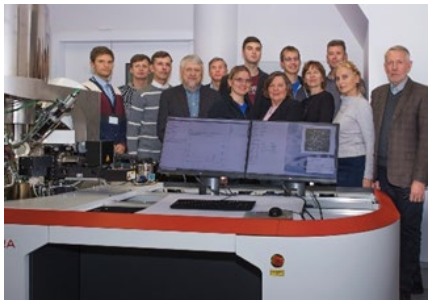
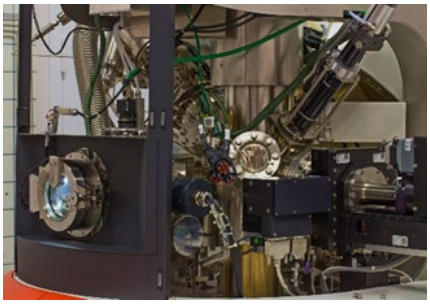

OAC offers open access facilities for characterisation of solid material surface structure, morphology, inner and crystalline structure, chemical and phase composition. The OAC infrastructure has been improved significantly during last 10 years, and now is equipped with modern electron microscopes (FE-SEM-FIB and TEM), X-ray diffractometers, X-ray fluorescence (WD-XRF), X-ray photoelectron (XPS) and Auger electron spectrometers. The OAC provides characterisation services of solid materials for customers from academic institutions and industry in Lithuania and abroad. Among the customers, there are universities of Southampton, Hoseo (South Korea), Riga, Vilnius and Kaunas. OAC provided structure characterisation services for such companies as Translucent Inc (from Palo Alto), IQE (North Carolina), Brolis Semiconductor, Altechna, Optolita and many others. For more information, please visit https://litexbeam.ftmc.lt.

Prototype formation and integration

Clean room technology for prototyping of semiconductor-based devices

Based on a collaboration between the Departments for Physical Technologies and Optoelectronics, a complete cycle of the clean room (CR) micro-processing line has started to function. It is ready to produce the working models and the demonstration prototypes of chemical and photo-sensitive devices as single units and as limited batches of products. The prototyping of innovative devices is based on a few key enabling technologies including the PECVD/CVD for the synthesis of 2D materials, namely graphene and MoS2, multi-mode magnetron sputtering for deposition of multicomponent functional films and molecule beam epitaxy for GaAs based optoelectronic devices.

The CR services include: 1) CR (ISO7–ISO5 about 300 m^2) operations, 2) photolithography, 3) laser lithography, 4) wet chemical processing, 5) thermal processing, 6) metal and oxide coatings, 7) assemblage and testing.

Characterisation and testing of prototypes

The R&D projects in the OAC can range from proof of concepts (TRL – Technological Readiness Level- 3), validation of technologies in the laboratory (TRL 4) or relevant environment (TRL 5),

and up to demonstration in a relevant environment (TRL 6). In specific cases, collaboration can reach prototyping in an operational environment (TRL 7). For this, we use the methods acceptable to characterise the components and devices at the nanometre scale level and the level of the complete unit.

The characterization includes: 1) topography, force spectroscopy, tunnelling current spectroscopy by scanning probe microscopy, 2) standard I-V and C-V characteristics in the dc- and ac-modes by the probe station, 3) photovoltaic parameters with the A1.5 solar source by special set-up, 4) gas response in the synthetic atmosphere under strictly controlled conditions by gas flow control system. We also carry out special set of tests to determine the response and resistivity to the microwave irradiation.

BALTFAB processing technologies

is a joint open user facility between departments of Laser technologies and Nanoengineering, offering a full range of nano/micro and macro fabrication as well as laser patterning, marking and cutting on any required material. State of the art laser microfabrication workstations are equipped with full variety of industrial ns-, ps- and fs- lasers. The BALTFAB team include experts to set-up, test and develop laser micro-machining processes and systems. Soft nano-lithography tools for rapid creation of nano-structures are tested to be live cell compatible. The patterns are routinely applied to improve the bio-compatibility of medical devices. The team is developing tools for detection of molecules on surfaces, to fasten the testing and evaluation of cells or drugs. More: see www.baltfab.com

Services include: 1) Laser processing: in-Glass marking; laser beam interference ablation; laser direct writing; ultrashort pulse

laser ablation. 2) Molecular: dip pen nanolithography; microcontact printing; piezoelectric inkjet printing; colloidal nanolithography. 3) Analytical: bio AFM; electrochemical sensors; imaging surface plasmon ellipsometry.

Available equipment: Multi-axis workstations with ultrashort pulse lasers for experimentation, rent and user training services. Dip pen nanolithography and imaging ellipsometry for creating and imaging of molecular surfaces.

Converse and chemical coatings

specializes in aluminium and its alloys anodization, galvanic precious metals plating and related fields. The services provide: electrodeposition of protective, decorative as well as technical converse (anodic) coatings, structural etching of decoration elements, adsorption colouring of anodized surfaces, modify-cation of aluminium and its alloys surfaces with a passivation film that ensures the required conductivity, protection and other properties, chemical deposition of passivation coatings onto alloy steels.

Available equipment: Experimental equipment for environ-ment-friendly galvanic processes, anodizing line.

Chemical passivation line for chromium-free passivation process of aluminium and its alloys, IRIDITE NCP.

Microwave transmission, reflection and absorption

In the new microwave anechoic chamber we developed a setup for microwave transmission and reflection measurement in a frequency range from 1 GHz to 18 GHz. Measured sample is placed in the aperture of the absorbing panel. Using this technique, it is possible to measure microwave properties of various modern materials: windowpanes, absorbing textiles, shielding materials, etc.

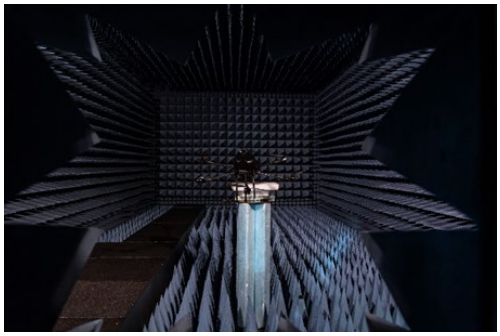

Setup for microwave signal transmission, reflection and absorp-tion in an anechoic chamber.

PROJECTS

Research Executive Agency (REA) project “A multi-spectroscopic approach to probe amyloid aggregatiion at biological surfaces” (MultiSpecAMYLOID)

S. Strazdaitė

MultiSpecAMYLOID

European Commission project “European Joint Research Programme in the management and disposal of radioactive waste” (EURAD)

R. Plukienė

EURAD

European Defence Agency (EDA) project “Adaptive camouflage for the Soldier II” (ACAMSII)

A. Abraitienė

European Space Agency (ESA) project “Terahertz Time Domain Gas-Phase Spectroscopy”

R. Adomavičius

European Commission project “Advancing Science and TEchnology thRough dIamond Quantum Sensing” (ASTERIQS)

A. Alkauskas

ASTERIQS

ResearchExecutive Agency (REA) project “Chalcopyrite-perovskites for infrared photovoltaics”(IRPV)

R. Kondrotas

IRPV

European Commission project “In-built Triggered Enzymes to Recycle Multi-layers: an Inovation for Uses in Plastic-packaging” (TERMINUS)

S. Asadauskas

Science for Peace and Security Programme project “Tuned optical sensors for detection and identification of airborne hostile agents” (HOSTITUNOP)

A. Rodin

Research Executive Agency (REA) “Dirac Semimetals based Terahertz Components” (DiSeTCom)

G. Valušis

DiSeTCom

Horizon 2020 programme project “PRE-DISposal management of radioactive waste“ (PRE-DIS)

R. Plukienė

PRE-DIS

European Space Agency (ESA) project “Bismide-based Intersubband Devices for Mid-Infrared Applications” (BISMIRA)

J. Devenson

Horizon 2020 programme project “Fostering the PAN-European infrastructure for empowering SMEs digital competences in laser-based advanced and additive manufacturing” (PULSATE)

G. Račiukaitis

PULSATE

European Space Agency (ESA) project “Optical fiber-based source of entangled photons for satellite-based quantum communications” (EPhOS)

V. Tomkus

Research Executive Agency (REA) project “Terahertz Photonics for Communica-tions, Space, Security, Radio-Astronomy, and Material Science” (TERAOPTICS)

I. Kašalynas

TERAOPTICS

EVENTS

Gintaras Valušis elected to EARTO Executive Board

The FTMC became the Member of European Association of Research and Technology Organisations (EARTO) Executive Board. After the vote **on April 3, 2020**, General Assembly of EARTO announced the FTMC director G. Valušis as the Member of the EARTO Executive Board. 'We are very pleased to be elected to Executive Board and work together with the 22 strongest scientific institutions of Europe. The EARTO Association unites more than 350 European research centers and institutes, whose main activities are focused on applied research and the creation and development of high technologies. Research organizations are admitted to EARTO only after a thorough professional examination of their scientific and technological merits' told G. Valušis.

Understanding processes behind neurodegenerative diseases

In May 2020, a prestigious science journal, *Langmuir*, published a unique scientific study of Ph.D. Simona Strazdaitė and her collegues from the FTMC *Structure Determination of Hen Egg-White Lysozyme Aggregates Adsorbed to Lipid/Water and Air/Water Interfaces*. The illustration from this research was published on the cover of the journal. Our scientists studied important molecular interactions between protein aggregates and a model cell membrane. The researchers found that protein aggregates get adsorbed to the membrane not only due to attraction between opposite charges, but also due to hydrophobic interaction, which potentially can be amplified if the membrane is disordered.

Exhibition "Science and scientists on coins and banknotes"

An original numismatic exhibition "Science and scientists on coins and banknotes" was organized at the Center by Eugenijus Norkus. This exhibition was dedicated to the 10th Anniversary of the FTMC, where prof. Norkus works as the Chief Research Associate and Head of Catalysis Department. He is the full Member of the Lithuanian Academy of Sciences, well-known for his works in catalysis, has been honoured and awarded many prizes for his research, including the Lithuanian National Science Award (2000 and 2015).

FTMC anniversary conference *10 years of scientific excellence and high-tech innovations*

On September 28-29, the FTMC was celebrating the 10th anniversary of its activity. To commemorate the event, the two-day international scientific conference *10 years of scientific excellence and high-tech innovation* was held in Vilnius. It was opened and welcomed by Eugenijus Jovaiša, Chairman of the Committee on Education and Science of the Parliament of Lithuania. He emphasized local and international scientific activities of the FTMC and its highly valuable feature, entrepreneurship. Prime Minister of Lithuania Saulius Skvernelis had passed his written greetings to the community of the FTMC thanking for the dissemination of competent knowledge and experience, innovations, strengthening the international scientific community and cooperation. In the FTMC's 10th anniversary conference, which was held in center, and also broadcasted online, participated the world famous leaders in science and high-tech, members of the FTMC's International Advisory Board: chemistry, optoelectronics and photonics, materials engineering, life sciences stars from Finland, the USA, the Netherlands, Germany and other countries.

The FTMC's 10th anniversary program also included interesting cultural events. In the FTMC lobby there was arranged the exclusive numismatic exhibition from FTMC prof E. Norkus' own collection "Science and Scientists on Coins and Banknotes". At the end of first day of the Conference, the chamber group of the Vilnius Music lovers symphony orchestra arranged evening concert.

APROPOS 17: when optics meet electronics - spectacular phenomena and innovations

Lithuanian scientists and world-famous researchers in the field participated in 17th International Conference APROPOS 17 - *Advanced Properties and Processes in Optoelectronic Materials and Systems* which was held **on September 30 - October 1** in FTMC, Vilnius. The APROPOS 17 conference continues the series of symposia held in Vilnius since 1971 with the initial title *Plasma and instabilities in semiconductors* and later *Ultrafast Phenomena in Semiconductors* (*UFPS*). It was an international event on plasma and semiconductor physics (initiated by the former Institute of Semiconductor Physics) bringing together scientists from all over the world. The conferences every three years were held in Vilnius.

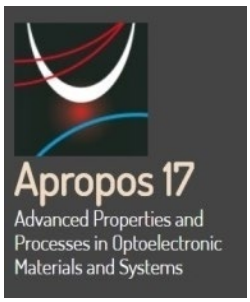

The conference APROPOS 17 aims to reveal and share the new ideas in technology, research and application of new advanced optoelectronic materials, discover new trends in optoelectronics research and discuss processes and phenomena arising when optics meets electronics. Special emphasis is on applications of ultrafast methods for advanced materials. Lithuanian-Polish Workhop, a satellite seminar-workshop of Lithuanian and Polish scientists, was an important part of the APROPOS 17. This event was greeted by Urszula Doroszewska, the Ambassador of Poland to Lithuania.

Visit of the President of Lithuania to FTMC

On October 21, the President of Lithuania Gitanas Nausėda and group of his advisers for education, science, culture and social politics visited FTMC. The honorary guests got acquainted with micro-lasers fabrication and material processing technologies, visited the Departments of Optoelectronics Technology and Nuclear Research, communicated with the scientists and PhDs of the Center. Gintaras Valušis, the director of FTMC, and Dr. Renata Butkutė introduced the achievements of our scientists in the field of photonics, talked about international projects and science - business communication. The President visited the exposition of innovative products, examined the products of modern micro- and nano-structured many-component device fabrication technologies. In Mass Spectrometry Laboratory the guests got acquainted with the most modern equipment for the radioactive carbon dating and other research in the field of nuclear and environmental safety.

The Award for Lithuanian ideas leading globally to Audrius Alkauskas

The FTMC chief researcher and Audrius Alkauskas was awarded Global Lithuanian Award for the developments in computational material science applied to quantum information processing. Global Lithuanian Leaders promote the culture of sharing of ideas and experience, connect the overachievers with international experience and encourage their engagement for the welfare of Lithuania. The scientific advances of Alkauskas group in material science related to quantum information technologies appeared on the cover of the Applied Physics Letters. His international team presented their results on single-photon emitters in two-dimensional semiconductors. They recently joined an EU Quantum Technology Flagship project on diamond-based quantum sensors. Audrius Alkauskas has received his PhD at the University of Basel, worked at the Swiss Federal Institute of Technology in Lausanne, as well as at the University of California, Santa Barbara. Most of his present research is conducted in Lithuania.

AWARDS

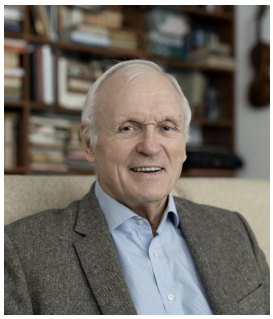

Gediminas Trinkūnas
– for life achievements

After defending his PhD at the Institute of Physics, Gediminas Trinkūnas moved to the problems related to the theory of photo-induced phenomena in molecular systems, to studies of light-induced photosynthetic reactions, in particular. Problems of excitation energy transfer and photoinduced charge generation in photosynthetic bacteria and plant photosynthesis were under his interest. While solving the scientific problems, he was also active as a deputy Director of the Institute Physics and a manager of the Science Park of the FTMC and was also involved in development of new science-related technologies.

Audrius Alkauskas
– for scientific achievements

For highest quality science, scientific curiosity and leadership. For particular attention to education of students and PhDs. For inspiring work and enthusiasm managing the seminars of the Center.

Steigvilė Byčenkienė
– for innovational activity

For innovative style of work, new themes, leadership and team building. For her activity as a member of EC Platform on Sustainable Finance. For participation in Commission expert group in the Mission Board for adaptation to climate change including societal transformation.

Ramunė Kriaučionytė
– for scientifically invisible work

For her precise and remarkable work managing Financial Department and creating an inspiring atmosphere. Over the years, Ramunė gained a large scale experience in managing financial parts of various scientific projects and contracts with particular focus to EU related activities. She and her team make sincere efforts to remove the burden of financial project management from the scientists to allow them to concentrate on purely scientific tasks.

Aldona Balčiūnaitė
– breakthrough of the year

For productive scientific work, enthusiasm and innovative ideas. For being elected to the Young Academy of the Lithuanian Academy of Sciences.

Linas Minkevičius
– special award

For breakthrough scientific-technological activity which allowed to become the Young Academy Member of the Lithuanian Academy of Sciences.

Eugenijus Norkus
– FTMC Patronage award

For beginning of the patronage tradition, for unique numismatic collection donated to our Center.

Brian Olley
British Ambassador to Lithuania
– FTMC Patronage Award

For kindness and sincere support in acquiring a special equipment for studies of the face masks filtration efficiency.

DOCTORAL THESES

Doctoral theses defended in 2020

Giedrius Abromavičius – Microstructural and optical properties of metal oxide optical coatings deposited by ion beam sputtering and their application in UV spectral range (*T008*).

Scientific supervisor: dr. R. Drazdys.

Rokas Žalnėravičius – Synthesis, characterization and antimicrobial properties of metallic and semiconductor nanoparticles (*N003*).

Scientific supervisor: dr. A. Jagminas.

Tadas Matijošius – Tribological investigation of biocompatible nanostructured coatings and lubricating materials (*N003*).

Scientific supervisor: dr. S. Asadauskas.

Aušra Baradokė – Fabrication of miniaturised electrochemical sensor for cancerogenic biomarker detection (*N003*).

Scientific supervisor: prof. dr. R. Pauliukaitė.

Daina Upskuvienė – Synthesis, characterization and investigation of properties of gold nanoparticles (*N003*).

Scientific supervisor: dr. L. Tamašauskaitė Tamašiūnaitė.

Elena Lagzdina – Radiological and structural characterization of RBMK-1500 reactor graphite and application of the ion implantation method to investigate irradiation damage in graphite (*N002*).

Scientific supervisor: dr. R. Plukienė.

Vidmantas Jašinskas – Charge carrier generation and motion in single wall carbon nanotube/fullerene derivative films (*N002*).

Scientific supervisor: prof. habil. dr. V. Gulbinas.

Mažena Mackoit-Sinkevičienė – Point defects as single-photon emitters in hexagonal boron nitride: theoretical study (*N002*).

Scientific supervisor: prof. dr. A. Alkauskas.

Julija Pauraitė-Dudek – The impact of submicron aerosol source and physical-chemical parameters on atmospheric radiative balance (*N002*).

Scientific supervisor: dr. V. Ulevičius.

Vytautas Janonis – Development of terahertz diffractive optics and plasmon-phonon polaritonics components (*T008*).

Scientific supervisor: dr. I. Kašalynas.

Martynas Šapurov – Development of smooth asymmetric reactive power compensators (*T001*).

Scientific supervisor: dr. A. Baškys.

Edvardas Bielskis – Development of energy efficient photovoltaic microinverter (*T001*).

Scientific supervisor: dr. A. Baškys.

Agnė Mikalauskaitė – Investigation on the surface decoration of magnetic iron oxide nanoparticles with gold nanocomposites (*N003*).

Scientific supervisor: dr. A. Jagminas.

Audrius Drabavičius – Formation of chalcogenide solar cell absorber layers using electrochemical deposition of precursors (*N003*).

Scientific supervisor: habil.dr. R. Juškėnas.

Domas Jokubauskis – Development and applications of compact spectroscopic terahertz imaging systems using principles of optical beam engineering (*N002*).

Scientific supervisor: prof. habil. dr. G. Valušis.

Rokas Naujalis – Star Clusters in Galaxies. Multicolour HST photometry (*N002*).

Scientific supervisor: prof. dr. V. Vansevičius.

Monika Kirsnytė – Semiconductor polymeric composites formation by bioinspired in situ polymerization process with non-conductive substrates (*N003*).

Scientific supervisor: dr. A. Stirkė.

Jonas Klimantavičius – Tuning of magnetoresistive properties of nanostructured La-Sr-Mn-O films (*T001*).

Scientific supervisor: prof. habil. dr. N. Žurauskienė.

PUBLICATIONS

with FTMC affiliations in 2020 in the top quartiles (Q1-O4) journals

1. Adliene, D.; Griciene, B.; Skovorodko, K.; Laurikaitiene, J.; Puiso, J. Occupational radiation exposure of health professionals and cancer risk assessment for Lithuanian nuclear medicine workers // *Environmental research*. ISSN 0013-9351. 2020, vol. 183, art. no. 109144, p. 1-10.
2. Adomaitienė, E.; Ašmontas, S.; Bumelienė, S.; Tamaševičius, A. V. Local control of an array of the diffusively coupled FitzHugh–Nagumo oscillators via repulsive mean field // *Journal of applied physics*. ISSN 0021-8979. 2020, vol. 128, iss. 7, art. no. 074902, p. 1-7.
3. Adomaitienė, E.; Ašmontas, S.; Bumelienė, S.; Tamaševičius, A.V. Pinning control of an array of globally coupled FitzHugh–Nagumo oscillators by means of a four-terminal controller // *Physica scripta*. ISSN 0031-8949. 2020, vol. 95, no. 7, art. no. 075210, p. 1-6.
4. Adomaitienė, E.; Ašmontas, S.; Bumelienė, S.; Tamaševičius, A. V. Quenching coupled FitzHugh-Nagumo oscillators by repulsive feedback // *Physica scripta*. ISSN 0031-8949. 2020, vol. 95, no. 10, art. no. 105202, p. 1-6.
5. Adomaitienė, E.; Bumelienė, S.; Mykolaitis, G.; Tamaševičius, A.V. Destroying synchrony in an array of the FitzHugh–Nagumo oscillators by external DC voltage source // *Nonlinear analysis: modelling and control*. ISSN 1392-5113. 2020, vol. 25, no. 1, p. 57-68.
6. Adomaitienė, E.; Bumelienė, S.; Tamaševičius, A.V. Local control of an array of the globally coupled oscillators // *Nonlinear dynamics*. ISSN 0924-090X. 2020, vol. 99, iss. 3, p. 2129-2137.
7. Adomavičius, R.; Nevinskas, I.; Treu, J.; Xu, X.; Koblmüller, G.; Krotkus, A. Pulsed THz emission from wurtzite phase catalyst-free InAs nanowires // *Journal of physics D: Applied physics*. ISSN 0022-3727. 2020, vol. 53, iss. 19, art. no. 19LT01, p. 1-8.
8. Agafonov, V.; Nargelienė, V.; Balakauskas, S.; Bukauskas, V.; Kamarauskas, M.; Lukša, A.; Mironas, A.; Rėza, A.; Šetkus, A. Single variable defined technology control of the optical properties in MoS2 films with controlled number of 2D-layers // *Nanotechnology*. ISSN 0957-4484. 2020, vol. 31, iss. 2, art. no. 025602, p. 1-12.
9. Ali Santoro, M.C.; Anagnostakis, M.J.; Boshkova, T.; Camacho, A.; Fornaciari Iljadica, M.C.; Collins, S.M.; Diaz Perez, R.; Delgado, J.U.; Đurašavić, M.; Duch, M.A.; Elvira, V.H.; Gomes, R.S.; Gudelis, A.; Gurau, D.; Hurtado Bermudez, S.; Idoeta, R.; Jevremović, A.; Kandić, A.; Korun, M.; Karfopolous, K.; Laubenstein, M.; Long, S.; Margineanu, R.M.; Mitsios, I.; Mulas, D.; Nikolić, J.K.; Pantelica, A.; Peyres Medina, V.; Pibida, L.; Potiriadis, C.; Silva, R.L.; Siri, S.; Šešlak, B.; Verheyen, L.; Vodenik, B.; Vukanac, I.; Wiedner, H.; Zorko, B. Determining the probability of locating peaks using computerized peak-location methods in gamma-ray spectra as a function of the relative peak-area uncertainty // *Applied radiation and isotopes*. ISSN 0969-8043. 2020, vol. 155, art. no. 108920, p. 1-6.
10. Ardaravičius, L.; Keršulis, S.; Kiprijanovič, O.; Šimkevičius, Č.; Ašmontas, S. The Barkhausen method to investigate powerful processes during action of piezoelectric igniters // *Materials science-Medžiagotyra*. ISSN 1392-1320. 2020, vol. 26, iss. 3, p. 358-362.
11. Ardaravičius, L.; Kiprijanovič, O.; Ramonas, M.; Šermukšnis, E.; Šimukovič, A.; Matulionis, A. Estimation of the charged defect density from hot-electron transport studies in epitaxial ZnO // *Lithuanian journal of physics*. ISSN 1648-8504. 2020, vol. 60, no. 1, p. 48-56.
12. Ašmontas, S.; Anbinderis, M.; Čerškus, A.; Gradauskas, J.; Sužiedėlis, A.; Šilėnas, A.; Širmulis, E.; Umansky, V. Gated bow-tie diode for microwave to sub-terahertz detection // *Sensors*. ISSN 1424-8220. 2020, vol. 20, iss. 3, art. no. 829, p. 1-9.
13. Ašmontas, S.; Anbinderis, M.; Gradauskas, J.; Juškėnas, R.; Leinartas, K.; Lučun, A.; Selskis, A.; Staišiūnas, L.; Stanionytė, S.; Sužiedėlis, A.; Šilėnas, A.; Širmulis, E. Low resistance TiO2/p-Si heterojunction for tandem solar cells // *Materials*. ISSN 1996-1944. 2020, vol. 13, iss. 12, art. no. 2857, p. 1-10.
14. Ašmontas, S.; Bumelienė, S.; Gradauskas, J.; Raguotis, R.; Sužiedėlis, A. Impact ionization and intervalley electron scattering in InSb and InAs induced by a single terahertz pulse // *Scientific reports*. ISSN 2045-2322. 2020, vol. 10, art. no. 10580, p. 1-7.
15. Ašmontas, S.; Fedorenko, L.; Vlasiuk, V.; Gorbanyuk, T.; Kostylyov, V.; Lytovchenko, V.; Gradauskas, J.; Sužiedėlis, A.; Širmulis, E.; Žalys, O.A.; Masalskyi, O. Suppression of hot carriers by nanoporous silicon for improved operation of a solar cell // *Ukrainian journal of physical optics*. ISSN 1609-1833. 2020, vol. 21, iss. 4, p. 207-214.
16. Baah, M.; Obraztsov, P.; Paddubskaya, A.; Bičiūnas, A.; Suvanto, S.; Svirko, Y.; Kuzhir, P.; Kaplas, T. S. Electrical, transport, and optical properties of multifunctional graphitic films synthesized on dielectric surfaces by nickel nanolayer-assisted pyrolysis // *ACS applied materials & interfaces*. ISSN 1944-8244. 2020, vol. 12, iss. 5, p. 6226-6233.
17. Babichev, A. V.; Pashnev, D.; Denisov, D.V.; Gladyshev, A.G.; Yu.K., Bobretsova; Slipchenko, S.O.; Karachinsky, L.Ya.; Novikov, I.I.; Firsov, D.A.; Vorobjev, L.E.; Pikhtin, N.A.; Egorov, A.Yu. Study of the spectra of arched-cavity quantum-cascade lasers // *Optics and spectroscopy*. ISSN 0030-400X. 2020, vol. 128, no. 6, p. 702-706.
18. Babichev, A. V.; Pashnev, D.; Gladyshev, A. G.; Denisov, D. V.; Voznyuk, G. V.; Karachinsky, L. Ya.; Novikov, I. I.; Mitrofanov, M. I.; Evtikhiev, V. P.; Firsov, D. A.; Vorob'ev, L. E.; Pikhtin, N. A.; Egorov, A. Yu. Quantum-cascade lasers with a distributed Bragg reflector formed by Ion-beam etching // *Technical physics letters*. ISSN 1063-7850. 2020, vol. 46, no. 4, p. 312-315.
19. Babichev, A. V.; Pashnev, D.; Gladyshev, A. G.; Kurochkin, A. S.; Kolodeznyi, E. S.; Karachinsky, L. Ya.; Novikov, I. I.; Denisov, D. V.; Dudelev, V. V.; Sokolovskii, G. S.; Firsov, D. A.; Vorob'ev, L. E.; Slipchenko, S. O.; Lutetskiy, A. V.; Pikhtin, N. A.; Egorov, A. Yu. Spectral characteristics of half-ring quantum-cascade lasers // *Optics and spectroscopy*. ISSN 0030-400X. 2020, vol. 128, no. 8, p. 1187-1192.
20. Bagdžiūnas, G.; Palinauskas, D. Poly(9H-carbazole) as a Organic Semiconductor for Enzymatic and Non-Enzymatic Glucose Sensors // *Biosensors*. eISSN 2079-6374. 2020, vol. 10, iss. 9, art. no. 104, p. 1-15.
21. Bagdžiūnas, Gi.; Palinauskas, D.; Ramanavičius, A. Towards colourless-to-green electrochromic smart glass based on a redox active polymeric semiconductor containing carbazole moiety // *Dyes and pigments*. ISSN 0143-7208. 2020, vol. 177, art. no. 108328, p. 1-8.

22. Bagdžiūnas, G. Theoretical design of molecularly imprinted polymers based on polyaniline and polypyrrole for detection of tryptophan // *Molecular systems design & engineering*. eISSN 2058-9689. 2020, vol. 5, iss. 9, p. 1504-1512.

23. Balevičius, S.; Žurauskienė, N.; Stankevič, V.; Keršulis, S.; Baškys, A.; Bleizgys, V.; Dilys, J.; Lučinskis, A.; Tyshko, A.; Brazil, S. Hand-held magnetic field meter based on colossal magnetoresistance-B-scalar sensor // I*EEE transactions on instrumentation and measurement*. ISSN 0018-9456. 2020, vol. 69, iss. 6, p. 2808-2816.

24. Balion, Z.; Cėpla, V.; Svirskienė, N.; Svirskis, G.; Druceikaitė, K.; Inokaitis, H.; Rusteikaitė, J.; Masilionis, I.; Stankevičienė, G.; Jelinskas, T.; Ulčinas, A.; Samanta, A.; Valiokas, R.; Jekabsone, A. Cerebellar cells self-assemble into functional organoids on synthetic, chemically crosslinked ECM-mimicking peptide hydrogels // *Biomolecules*. ISSN 2218-273X. 2020, vol. 10, iss. 5, art. no. 754, p. 1-25.

25. Balion, Z.; Sipailaitė, E.; Stasyte, G.; Vailionyte, A.; Mazetyte-Godiene, A.; Seskeviciute, I.; Bernotienė, R.; Phopase, J.; Jekabsone, A. Investigation of cancer cell migration and proliferation on synthetic extracellular matrix peptide hydrogels: research article // *Frontiers in bioengineering and biotechnology*. ISSN 2296-4185. 2020, vol. 8, art. no. 773, p. 1-13.

26. Baltrėnas, P.; Urbanas, D.; Sukackienė, Z.; Stalnionienė, I.; Stalnionis, G.; Jasulaitienė, V.; Tamašauskaitė-Tamašiūnaitė, L. Flue gas purification from NO using supported Cu–Mn and Cu–Mn–Nb catalysts synthesized by electroless metal deposition method // *International journal of environmental science and technology*. ISSN 1735-1472. 2020, vol. 17, iss. 9, p. 3857-3874.

27. Baltrukonis, J.; Ulčinas, O.; Orlovas, S.; Jukna, V. Void and micro-crack generation in transparent materials with high-energy first-order vector Bessel beam // *Journal of the Optical Society of America* B. ISSN 0740-3224. 2020, vol. 37, iss. 7, p. 2121-2127.

28. Barauskas, R.; Sankauskaite, A.; Rubeziene, V.; Gadeikyte, A.; Skurkyte-Papieviene, V.; Abraitiene, A. Investigation of thermal properties of spacer fabrics with phase changing material by finite element model and experiment // *Textile research journal*. ISSN 0040-5175. 2020, vol. 90, iss. 15-16, p. 1837-1850.

29. Barisevičiūtė, R.; Maceika, E.; Ežerinskis, Ž.; Šapolaitė, J.; Butkus, L.; Mažeika, J.; Rakauskas, V.; Juodis, L.; Steponėnas, A.; Druteikienė, R.; Remeikis, V. Distribution of radiocarbon in sediments of the cooling pond of RBMK type Ignalina Nuclear Power Plant in Lithuania // *PloS one*. 2020, vol. 15, no. 8, art. no. e0237605, p. 1-14.

30. Bartašiūnas, A.; Miškinis, R.; Smirnov, D.; Urba, E. Investigation of the Lithuanian national standard of electric resistance // *Metrology and measurement systems*. ISSN 0860-8229. 2020, vol. 27, iss. 4, p. 615-627.

31. Bartulevičius, T.; Madeikis, K.; Veselis, L.; Petrauskienė, V.; Michailovas, A. Active fiber loop for synthesizing GHz bursts of equidistant ultrashort pulses // *Optics express*. ISSN 1094-4087. 2020, vol. 28, no. 9, p. 13059-13067.

32. Bertašius, P.; Macutkevič, J.; Banys, J.; Gaidukovs, S.; Barkane, A.; Vaivodiss, R. Synergy effects in dielectric and thermal properties of layered EVA composites with carbon and Fe3O4 nanoparticles // *Journal of applied polymer science*. ISSN 0021-8995. 2020, vol. 137, iss. 24, art. no. 48814, p. 1-8.

33. Berzinš, J.; Indrišiūnas, S.; Fasold, S.; Steinert, M.; Žukovskaja, O.; Cialla-May, D.; Gečys, P.; Bäumer, S. M. B.; Pertsch, T.; Setzpfandt, F. Laser-induced spatially-selective tailoring of high-index dielectric metasurfaces // *Optics express*. ISSN 1094-4087. 2020, vol. 28, iss. 2, p. 1539-1553.

34. Berzinš, J.; Indrišiūnas, S.; van Erve, K.; Nagarajan, A.; Fasold, S.; Steinert, M.; Gerini, G.; Gečys, P.; Pertsch, T.; Bäumer, S. M. B.; Setzpfandt, F. Direct and high-throughput fabrication of mie-resonant metasurfaces via single-pulse laser interference // *ACS nano*. ISSN 1936-0851. 2020, vol. 14, iss. 5, p. 6138-6149.

35. Bialopetravičius, J.; Narbutis, D. Deriving star cluster parameters with convolutional neural networks. II. Extinction and cluster-background classification // *Astronomy & astrophysics*. ISSN 0004-6361. 2020, vol. 633, art. no. A148, p. 1-17.

36. Bialopetravičius, J.; Narbutis, D. Study of star clusters in the M83 galaxy with a convolutional neural network // *The astronomical journal*. ISSN 0004-6256. 2020, vol. 160, no. 6, art. no. 264, p. 1-11.

37. Bielskis, E.; Baškys, A.; Valiulis, G. Controller for the grid-connected microinverter output current tracking // *Symmetry*. ISSN 2073-8994. 2020, vol. 12, iss. 1, art. no. 112, p. 1-13.

38. Bikulčius, G.; Češūnienė, A. O.; Selskienė, A.; Matijošius, T.; Pakštas, V.; Bučinskienė, D. A novel Cr–CeO_2/La_2O_3 nanocomposite electro-deposited in sulphate Cr (III) bath // *Transactions of the Institute of Metal Finishing*. ISSN 0020-2967. 2020, vol. 98, iss. 4, p. 199-208.

39. Braver, J.; Valkūnas, L.; Gelžinis, A. Benchmarking the forward–backward trajectory solution of the quantum-classical Liouville equation // *Journal of chemical physics*. ISSN 0021-9606. 2020, vol. 152, iss. 21, art. no. 214116, p. 1-12.

40. Bružaitė, I.; Rožėnė, J.; Morkvėnaitė-Vilkončienė, I.; Ramanavičius, A. Towards microorganism-based biofuel cells: the viability of saccharomyces cerevisiae modified by multiwalled carbon nanotubes // *Nanomaterials*. ISSN 2079-4991. 2020, vol. 10, iss. 5, art. no. 954, p. 1-4.

41. Buchnev, O.; Belosludtsev, A.; Reshetnyak, V.; Evans, D.R.; Fedotov, V.A. Observing and controlling a Tamm plasmon at the interface with a metasurface // *Nanophotonics*. ISSN 2192-8606. 2020, vol. 9, iss. 4, p. 897-903.

42. Bužavaitė-Vertelienė, E.; Plikusienė, I.; Tolenis, T.; Valavičius, A.; Anulytė, J.; Ramanavičius, A.; Balevičius, Z. Hybrid Tamm-surface plasmon polariton mode for highly sensitive detection of protein interactions // *Optics express*. ISSN 1094-4087. 2020, vol. 28, no. 20, p. 29033-29043.

43. Bužavaitė-Vertelienė, E.; Valavičius, A.; Grinevičiūtė, L.; Tolenis, T.; Lukošė, R.; Niaura, G.; Balevičius, Z. Influence of the graphene layer on the strong coupling in the hybrid Tamm-plasmon polariton mode // *Optics express*. ISSN 1094-4087. 2020, vol. 28, no. 7, p. 10308-10319.

44. Carpeggiani, P.A.; Coccia, G.; Fan, G.; Kaksis, E.; Pugžlys, A.; Baltuška, A.; Piccoli, R.; Jeong, Y.-G.; Rovere, A.; Morandotti, R.; Razzari, L.; Schmidt, B.E.; Voronin, A.A.; Zheltikov, A.M. Extreme Raman red shift: ultrafast multimode nonlinear space-time dynamics, pulse compression, and broadly tunable frequency conversion // *Optica*. ISSN 2334-2536. 2020, vol. 7, iss. 10, p. 1349-1354.

45. Cėpla, V.; Rakickas, T.; Garbenčiūtė, G.; Mazėtytė-Godienė, A.; Baradokė, A.; Ruželė, Ž.; Valiokas, R. Photografting and patterning of poly (ethylene glycol) methacrylate hydrogel on glass for biochip applications // *ACS applied materials and interfaces*. ISSN 1944-8244. 2020, vol. 12, iss. 29, p. 32233-32246.

46. Černašėjus, O.; Škamat, J.; Markovič, V.; Višniakov, N.; Indrišiūnas, S. Effect of laser processing on surface properties of additively manufactured 18-percent nickel maraging steel parts // *Coatings*. ISSN 2079-6412. 2020, vol. 10, iss. 6, art. no. 600, p. 1-15.

47. Čerškus, A.; Ašmontas, S.; Petrauskas, K.; Sužiedėlis, A.; Gradauskas, J.; Opanasyuk, A.S.; Vengalis, B. Photoluminescence properties of hybrid perovskites in solar cells with TiO2 and Mg02Zn08O electron transport layers // *Lithuanian journal of physics*. ISSN 1648-8504. 2020, vol. 60, no. 3, p. 172-184.

48. Charkova, T.; Zdaniauskienė, A. Synthesis and comparison of gold nanoparticles coated with silicon, manganese and titanium dioxides // Chemija. ISSN 0235-7216. 2020, vol. 31, no. 4, p. 197-202.

49. Chelnokova, I.A.; Golubewa, L.; Starodubtseva, M. N.; Kulahava, T. A.; Kunitskaya, Y. N.; Bulai, P. M.; Starodubtsev, I. E.; Kharin, Yu. S.; Shuba, M. V. Effect of single-walled carbon nanotubes on the

structural, physical, and mechanical properties of rat glial cell surface // *Journal of Nanoparticle Research*. ISSN 1388-0764. 2020, vol. 22, iss. 6, art. no. 144, p. 1-11.

50. Chernyakova, K.; Tzaneva, B.; Vrublevsky, I.; Videkov, V. Effect of aluminum anode temperature on growth rate and structure of nanoporous anodic alumina // *Journal of the electrochemical society*. ISSN 0013-4651. 2020, vol. 167, iss. 10, art. no. 103506, p. 1-6.

51. Chernyakova, K.; Ispas, A.; Karpič, R.; Ecke, G.; Vrublevsky, I.; Bund, A. Formation of ordered anodic alumina nanofibers during aluminum anodizing in oxalic acid at high voltage and electrical power // *Surface and coatings technology*. ISSN 0257-8972. 2020, vol. 394, art. no. 125813, p. 1-6.

52. Damberga, D.; Fedorenko, V.; Grundšteins, K.; Altundal, Ş.; Šutka, A.; Ramanavičius, A.; Coy, E.; Mrówczyński, R.; Iatsunskyi, I.; Viter, R. Influence of PDA coating on the structural, optical and surface properties of ZnO nanostructures // *Nanomaterials*. ISSN 2079-4991. 2020, vol. 10, iss. 12, art. no. 2438, p. 1-11.

53. Dansette, P.-M.; Burokas, R.; Veselis, L.; Zaukevičius, A.; Michailovas, A.; Rusteika, N. Peculiarities of second harmonic generation with chirped femtosecond pulses at high conversion efficiency // *Optics communications*. ISSN 0030-4018. 2020, vol. 455, art. no. 124462, p. 1-11.

54. de Alleluia, A.B.; Abdelshafy, A.F.; Ragulis, P.; Kuskov, A.; Andreev, D.; Othman, M.A.K.; Martinez-Hernandez, B.; Schamiloglu, E.; Figotin, A.; Capolino, F. Experimental testing of a 3-D-printed metamaterial slow wave structure for high-power microwave generation // *IEEE transactions on plasma science*. ISSN 0093-3813. 2020, vol. 48, iss. 12, p. 4356-4364.

55. Dementjev, A.; Rudys, R.; Karpič, R.; Rutkauskas, D. Optimization of wide-field second-harmonic generation microscopy for fast imaging of large sample areas in biological tissues // *Lithuanian journal of physics*. ISSN 1648-8504. 2020, vol. 60, no. 3, p. 145-153.

56. Dementjev, A.; Rutkauskas, D.; Polovy, I.; Mačernis, M.; Abramavičius, D.; Valkūnas, L.; Dovbeshko, G. Characterization of thymine microcrystals by CARS and SHG microscopy // *Scientific reports*. eISSN 2045-2322. 2020, vol. 10, art. no. 17097, p. 1-9.

57. Diethelm, M.; Schiller, A.; Kawecki, M.; Devižis, A.; Blülle, B.; Jenatsch, S.; Knapp, E.; Grossmann, Q.; Ruhstaller, B.; Nüesch, F.; Hany, R. The dynamic emission zone in sandwich polymer light-emitting electrochemical cells // *Advanced functional materials*. ISSN 1616-301X. 2020, vol. 30, iss. 33, art. no. 1906803, p. 1-10.

58. Ding, K.; Avrutin, V.; Izyumskaya, N.; Özgür, Ü.; Morkoç, H.; Šermukšnis, E.; Matulionis, A. High-performance BeMgZnO/ZnO heterostructure field-effect transistors // *Physica status solidi - rapid research letters*. ISSN 1862-6254. 2020, vol. 14, iss. 12, art. no. 2000371, p. 1-5.

59. Dobrozhan, O.; Shelest, I.; Stepanenko, A.; Kurbatov, D.; Yermakov, M.; Čerškus, A.; Plotnikov, S.; Opanasyuk, A. Structure, substructure and chemical composition of ZnO nanocrystals and films deposited onto flexible substrates // *Materials science in semiconductor processing*. ISSN 1369-8001. 2020, vol. 108, art. no. 104879, p. 1-8.

60. Drabavičius, A.; Naujokaitis, A.; Stalnionis, G.; Giraitis, R.; Mockus, Z.; Kanapeckaitė, S.; Kalinauskas, P.; Nedzinskas, R.; Niaura, G.; Juškėnas, R. Photoelectrochemical, Raman spectroscopy, XRD and photoluminescence study of disorder in electrochemically deposited kesterite thin film // *Journal of alloys and compounds*. ISSN 0925-8388. 2020, vol. 824, art. no. 153853, p. 1-9.

61. Drabik, D.; Gavutis, M.; Valiokas, R.; Ulčinas, A. Determination of the mechanical properties of model lipid bilayers using atomic force microscopy indentation // *Langmuir*. ISSN 0743-7463. 2020, vol. 36, iss. 44, p. 13251-13262.

62. Dreyer, C.E.; Alkauskas, A.; Lyons, J.L.; Van de Walle, Ch.G. Radiative capture rates at deep defects from electronic structure calculations // *Physical review B*. ISSN 2469-9950. 2020, vol. 102, iss. 8, art. no. 085305, p. 1-6.

63. Drigo, N.; Roldan-Carmona, C.; Franckevičius, M.; Lin, K.-H.; Gegevičius, R.; Kim, H.; Schouwink, P.A.; Sutanto, A.A.; Olthof, S.; Sohail, M.; Meerholz, K.; Gulbinas, V.; Corminboeuf, C.; Paek, Sa.; Nazeeruddin, M.K. Doped but stable: spirobisacridine hole transporting materials for hysteresis-free and stable perovskite solar cells // *Journal of the American Chemical Society*. ISSN 0002-7863. 2020, vol. 142, iss. 4, p. 1792-1800.

64. Drogowska-Horna, K.A.; Mirza, I.; Rodriguez, A.; Kovaříček, P.; Sládek, J.; J.-Y. Derrien, T.; Gedvilas, M.; Račiukaitis, G.; Frank, O.; M. Bulgakova, N.; Kalbáč, M. Periodic surface functional group density on graphene via laser-induced substrate patterning at Si/SiO2 interface // *Nano research*. ISSN 1998-0124. 2020, vol. 13, iss. 9, p. 2332-2339.

65. Dudutis, J.; Pipiras, J.; Schwarz, S.; Rung, S.; Hellmann, R.; Račiukaitis, G.; Gečys, P. Laser-fabricated axicons challenging the conventional optics in glass processing applications // *Optics express*. ISSN 1094-4087. 2020, vol. 28, no. 4, p. 5715-5730.

66. Dudutis, J.; Pipiras, J.; Stonys, R.; Daknys, E.; Kilikevičius, A.; Kasparaitis, A.; Račiukaitis, G.; Gečys, P. In-depth comparison of conventional glass cutting technologies with laser-based methods by volumetric scribing using Bessel beam and rear-side machining // *Optics express*. ISSN 1094-4087. 2020, vol. 28, iss. 21, p. 32133-32151.

67. Dzedzickis, A.; Šutinys, E.; Bučinskas, V.; Samukaitė-Bubnienė, U.; Jakštys, B.; Ramanavičius, A.; Morkvėnaitė-Vilkončienė, I. Polyethylene-carbon composite (Velostat®) based tactile sensor // *Polymers: Special Issue High-Performance Polymeric Sensors*. eISSN 2073-4360. 2020, vol. 12, iss. 12, art. no. 2905, p. 1-17.

68. Gabriūnaitė, I.; Valiūnienė, A.; Poderytė, M.; Ramanavičius, A. Silane-based self-assembled monolayer deposited on fluorine doped tin oxide as model system for pharmaceutical and biomedical analysis // *Journal of pharmaceutical and biomedical analysis*. ISSN 0731-7085. 2020, vol. 177, art. no. 112832, p. 1-4.

69. Garbarienė, I.; Garbaras, A.; Masalaite, A.; Ceburnis, D.; Krugly, E.; Kauneliene, V.; Remeikis, V.; Martuzevicius, D. Identification of wintertime carbonaceous fine particulate matter (PM2.5) sources in Kaunas, Lithuania using polycyclic aromatic hydrocarbons and stable carbon isotope analysis // *Atmospheric environment*. ISSN 1352-2310. 2020, vol. 237, art. no. 117673, p. 1-9.

70. Gedvilas, M.; Račiukaitis, G. Spatial zigzag evolution of cracks in moving sapphire initiated by bursts of picosecond laser pulses for ultrafast wafer dicing // *RSC advances*. eISSN 2046-2069. 2020, vol. 10, iss. 55, p. 33213-33220.

71. Gelžinis, A.; Valkūnas, L. Analytical derivation of equilibrium state for open quantum system // *Journal of chemical physics*. ISSN 0021-9606. 2020, vol. 152, iss. 5, art. no. 051103, p. 1-6.

72. German, N.; Popov, A.; Ramanavičienė, A.; Ramanavičius, A. Formation and electrochemical characterisation of enzyme-assisted formation of polypyrrole and polyaniline nanocomposites with embedded glucose oxidase and gold nanoparticles // *Journal of the electrochemical society*. ISSN 0013-4651. 2020, vol. 167, iss.16, art. no. 165501, p. 1-8.

73. German, N.; Ramanavičienė, A.; Ramanavičius, A. Formation and electrochemical evaluation of polyaniline and polypyrrole nano-composites based on glucose oxidase and gold nanostructures // *Polymers*. eISSN 2073-4360. 2020, vol. 12, iss. 12, art. no. 3026, p. 1-20.

74. Gicevičius, Mi.; Cechanavičiūtė, I.A.; Ramanavičius, A. Electro-chromic textile composites based on polyaniline-coated metallized conductive fabrics // J-. ISSN 0013-4651. 2020, vol. 167, art. no. 155515, p. 1-5.

75. Girčienė, O.; Gudavičiūtė, L.; Selskienė, A.; Kirdeikienė, A.; Ramanauskas, R. Electrochemical investigations of the anticorrosive

behaviour of the phosphated electrogalvanized steel additionally coated with conversion layer of cerium oxide // Chemija. ISSN 0235-7216. 2020, vol. 31, no. 2, p. 77-86.

76. Gnatyuk, I.; Dementjev, A.; Karpič, R.; Shcherban, N.; Gavrilko, T.; Baran, J. CARS imaging of nematic liquid crystal confined to mesoporous silica-based particles // *Molecular crystals and liquid crystals*. ISSN 1542-1406. 2020, vol. 697, iss. 1, p. 1-10.

77. Golubewa, L.; Karpič, R.; Matulaitienė, I.; Selskis, A.; Rutkauskas, D.; Pushkarchuk, A.; Khlopina, T.; Michels, D.; Lyakhov, D.; Kulahava, T.; Shah, A.; Svirko, Y.; Kuzhir, P. Surface-enhanced Raman spectroscopy of organic molecules and living cells with gold-plated black silicon // *ACS applied materials & interfaces*. ISSN 1944-8244. 2020, vol. 12, iss. 45, p. 50971-50984.

78. Golubewa, L.; Kulahava, T.; Kunitskaya, Y.; Bulai, P.; Shuba, M.; Karpič, R. Enhancement of single-walled carbon nanotube accumulation in glioma cells exposed to low-strength electric field: Promising approach in cancer nanotherapy // *Biochemical and biophysical research communications*. ISSN 0006-291X. 2020, vol. 529, no. 3, p. 647-651.

79. Golubewa, L.; Rehman, H.; Kulahava, Ta.; Karpič, R.; Baah, M.; Kaplas, T.; Shah, A.; Malykhin, S.; Obraztsov, A.; Rutkauskas, D.; Jankunec, M.; Matulaitienė, I.; Selskis, A.; Denisov, A.; Svirko, Y.; Kuzhir, P. Macro-, micro- and nano-roughness of carbon-based interface with the living cells: towards a versatile bio-sensing platform // *Sensors*. ISSN 1424-8220. 2020, vol. 20, iss. 18, art. no. 5028, p. 1-14.

80. Golubewa, L.; Timoshchenko, I.; Romanov, O.; Karpič, R.; Kulahava, T.; Rutkauskas, D.; Shuba, M.; Dementjev, A.; Svirko, Yu.; Kuzhir, P. Single-walled carbon nanotubes as a photo-thermo-acoustic cancer theranostic agent: theory and proof of the concept experiment // *Scientific reports*. ISSN 2045-2322. 2020, vol. 10, art. no. 22174, p. 1-9.

81. Gradauskas, J.; Ašmontas, S.; Sužiedėlis, A.; Šilėnas, A.; Vaičikauskas, V.; Čerškus, A.; Širmulis, E.; Žalys, O.A.; Masalskyi, O. Influence of hot carrier and thermal components on photovoltage formation across the p–n junction // *Applied sciences*. ISSN 2076-3417. 2020, vol. 10, iss. 21, art. no. 7483, p. 1-8.

82. Gric, T.; Rafailov, E. A systematic insight into the surface plasmon polaritons guided by the graphene based heterostructures // *Optical and quantum electronics*. ISSN 0306-8919. 2020, vol. 52, iss. 9, art. no. 404, p. 1-11.

83. Gric, T.; Rafailov, E. Enhancement of the Purcell effect by the wire metamaterials formed by the hexagonal unit cells // *Applied Sciences*. ISSN 2076-3417. 2020, vol. 10, iss. 16, art. no. 5687, p. 1-8.

84. Gric, T.; Sokolovski, S.; Navolokin, N.; Glushkobskaya, O.; Rafailov, E. Metamaterial formalism approach for advancing the recognition of glioma areas in brain tissue biopsies // *Optical materials express*. ISSN 2159-3930. 2020, vol. 10, iss. 7, p. 1607-1615.

85. Grigaliūnaitė-Vonsevičienė, G.; Vengalis, B.; Maneikis, A.; Juškėnas, R. Magnetic and electrical properties of postannealed Co2MnSi Heusler alloy films // *Applied nanoscience*. ISSN 2190-5509. 2020, vol. 10, iss. 7, p. 2229-2237.

86. Grigelionis, I.; Diakonova, N.; Knap, W.; Teppe, F.; Prystawko, P.; Kašalynas, I. Radiation from shallow oxygen impurity in AlGaN/GaN HEMT structures in magnetic field // *Solid state communications*. ISSN 0038-1098. 2020, vol. 320, art. no. 114019, p. 1-4.

87. Grigelionis, I.; Kašalynas, I. Terahertz spectroscopy of thermal radiation from AlGaN/GaN heterostructure on sapphire at low temperatures // *Applied sciences*. eISSN 2076-3417. 2020, vol. 10, iss. 3, art. no. 851, p. 1-7.

88. Grinevičiūtė, L.; Buzelis, R.; Mažulė, L.; Melninkaitis, A.; Kičas, S.; Tolenis, T. Enhancement of high reflectivity mirrors using the combination of standard and sculptured thin films // *Optics & laser technology*. ISSN 0030-3992. 2020, vol. 129, art. no. 106292, p. 1-7.

89. Grivickas, P.; Ščajev, Patrik; Kazuchits, N.; Mazanik, A.; Korolik, O.; Voss, L. F.; Conway, A. M.; Hall, D. L.; Bora, M.; Subačius, L.; Bikbajevas, V.; Grivickas, V. Carrier recombination parameters in diamond after surface boron implantation and annealing // *Journal of applied physics*. ISSN 0021-8979. 2020, vol. 127, iss. 24, art. no. 245707, p. 1-6.

90. Gryaznov, D.; Stauffer, S. K.; Kotomin, E.A.; Vilčiauskas, L. Hybrid density functional theoretical study of NASICON-type NaxTi2(PO4)3 (x=1–4) // *Physical chemistry chemical physics*. ISSN 1463-9076. 2020, vol. 22, p. 11861-11870.

91. Gulbinas, V. Charge carrier mobility dynamics in organic semiconductors and solar cells // *Lithuanian Journal of Physics*. ISSN 1648-8504. 2020, vol. 60, no. 1, p. 1-25.

92. Ibenskas, A.; Šimėnas, M.; Kizlaitis, K.J.; Tornau, E. Pinwheel structures of deprotonated trimesic acid on Ag (111): model and simulations // *The journal of physical chemistry C.* ISSN 1932-7447. 2020, vol. 124, iss. 20, p. 11212-11220.

93. Ibenskas, A.; Tornau, E. Modeling of ribbon and oblique structures of benzene-1,3,5-triyl-tribenzoic acid // *Journal of physical chemistry C*. ISSN 1932-7447. 2020, vol. 124, iss. 34, p. 18650-18659.

94. Ioannidis, A.; Gric, T.; Rafailov, E. Surface plasmon polariton waves propagation at the boundary of graphene based metamaterial and corrugated metal in THz range // *Optical and quantum electronics*. ISSN 0306-8919. 2020, vol. 52, art. no. 10, p. 1-12.

95. Jablonskienė, J.; Šimkūnaitė, D.; Vaičiūnienė, J.; Selskis, A.; Drabavičius, A.; Jasulaitienė, V.; Tamašauskaitė-Tamašiūnaitė, L.; Norkus, E. Surfactant-assisted microwave synthesis of carbon supported MnO_2 nanocomposites and their application for electrochemical supercapacitors // *Chemija*. ISSN 0235-7216. 2020, vol. 31, no. 1, p. 11-24.

96. Jablonskienė, J.; Šimkūnaitė, D.; Vaičiūnienė, J.; Stalnionis, G.; Drabavičius, A.; Tamašauskaitė-Tamašiūnaitė, L.; Norkus, E. Carbon supported manganese (IV)–cobalt (II/III) oxides nanoparticles for high-performance electrochemical supercapa-citors // *Chemija*. ISSN 0235-7216. 2020, vol. 31, no. 2, p. 87-94.

97. Jagminas, A.; Naujokaitis, A.; Gaigalas, P.; Ramanavičius, S.; Kurtinaitienė, M.; Trusovas, R. Substrate impact on the structure and electrocatalyst properties of molybdenum disulfide for HER from water // *Metals*. ISSN 2075-4701. 2020, vol. 10, iss. 9, art. no. 1251, p. 1-12.

98. Janonis, V.; Tumėnas, S.; Prystawko, P.; Kacperski, J.; Kašalynas, I. Investigation of n-type gallium nitride grating for applications in coherent thermal sources // *Applied Physics Letters*. ISSN 0003-6951. 2020, vol. 116, iss. 11, art. no. 112103, p. 1-5.

99. Janulevičius, M.; Klimkevičius, V.; Mikoliūnaitė, L.; Vengalis, B.; Vargalis, R.; Šakirzanovas, S.; Plaušinaitienė, V.; Žilinskas, A.; Katelnikovas, Artūras. Ultralight magnetic nanofibrous $GdPO_4$ aerogel // *ACS Omega*. eISSN 2470-1343. 2020, vol. 5, no. 23, p. 14180-14185.

100. Jasaitis, D.; Klima, V.; Pečiulienė, M.; Vasiliauskienė, V.; Konstantinova, M. Comparative assessment of radiation background due to natural and artificial radionuclides in soil in specific areas on the territories of State of Washington (USA) and Lithuania // *Water, air & soil pollution*. ISSN 0049-6979. 2020, vol. 231, iss. 7, art. no. 347, p. 1-10.

101. Jasiūnas, R.; Gegevičius, R.; Franckevičius, M.; Jašinskas, V.; Gulbinas, V. Energy barriers restrict charge carrier motion in MAPI perovskite films // *Advanced optical materials*. ISSN 2195-1071. 2020, vol. 8, iss. 16, art. no. 2000036, p. 1-8.

102. Jasiūnas, R.; Gegevičius, R.; Franckevičius, M.; Phung, N.; Abate, A.; Gulbinas, V. Suppression of electron trapping in MAPbI3 Perovskite by Sr2+ doping // *Physica Status Solidi - Rapid Research Letters*. ISSN 1862-6254. 2020, vol. 14, issue 11, art. no. 2000307, p. 1-5.

103. Jasiūnas, R.; Zhang, H.; Yuan, J.; Zhou, X.; Qian, D.; Zou, Y.; Devižis, A.; Šulskus, J.; Gao, F.; Gulbinas, V. From generation to extraction: a time-resolved investigation of photophysical processes in non-fullerene organic solar cells // *Journal of physical chemistry C*. ISSN 1932-7447. 2020, vol. 124, no. 39, p. 21283-21292.

104. Javorskis, T.; Karpavičienė, I.; Jurys, A.; Snarskis, G.; Bukšnaitienė, R.; Orentas, E. An enolate-structure-enabled anionic cascade cyclization reaction: easy access to complex scaffolds with contiguous six-, five-, and four-membered rings // *Angewandte chemie international edition.* ISSN 1433-7851. 2020, vol. 59, iss. 45, p. 20120-20128.

105. Jefanova, O.; Baužienė, I.; Lujanienė, G.; Švedienė, J.; Raudonienė, V.; Bridžiuvienė, D.; Paškevičius, A.; Levinskaitė, L.; Žvirgždas, J.; Petrošius, R.; Skuratovič, Ž.; Mažeika, J. Initiation of radioecological monitoring of forest soils and plants at the Lithuanian border region before the start of the Belarusian nuclear power plant operation // *Environmental monitoring and assessment*. ISSN 0167-6369. 2020, vol. 192, iss. 10, art. no. 666, p. 1-18.

106. Jonauskė, V.; Ramanauskas, R.; Platakytė, R.; Niaura, G.; Mikoliūnaitė, L.; Ishikawa, K.; Kareiva, A. Formation of 2D calcium hydroxyapatite on stainless steel modified with a TiN sublayer // *Mendeleev communications*. ISSN 0959-9436. 2020, vol. 30, iss. 4, p. 512-515.

107. Jorudas, J.; Šimukovič, A.; Dub, M.; Sakowicz, M.; Prystawko, P.; Indrišiūnas, S.; Kovalevskij, V.; Rumyantsev, S.; Knap, W.; Kašalynas, I. AlGaN/GaN on SiC devices without a GaN buffer layer: electrical and noise characteristics // *Micromachines*. ISSN 2072-666X. 2020, vol. 11, iss. 12, art. no. 1131, p. 1-13.

108. Judžentienė, A.; Būdienė, J.; Švedienė, J.; Garjonytė, R. Toxic, radical scavenging, and antifungal activity of rhododendron tomentosum H. essential oils // *Molecules*. eISSN 1420-3049. 2020, vol. 25, iss. 7, art. no. 1676, p. 1-17.

109. Judžentienė, A. Review: Marsh rosemary (Rhododendron tomentosum Harmaja (ex Ledum palustre Linn) growing in Lithuania) essential oils and their properties // *Chemija*. ISSN 0235-7216. 2020, vol. 31, no. 4, p. 269-277.

110. Juodkazytė, J.; Petrulevičienė, M.; Parvin, M.; Šebeka, B.; Savickaja, I.; Pakštas, V.; Naujokaitis, A.; Virkutis, J.; Gegeckas, A. Activity of sol-gel derived nanocrystalline WO3 films in photo-electronchemical generation of reactive chlorine species // *Journal of electroanalytical chemistry*. ISSN 1572-6657. 2020, vol. 871, art. no. 114277, p. 1-9.

111. Juzeliūnas, E.; Fray, D.J. Silicon electrochemistry in molten salts // *Chemical reviews*. ISSN 0009-2665. 2020, vol. 120, iss. 3, p. 1690-1709.

112. Kaare, K.; Yu, E.; Volperts, A.; Dobele, G.; Zhurinsh, A.; Dyck, A.; Niaura, G.; Tamašauskaitė-Tamašiūnaitė, L.; Norkus, E.; Andrulevičius, M.; Danilson, M.; Kruusenberg, I. Highly active wood-derived nitrogen-doped carbon catalyst for the oxygen reduction reaction // *ACS Omega*. ISSN 2470-1343. 2020, vol. 5, no. 37, p. 23578-23587.

113. Kaciulis, S.; Bolli, E.; Mezzi, A.; Vagner, M.; Plaušinaitienė, V.; Keršulis, S.; Žurauskienė, N.; Lukošė, R. Surface and structural analysis of epitaxial La1−xSrx (Mn1−yCoy)zO3 films // *Surface and interface analysis*. ISSN 0142-2421. 2020, vol. 52, iss. 12, p. 900-906.

114. Kairytė, A.; Kremensas, A.; Balčiūnas, G.; Matulaitienė, I.; Czlonka, S.; Sienkiewicz, N. Evaluation of self-thermally treated wood plastic composites from wood bark and rapeseed oil-based binder // *Construction and building materials*. ISSN 0950-0618. 2020, vol. 250, art. no. 118842, p. 1-9.

115. Kalanda, N.; Yarmolich, M.; Kim, D.-H.; Baltrūnas, D.; Mažeika, K.; Tamulevičius, S.; Andrulevičius, M.; Sobolev, N.A. Valence state of iron and molybdenum cations under Conditions of anionic deficiency in Sr2FeMoO6– δ // *Physica status solidi B: Basic solid state physics*. ISSN 0370-1972. 2020, vol. 257, iss. 3, art. no. 1900387, p. 1-8.

116. Kalinauskas, P.; Norkus, E.; Mockus, Z.; Giraitis, R.; Stalnionis, G.; Jasulaitienė, V.; Juškėnas, R. The influence of removal of secondary phases and dissolution by-product from the surface of Cu2ZnSnS4 film on the photoelectrochemical response of this film // *Journal of the electrochemical society*. ISSN 0013-4651. 2020, vol. 167, iss. 2, art. no. 026513, p. 1-6.

117. Kamarauskas, M.; Agafonov, V.; Daugalas, T.; Balakauskas, S.; Mironas, A.; Nedzinskas, R.; Niaura, G.; Treideris, M.; Šetkus, A. Photovoltaic effect-driven IR response of heterojunctions obtained by direct CVD synthesis of MoS2 nanolayers on crystalline silicon // *Nanotechnology*. ISSN 0957-4484. 2020, vol. 31, iss. 42, art. no. 425603, p. 1-12.

118. Kamarauskas, M.; Treideris, M.; Agafonov, V.; Mironas, A.; Strazdienė, V.; Rėza, A.; Šetkus, A. Black silicon quality control by conditions of nickel-assisted etching of crystalline silicon surfaces in photovoltaic devices // *Lithuanian journal of physics*. ISSN 1648-8504. 2020, vol. 60, no. 1, p. 57-66.

119. Karaliūnas, M.; Udal, A.; Valušis, G. Depopulation mechanism for incoherent terahertz source – THz torch – based on GaAsBi/GaAs quantum well in GaAs/AlGaAs parabolic quantum well // *Lithuanian journal of physics*. ISSN 1648-8504. 2020, vol. 60, no. 2, p. 113-124.

120. Karitonas, R.; Jurkonienė, S.; Sadauskas, K.; Vaičiūnienė, J.; Manusadžianas, L. Modifying effects of leaf litter extracts from invasive versus native tree species on copper-induced responses in Lemna minor // *PeerJ.* ISSN 2167-8359. 2020, vol. 8, art. no. e9444, p. 1-28.

121. Karoblis, D.; Diliautas, R.; Raudonytė-Svirbutavičienė, E.; Mažeika, K.; Baltrūnas, D.A.; Beganskienė, A.; Žarkov, A.; Kareiva,. The synthesis and characterization of sol-gel-derived SrTiO3-BiMnO3 solid solutions // *Crystals*. ISSN 2073-4352. 2020, vol. 10, iss. 12, art. no. 1125, p. 1-11.

122. Karoblis, D.; Griesiūtė, D.; Mažeika, K.; Baltrūnas, D.A.; Karpinsky, D.; Lukowiak, A.; Gluchowski, P.; Raudonis, R.; Katelnikovas, A.; Žarkov, A.; Kareiva, A. A Facile Synthesis and Characterization of Highly Crystalline Submicro-Sized BiFeO3 // *Materials*. ISSN 1996-1944. 2020, vol. 13, iss. 13, art. no. 3035, p. 1-10.

123. Karoblis, D.; Mažeika, K.; Baltrūnas, D.A.; Lukowiak, A.; Strek, W.; Žarkov, A.; Kareiva, A. Novel synthetic approach to the preparation of single-phase BixLa1−xMnO3+δ solid solutions // *Journal of sol-gel science and technology*. ISSN 0928-0707. 2020, vol. 93, p. 650-656.

124. Karoblis, D.; Žarkov, A.; Mažeika, K.; Baltrūnas, D.A.; Niaura, G.; Beganskienė, A.; Kareiva, A. Sol-gel synthesis, structural, morphological and magnetic properties of BaTiO3–BiMnO3 solid solutions // *Ceramics international*. ISSN 0272-8842. 2020, vol. 46, no 10, part B, p. 16459-16464.

125. Kašėta, V.; Kaušylė, A.; Kavaliauskaitė, J.; Petreikytė, M.; Stirkė, A.; Biziulevičienė, G. Detection of intracellular biomarkers in viable cells using millisecond pulsed electric fields // *Experimental cell research*. ISSN 0014-4827. 2020, vol. 389, iss. 1, art. no. 111877, p. 1-7.

126. Kaušaitė-Minkštimienė, A.; Glumbokaitė, L.; Ramanavičienė, A.; Ramanavičius, A. Reagent-less amperometric glucose biosensor based on nanobiocomposite consisting of poly(1,10-phenanthroline-5,6-dione), poly(pyrrole-2-carboxylic acid), gold nanoparticles and glucose oxidase // *Microchemical journal*. ISSN 0026-265X. 2020, vol. 154, art. no. 104665, p. 1-7.

127. Kepenienė, V.; Stagniūnaitė, R.; Balčiūnaitė, A.; Tamašauskaitė-Tamašiūnaitė, L.; Norkus, E. Microwave-assisted synthesis of a AuCeO2/C catalyst and its application for the oxidation of alcohols in an alkaline medium // *New journal of chemistry*. ISSN 1144-0546. 2020, vol. 44, iss. 42, p. 18308-18318.

128. Kepenienė, V.; Stagniūnaitė, R.; Tamašauskaitė-Tamašiūnaitė, L.; Pakštas, V.; Jasulaitienė, V.; Léger, B.; Rousseau, J.; Ponchel, A.; Monflier, E.; Norkus, E. Co3O4/C and Au supported Co3O4/C nanocomposites – Peculiarities of fabrication and application

towards oxygen reduction reaction // *Materials chemistry and physics*. ISSN 0254-0584. 2020, vol. 241, art. no. 122332, p. 1-11.

129. Kepenienė, V.; Stagniūnaitė, R.; Upskuvienė, D.; Tamašauskaitė-Tamašiūnaitė, L.; Pakštas, V.; Drabavičius, A.; Andrulevičius, M.; Norkus, E. Electrocatalytic activity of AuCeO2/C towards ethylene glycol oxidation and oxygen reduction reactions // Chemija. ISSN 0235-7216. 2020, vol. 31, no. 2, p. 57-68.

130. Kiprijanovič, O.; Ardaravičius, L.; Gradauskas, J.; Šimkevičius, Č.; Keršulis, S.; Ašmontas, S. S-N border instability, magnetic flux trapping and cumulative effect during pulsed S-N switching of high quality YBaCuO thin films // *Superconductor science and technology*. ISSN 0953-2048. 2020, vol. 33, no. 9, art. no. 095013, p. 1-8.

131. Klimkevičius, V.; Janulevičius, M.; Babičeva, A.; Drabavičius, A.; Katelnikovas, A. Effect of cationic brush-type copolymers on the colloidal stability of GdPO4 particles with different morphologies in biological aqueous media // *Langmuir*. ISSN 0743-7463. 2020, vol. 36, no. 26, p. 7533-7544.

132. Kochanė, T.; Zabarauskė, I.; Klimkevičienė, L.; Strakšys, A.; Mačiulytė, S.; Navickaitė, L.; Gailiūnaitė, S.; Budrienė, S. Starch hydrolysis using maltogenase immobilized via different techniques // *International journal of biological macromolecules*. ISSN 0141-8130. 2020, vol. 144, p. 544-552.

133. Kolenda, M.; Kezys, D.; Reklaitis, I.; Radiunas, E.; Ritasalo, R.; Kadys, A.; Grinys, T.; Malinauskas, T.; Stanionytė, S.; Skapas, M.; Petruškevičius, R.; Tomašiūnas, R. Development of polarity inversion in a GaN waveguide structure for modal phase matching // *Journal of materials science*. ISSN 0022-2461. 2020, vol. 55, p. 12008-12021.

134. Konkel, R.; Toruńska-Sitarz, A.; Cegłowska, M.; Ežerinskis, Ž.; Šapolaitė, J.; Mažeika, J.; Mazur-Marzec, H. Blooms of toxic cyanobacterium Nodularia spumigena in Norwegian fjords during Holocene warm periods // *Toxins*. eISSN 2072-6651. 2020, vol. 12, iss. 4, art. no. 257, p. 1-12.

135. Koroliov, A.; Reklaitis, J.; Varsockaja, K.; Germanas, D.; Plukis, A.; Remeikis, V. X-ray pulse emission of alkali metal halide salts irradiated by femtosecond laser pulses // *Applied physics B. Lasers and optics*. ISSN 0946-2171. 2020, vol. 126, iss. 9, art. no. 144, p. 1-7.

136. Korotieiev, V.; Kochelap, V.A. Plasma wave oscillations in a nonequilibrium two-dimensional electron gas: Electric field induced plasmon instability in the terahertz frequency range // *Physical review B.* ISSN 2469-9950. 2020, vol. 101, iss. 23, art. no 235420, p. 1-15.

137. Koulouklidis, A.D.; Gollner, C.; Shumakova, V.; Fedorov, V.Yu.; Pugžlys, A.; Baltuška, A.; Tzortzakis, S. Observation of extremely efficient terahertz generation from mid-infrared two-color laser filaments // *Nature communications*. eISSN 2041-1723. 2020, vol. 11, art. no. 292, p. 1-8.

138. Kristensson, A.; Ausmeel, S.; Pauraitė, J.; Eriksson, A.; Ahlberg, E.; Byčenkienė, S.; Degórska, A. Source contributions to rural carbonaceous winter aerosol in North-Eastern Poland // *Atmosphere*. ISSN 2073-4433. 2020, vol. 11, iss. 3, art. no. 263, p. 1-19.

139. Ksenevich, V.; Dorosinets, V.; Adamchuk, D.; Macutkevič, J.; Banys, J. Weak localization in polycrystalline tin dioxide films // *Materials*. ISSN 1996-1944. 2020, vol. 13, iss. 23, art. no. 5415, p. 1-14.

140. Kumagai, T.; To, N.; Balčytis, A.; Seniutinas, G.; Juodkazis, S.; Nishijima, Y. Kirchhoff's thermal radiation from lithography-free black metals // *Micromachines*. ISSN 2072-666X. 2020, vol. 11, iss. 9, art. no. 824, p. 1-13.

141. Kuodis, Z.; Matulaitienė, I.; Špandyreva, M.; Labanauskas, L.; Stončius, S.; Eicher-Lorka, O.; Sadzevičienė, R.; Niaura, G. Reflection absorption infrared spectroscopy characterization of SAM formation from 8-Mercapto-N-(phenethyl)octanamide thiols with phe ring and amide groups // *Molecules*. ISSN 1420-3049. 2020, vol. 25, iss. 23, art. no. 5633, p. 1-14.

142. Laurikėnas, A.; Mažeika, K.; Baltrūnas, D.A.; Skaudžius, R.; Beganskienė, A.; Kareiva, A. Hybrid organic-inorganic $Fe_3O(TFBDC)_3(H_2O)_3\cdot(DMF)_3$ compound synthesized by slow evaporation method: characterization and comparison of magnetic properties // *Lithuanian journal of physics*. ISSN 1648-8504. 2020, vol. 60, no. 1, p. 78-89.

143. Ledesma, M.; Gorokhova, E.; Holmstrand, H.; Garbaras, A.; Karlson, A.M.L. Nitrogen isotope composition of amino acids reveals trophic partitioning in two sympatric amphipods // *Ecology and evolution*. ISSN 2045-7758. 2020, vol. 10, iss. 19, p. 10773-10784.

144. Ledinauskas, E.; Zubovas, K. Evolution of dwarf galaxy observable parameters // *Monthly notices ofthe Royal Astronomical Society*. ISSN 0035-8711. 2020, vol. 493, iss. 1, p. 638-650.

145. Leinartas, K.; Juzeliūnas, E.; Staišiūnas, L.; Selskis, A.; Grigucevičienė, A.; Bučinskienė, D.; Juškėnas, R.; Ručinskienė, A. Early stages of Mg–Nb alloy corrosion in a balanced salt solution – STEM-HAADF and EIS study // *Chemija*. ISSN 0235-7216. 2020, vol. 31, no. 3, p. 119-129.

146. Liashenko, T.; Pushkarev, A.; Naujokaitis, A.; Pakštas, V.; Franckevičius, M.; Zakhidov, A.; Makarov, S. Suppression of electric field-induced segregation in sky-blue perovskite light-emitting electrochemical cells // *Nanomaterials*. ISSN 2079-4991. 2020, vol. 10, iss. 10, art. no. 1937, p. 1-13.

147. Linklater, D.P.; Haydous, F.; Xi, Ch.; Pergolesi, D.; Hu, J.; Ivanova, E.P.; Juodkazis, S.; Lippert, Th.; Juodkazytė, J. Black-Si as a photoelectrode // *Nanomaterials*. ISSN 2079-4991. 2020, vol. 10, iss. 5, art. no. 873, p. 1-13.

148. Lu, S.; Ding, H.; Hu, J.; Liu, Yu.; Zhu, J.; Kondrotas, R.; Chen, Ch.; Tang, J. In situ investigation of interfacial properties of Sb2Se3 heterojunctions // *Applied physics letters*. ISSN 0003-6951. 2020, vol. 116, iss. 24, art. no. 241602, p. 1-5.

149. Mačiulis, V.M.; Malinovskis, U.; Erts, D.; Ramanavičius, A.; Ramanavičienė, A.; Balevičius, S.; Juciutė, S.; Plikusienė, I. Porous aluminium oxide coating for the development of spectroscopic ellipsometry based biosensor: evaluation of human serum albumin ddsorption // *Coatings*. ISSN 2079-6412. 2020, vol. 10, iss. 11, art. no. 1018, p. 1-10.

150. Mackonis, P.; Petrulėnas, A.; Rodin, A.; Girdauskas, V.; Michailovas, A. Two-stage transient stimulated Raman chirped-pulse amplification in KGd (WO4)2 with compression to 145 fs // *Optics letters*. ISSN 0146-9592. 2020, vol. 45, no. 24, p. 6627-6630.

151. Mackonis, Paulius; Rodin, Aleksej. Laser with 1.2 ps, 20 mJ pulses at 100 Hz based on CPA with a low doping level Yb:YAG rods for seeding and pumping of OPCPA // Optics express. ISSN 1094-4087. 2020, vol. 28, no. 2, p. 1261-1268.

152. Mackonis, P.; Rodin, A. OPCPA investigation with control over the temporal shape of 1.2 ps pump pulses // *Optics express*. ISSN 1094-4087. 2020, vol. 28, no. 8, p. 12020-12027.

153. Maminskas, J.; Pilipavičius, J.; Staisiunas, E.; Baranovas, G.; Alksne, M.; Daugela, P.; Juodzbalys, G. Novel Yttria-Stabilized Zirconium Oxide and Lithium Disilicate Coatings on Titanium Alloy Substrate for Implant Abutments and Biomedical Application // *Materials*. ISSN 1996-1944. 2020, vol. 13, no. 9, art. no. 2070, p. 1-19.

154. Markauskas, E.; Zubauskas, L.; Račiukaitis, G.; Gečys, P. Damage-free patterning of thermally sensitive CIGS thin-film solar cells: Can nanosecond pulses outperform ultrashort laser pulses? // *Solar energy*. ISSN 0038-092X. 2020, vol. 202, p. 514-521.

155. Marsden, Ch.; Shankar, F.; Ginolfi, M.; Zubovas, K. The case for the fundamental MBH-σ relation // *Frontiers in physics*. ISSN 2296-424X. 2020, vol. 8, art. no. 61, p. 1-13.

156. Mašalaitė-Nalivaikė, A.; Remeikis, V.; Zenker, K.; Westra, I.; Meijer, H.A.J.; Dusek, U. Seasonal changes of sources and volatility of carbonaceous aerosol at urban, coastal and forest sites in Eastern Europe (Lithuania) // *Atmospheric environment*. ISSN 1352-2310. 2020, vol. 225, art. no. 117374, p. 1-11.

157. Mascoli, V.; Gelžinis, A.; Chmeliov, J.; Valkūnas, L.; Croce, R. Light-harvesting complexes access analogue emissive states in different environments // *Chemical science*. ISSN 2041-6520. 2020, vol. 11, iss. 22, p. 5697-5709.

158. Matijošius, T.; Pivoriūnas, A.; Čebatariūnienė, A.; Tunaitis, V.; Staišiūnas, L.; Stalnionis, G.; Ručinskienė, A.; Asadauskas, S. Friction reduction using Nanothin Titanium layers on anodized aluminum as potential bioceramic material // *Ceramics international*. ISSN 0272-8842. 2020, vol. 46, iss. 10, pt. A, p. 15581-15593.

159. Matulis, A.; Acus, A. Negative flow of energy in a mechanical wave // *Lithuanian journal of physics*. ISSN 1648-8504. 2020, vol. 60, no. 4, p. 205-216.

160. Mažeikienė, R.; Niaura, G.; Malinauskas, A. Differential multi-wavelength Raman study of electrochemical redox transitions of polyaniline in solutions of different acidities // *Spectrochimica acta. Part A: Molecular and biomolecular spectroscopy*. ISSN 1386-1425. 2020, vol. 229, art. no. 117991, p. 1-8.

161. Meisak, D.; Macutkevič, J.; Plyushch, A.; Polina, K.; Selskis, A.; Banys, J. Dielectric relaxation in hybrid epoxy/MWCNT/$MnFe_2O_4$ composites // *Polymers*. eISSN 2073-4360. 2020, vol. 12, iss. 3, art. no. 697, p. 1-13.

162. Meisak, D.; Macutkevič, J.; Selskis, A.; Banys, J.; Kuzhir, P. Dielectric properties and electrical percolation in $MnFe_2O_4$/epoxy resin composites // *Physica status solidi A-Applications and materials science*. ISSN 1862-6300. 2020, vol. 217, iss. 6, art. no. 1900526, p. 1-6.

163. Melnikas, S.; Gimževskis, U.; Kičas, S. Stress compensated back side coated chirped mirror with high negative dispersion // *Optics and laser technology*. ISSN 0030-3992. 2020, vol. 121, art. no. 105820, p. 1-5.

164. Melvydas, V.B.; Švedienė, J.; Skridlaitė, G.; Vaičiūnienė, J.; Garjonytė, R. In vitro inhibition of Saccharomyces cerevisiae growth by Metschnikowia spp. triggered by fast removal of iron via two ways // *Brazilian journal of microbiology*. ISSN 1517-8382. 2020, vol. 51, iss. 4, p. 1953-1964.

165. Meškinis, Š.; Gudaitis, R.; Vasiliauskas, A.; Tamulevičius, S.; Niaura, G. Multiwavelength Raman scattering spectroscopy study of graphene synthesized on Si(100) and SiO_2 by microwave plasma-enhanced chemical vapor deposition // *Physica status solidi - rapid research letters: Special issue: Two-dimensional semiconductors*. ISSN 1862-6254. 2020, vol. 14, iss. 2, art. no.1900462, p. 1-5.

166. Mickiene, G.; Dalgėdienė, I.; Zvirblis, G.; Dapkunas, Z.; Plikusiene, I.; Bužavaitė-Vertelienė, E.; Balevičius, Z.; Rukšėnaitė, A.; Plečkaitytė, M. Human granulocyte-colony stimulating factor (G-CSF)/stem cell factor (SCF) fusion proteins: design, characterization and activity // *PeerJ*. eISSN 2167-8359. 2020, vol. 8, art. no. c9788, p. 1-23.

167. Minkevičius, L.; Qi, L.; Siemion, A.; Jokubauskis, D.; Sešek, A.; Švigelj, A.; Trontelj, J.; Seliuta, D.; Kašalynas, I.; Valušis, G. Titanium-based microbolometers: control of spatial profile of terahertz emission in weak power sources // *Applied sciences*. eISSN 2076-3417. 2020, vol. 10, iss. 10, art. no 3400, p. 1-12.

168. Mockus, Z.; Norkus, E.; Vaitkus, R.; Kalinauskas, P.; Grincienė, G.; Tamašauskaitė-Tamašiūnaitė, L. Inhibition of Sn(II) oxidation by air oxygen in acidic gluconate-containing solutions // *Journal of the electrochemical society*. ISSN 0013-4651. 2020, vol. 167, iss. 12, art. no. 122503, p. 1-8.

169. Mordas, G.; Jasulaitienė, V.; Steponavičiūtė, A.; Gaspariūnas, M.; Petkevič, R.; Selskienė, A.; Juškėnas, R.; Paul, D.F.; Mann, J.E.; Remeikis, V.; Račiukaitis, G. Characterisation of CoCrMo powder for additive manufacturing // *The international journal of advanced manufacturing technology*. ISSN 0268-3768. 2020, vol. 111, iss. 11-12, p. 3083-3093.

170. Nishijima, Y.; Enomonoto, K.; Okazaki, Sh.; Arakawa, T.; Balčytis, A.; Juodkazis, S. Pulsed laser deposition of Pt-WO3 of hydrogen sensors under atmospheric conditions // *Applied surface science*. ISSN 0169-4332. 2020, vol. 534, art. no. 147568, p. 1-6.

171. Norkus, R.; Nevinskas, I.; Krotkus, A. Terahertz emission from a bulk GaSe crystal excited by above bandgap photons // *Journal of applied physics*. ISSN 0021-8979. 2020, vol. 128, iss. 22, art. no. 225701, p. 1-6.

172. Onufrijevs, P.; Ščajev, P.; Medvids, A.; Andrulevicius, M.; Nargelas, S.; Malinauskas, T.; Stanionytė, S.; Skapas, M.; Grase, L.; Pludons, A.; Oehme, M.; Lyutovich, K.; Kasper, E.; Schulze, J.; Cheng, H.H. Direct-indirect GeSn band structure formation by laser radiation: the enhancement of Sn solubility in Ge // *Optics and laser technology*. ISSN 0030-3992. 2020, vol. 128, art. no. 106200, p. 1-7.

173. Orlovas, S.; Berškys, J. Vector-spherical-harmonics representation of vector complex source beams carrying vortices // *Physical review A*. ISSN 2469-9926. 2020, vol. 102, iss. 6, art. no. 063532, p. 1-10.

174. Orlovas, S.; Huber, Ch.; Marchenko, P.; Banzer, P.; Leuchs, G. Towards a corrected knife-edge-based reconstruction of tightly focused higher order beams // *Frontiers in physics*. ISSN 2296-424X. 2020, vol. 8, art. no. 527734, p. 1-10.

175. Pačebutas, V.; Čechavičius, B.; Krotkus, A. Single quantum well diodes from GaInAsBi emitting at wavelengths up to 2.5 μm // *Infrared physics & technology*. ISSN 1350-4495. 2020, vol. 111, art. no. 103567, p. 1-5.

176. Pačebutas, V.; Norkus, R.; Karpus, V.; Geižutis, A.; Strazdienė, V.; Stanionytė, S.; Krotkus, A. Band-offsets of GaInAsBi–InP heterojunctions // *Infrared physics & technology*. ISSN 1350-4495. 2020, vol. 109, art. no. 103400, p. 1-4.

177. Paddubskaya, A.; Rutkauskas, D.; Karpič, R.; Dovbeshko, G.; Nebogatikova, N.; Antonova, I.; Dementjev, A. Recognition of spatial distribution of CNT and graphene in hybrid structure by mapping with coherent anti-Stokes Raman microscopy // *Nanoscale research letters*. ISSN 1931-7573. 2020, vol. 15, art. no. 37, p. 1-7.

178. Padleckienė, I.; Stygienė, L.; Krauledas, S. Development and investigation of a textile heating element ensuring thermal physiological comfort // *Fibres & textiles in Eastern Europe*. ISSN 1230-3666. 2020, vol. 28, iss. 5, p. 56-62.

179. Paek, S.; Roldán-Carmona, C.; Cho, K.T.; Franckevičius, M.; Kim, H.; Kanda, H.; Drigo, N.; Lin, K.-H.; Pei, M.; Gegevičius, R.; Yun, H. J.; Yang, H.; Schouwink, P.A.; Corminboeuf, C.; Asiri, Abdullah M.; Nazeeruddin, M.K. Molecular design and operational stability: toward stable 3D/2D perovskite interlayers // *Advanced science*. eISSN 2198-3844. 2020, vol. 7, iss. 19, art. no. 2001014, p. 1-11.

180. Pakalniškis, A.; Baltrūnas, D.A.; Mažeika, K.; Skaudžius, R.; Ramanauskas, R.; Kareiva, A. Reinspection of low temperature synthesis of bulk Bi3Fe5O12 (BIG): An aqueous sol-gel processing // *Materials chemistry and physics*. ISSN 0254-0584. 2020, vol. 253, art. no. 123283, p. 1-6.

181. Pakštas, V.; Grincienė, G.; Kamarauskas, E.; Giraitis, R.; Skapas, M.; Selskis, A.; Juškėnas, R.; Niaura, G.; Franckevičius, M. Impact of CdS layer thickness on the composition, structure and photovoltaic performance of superstrate CZTSSe solar cells // *Solar energy*. ISSN 0038-092X. 2020, vol. 207, p. 1231-1239.

182. Palaimienė, E.; Macutkevič, J.; Banys, J.; Gruszka, I.; Kania, A. Broadband and infrared spectroscopy of Ag0.98Li0.02NbO3 ceramics // *Lithuanian journal of physics*. ISSN 1648-8504. 2020, vol. 60, no. 4, p. 247-252.

183. Palaimienė, E.; Schaefer, S.; Macutkevič, J.; Banys, J.; Selskis, A.; Fierro, V.; Alain, C. Electrical percolation and electromagnetic properties of polydimethylsiloxane composites filled with Ag

nanoparticles of different sizes // *Polymer composites*. ISSN 0272-8397. 2020, vol. 41, vol. 11, p. 4750-4756.

184. Pashnev, D.; Kaplas, T.S.; Korotyeyev, V.; Janonis, V.; Urbanovič, A.; Jorudas, J.; Kašalynas, I. Terahertz time-domain spectroscopy of two-dimensional plasmons in AlGaN/GaN heterostructures // *Applied physics letters*. ISSN 0003-6951. 2020, vol. 117, iss. 5, art. no. 051105, p. 1-5.

185. Pashnev, D.; Korotyeyev, V.; Jorudas, J.; Kaplas, T.S.; Janonis, V.; Urbanovič, A.; Kašalynas, I. Experimental evidence of temperature dependent effective mass in AlGaN/GaN heterostructures observed via THz spectroscopy of 2D plasmons // *Applied physics letters*. ISSN 0003-6951. 2020, vol. 117, iss. 16, art. no. 162101, p. 1-5.

186. Paulauskas, T.; Čechavičius, B.; Karpus, V.; Jočionis, L.; Tumėnas, S.; Devenson, J.; Pačebutas, V.; Stanionytė, S.; Strazdienė, V.; Geižutis, A.; Čaplovičová, M.; Vretenár, V.; Walls, M.; Krotkus, A. Pola-rization dependent photoluminescence and optical anisotropy in CuPtB-ordered dilute GaAs1–xBix alloys // *Journal of applied physics*. ISSN 0021-8979. 2020, vol. 128, iss. 19, art. no. 195106, p. 1-10.

187. Paulauskas, T.; Pačebutas, V.; Butkutė, R.; Čechavičius, B.; Naujokaitis, A.; Kamarauskas, M.; Skapas, M.; Devenson, J.; Čaplovičová, M.; Vretenár, V.; Li, X.; Kociak, M.; Krotkus, A. Atomic-resolution EDX, HAADF, and EELS study of GaAs1-xBix alloys // *Nanoscale research letters*. ISSN 1931-7573. 2020, vol. 15, art. no. 121, p. 1-12.

188. Paulauskas, T.; Pačebutas, V.; Geižutis, A.; Stanionytė, S.; Dudutienė, E.; Skapas, M.; Naujokaitis, A.; Strazdienė, V.; Čechavičius, B.; Čaplovičová, M.; Vretenár, V.; Jakieła, R.; Krotkus, A. GaAs1-xBix growth on Ge: anti-phase domains, ordering, and exciton localization // *Scientific reports*. eISSN 2045-2322. 2020, vol. 10, art. no. 2002, p. 1-12.

189. Pauliukaitė, R.; Voitechovič, E. Multisensor systems and arrays for medical applications employing naturally-occurring compounds and materials // *Sensors*. ISSN 1424-8220. 2020, vol. 20, iss. 12, art. no. 3551, p. 1-38.

190. Petronienė, J.J.; Morkvėnaitė-Vilkončienė, I.; Mikšiūnas, R.; Bironaite, D.; Ramanavičienė, A.; Mikoliūnaitė, L.; Kisieliūtė, A.; Ručinskas, K.; Janušauskas, V.; Plikusienė, I.; Labeit, S.; Ramanavičius, A. Evaluation of redox activity of human myocardium-derived mesenchymal stem cells by scanning electrochemical microscopy // *Electroanalysis*. ISSN 1040-0397. 2020, vol. 32, no. 6, p. 1337-1345.

191. Petronienė, J.J.; Morkvėnaitė-Vilkončienė, I.; Mikšiūnas, R.; Bironaitė, D.; Ramanavičienė, A.; Ručinskas, K.; Janušauskas, V.; Ramanavičius, A. Scanning electrochemical microscopy for the investigation of redox potential of human myocardium-derived mesenchymal stem cells grown at 2D and 3D conditions // *Electrochimica acta*. ISSN 0013-4686. 2020, vol. 360, art. no. 136956, p. 1-9.

192. Petrulevičienė, M.; Juodkazytė, J.; Parvin, M.; Tereshchenko, A.; Ramanavičius, S.; Karpič, R.; Samukaitė-Bubnienė, U.; Ramanavičius, A. Tuning the photo-luminescence properties of Wo3 layers by the adjustment of layer formation conditions // *Materials*. eISSN 1996-1944. 2020, vol. 13, iss. 12, art. no. 2814, p. 1-14.

193. Petruškevičius, R.; Balčytis, A.; Urbonas, D.; Vaškevičius, K.; Juodkazis, S. Microring resonators with circular element inner-wall gratings for enhanced sensing // *Japanese journal of applied physics.* ISSN 0021-4922. 2020, vol. 59, no. SO, art. no. SOOD02, p. 1-7.

194. Plaušinaitis, D.; Balčiūnas, D.; Ramanavičius, A. Synthesis of heterogeneously conductive polypyrrole layer from non-aqueous solution using the double-step potential technique // *Journal of the electrochemical society*. ISSN 0013-4651. 2020, vol. 167, iss. 8, art. no. 086510, p. 1-10.

195. Plaušinaitis, D.; Sinkevičius, L.; Samukaitė-Bubnienė, U.; Ratautaitė, V.; Ramanavičius, A. Evaluation of electrochemical quartz crystal microbalance based sensor modified by uric acid-imprinted polypyrrole // *Talanta*. ISSN 0039-9140. 2020, vol. 220, art. no. 121414, p. 1-7.

196. Plikusienė, I.; Balevičius, Z.; Ramanavičienė, A.; Talbot, J.; Mickienė, G.; Balevičius, S.; Stirkė, A.; Tereshchenko, A.; Tamošaitis, L.; Žvirblis, G.; Ramanavičius, A. Evaluation of affinity sensor response kinetics towards dimeric ligands linked with spacers of different rigidity: Immobilized recombinant granulocyte colony-stimulating factor based synthetic receptor binding with genetically engineered dimeric analyte derivatives // *Biosensors and bioelectronics*. ISSN 0956-5663. 2020, vol. 156, art. no. 112112, p. 1-8.

197. Polita, A.; Toliautas, S.; Žvirblis, R.; Vyšniauskas, A. The effect of solvent polarity and macromolecular crowding on the viscosity sensitivity of a molecular rotor BODIPY-C10 // *Physical chemistry chemical physics*. ISSN 1463-9076. 2020, vol. 22, iss. 16, p. 8296-8303.

198. Popov, A.; Brasiūnas, B.; Damaškaitė, A.; Plikusienė, I.; Ramanavičius, A.; Ramanavičienė, A. Electrodeposited gold nanostructures for the enhancement of electrochromic properties of PANI–PEDOT film deposited on transparent electrode // *Polymers*. eISSN 2073-4360. 2020, vol. 12, iss. 12, art. no. 2778, p. 1-14.

199. Prielaidas, Ž.; Juodkazis, S.; Stankevičius, E. Thermal control of SZ2080 photopolymerization in four-beam interference lithography // *Physical chemistry chemical physics*. ISSN 1463-9076. 2020, vol. 22, p. 5038-5045.

200. Prokopčiuk, N.; Franck, U.; Dudoitis, V.; Tarasiuk, N.; Juškienė, I.; Čepuraitė, D.; Štaras, K.; Valiulis, A.; Ulevičius, V.; Valiulis, A. Global Alliance against Chronic Respiratory Diseases demonstration project: aerosol pollution and its seasonal peculiarities in primary schools of Vilnius // *Chinese medical journal*. ISSN 0366-6999. 2020, vol. 133, iss. 13, p. 1516-1525.

201. Prokopčiuk, N.; Franck, U.; Dudoitis, V.; Tarasyuk, N.; Juškienė, I.; Valiulis, A.; Čepuraitė, D.; Štaras, K.; Ulevičius, V. On the seasonal aerosol pollution levels and its sources in some primary schools in Vilnius, Lithuania // *Environmental science and pollution research*. ISSN 0944-1344. 2020, vol. 27, iss. 13, p. 15592-15606.

202. Pyragas, K.; Fedaravičius, A.P.; Pyragienė, T. Entrainment of a network of interacting neurons with minimum stimulating charge // *Physical review E*. ISSN 2470-0045. 2020, vol.102, iss. 1, art. no. 012221, p. 1-10.

203. Pyragas, V.; Pyragas, K. Using reservoir computer to predict and prevent extreme events // *Physics letters A.* ISSN 0375-9601. 2020, vol. 384, iss. 24, art. no 126591, p. 1-9.

204. Ragulis, P.; Andreev, D.; De Alleluia, A.B.; Simniškis, R.; Kamarauskas, M.; Dagys, M.; Schamiloglu, E.; Kancleris, Ž. A. Short-pulse HPM measurements using a resistive sensor // *IET microwaves antennas & propagation*. ISSN 1751-8725. 2020, vol.14, iss. 13, p. 1655-1661.

205. Rakauskas, V.; Šidagytė-Copilas, E.; Stakėnas, S.; Garbaras, A. Invasive Neogobius melanostomus in the Lithuanian Baltic Sea coast: Trophic role and impact on the diet of piscivorous fish // *Journal of Great Lakes research*. ISSN 0380-1330. 2020, vol. 46, iss. 3, p. 597-608.

206. Ramanavičius, S.; Petrulevičienė, M.; Juodkazytė, J.; Grigucevičienė, A.; Ramanavičius, A. Selectivity of tungsten oxide synthesized by Sol-Gel method towards some volatile organic compounds and gaseous materials in a broad range of temperatures // *Materials*. eISSN 1996-1944. 2020, vol. 13, iss. 3, art. no. 523, p. 1-17.

207. Ramanavičius, S.; Ramanavičius, A. Insights in the application of stoichiometric and non-stoichiometric titanium oxides for the design of sensors for the determination of gases and VOCs (TiO2−x and TinO2n−1 vs. TiO2) // *Sensors*. ISSN 1424-8220. 2020, vol. 20, iss. 23, art. no. 6833, p. 1-18.

208. Ramanavičius, S.; Ramanavičius, A. Progress and insights in the application of MXenes as new 2D nano-materials suitable for

biosensors and biofuel cell design // *International journal of molecular sciences.* eISSN 1422-0067. 2020, vol. 21, iss. 23, art. no. 9224, p. 1-17.

209. Ramanavičius, S.; Tereshchenko, A.; Karpič, R.; Ratautaitė, V.; Samukaitė-Bubnienė, U.; Maneikis, A.; Jagminas, A.; Ramanavičius, A. TiO2-x/TiO2-structure based 'self-heated' sensor for the determination of some reducing gases // *Sensors*. ISSN 1424-8220. 2020, vol. 20, iss. 1, art. no. 74, p. 1-17.

210. Ramonas, M.; Liberis, J.; Šimukovič, A.; Šermukšnis, E.; Matulionis, A.; Avrutin, V.; Özgür, Ü.; Morkoç, H. Terahertz oscillations in gallium nitride quantum-well channels predicted by hot-electron noise temperature behavior at microwave frequency // *Journal of applied physics*. ISSN 0021-8979. 2020, vol. 128, iss. 5, art. no. 055702, p. 1-11.

211. Ratautas, K.; Jagminienė, A.; Stankevičienė, I.; Sadauskas, M.; Norkus, E.; Račiukaitis, G. Evaluation and optimisation of the SSAIL method for laser-assisted selective electroless copper deposition on dielectrics // *Results in physics*. ISSN 2211-3797. 2020, vol. 16, art. no. 102943, p. 1-10.

212. Ratautas, K.; Vosylius, V.; Jagminienė, A.; Stankevičienė, I.; Norkus, E.; Račiukaitis, G.. Laser-induced selective electroless plating on PC/ABS polymer: minimisation of thermal effects for supreme processing speed // *Polymers*. ISSN 2073-4360. 2020, vol. 12, iss. 10, art. no. 2427, p. 1-16.

213. Reklaitis, I.; Radiunas, E.; Malinauskas, T.; Stanionytė, S.; Juška, G.; Ritasalo, R.; Pilvi, T.; Taeger, S.; Strassburg, M. A comparative study on atomic layer deposited oxide film morphology and their electrical breakdown // *Surface & coatings technology*. ISSN 0257-8972. 2020, vol. 399, art. no. 126123, p. 1-15.

214. Remeikis, V.; Plukienė, R.; Plukis, A.; Barkauskas, V.; Gudelis, A.; Druteikienė, R.; Gvozdaitė, R.; Juodis, L.; Duškesas, G.; Lagzdina, E.; Germanas, D.; Ridikas, D.; Krutovcov, S. Characterisation of RBMK-1500 graphite: A method to identify the neutron activation and surface contamination terms // *Nuclear engineering and design*. ISSN 0029-5493. 2020, vol. 361, art. no. 110501, p. 1-10.

215. Rimkus, T.; Ežerinskis, Ž.; Šapolaitė, J.; Peseckas, K. Mesolithic AMS 14C evidence on microlithic and pressure blade technology in the lakeland of eastern Lithuania // *Lithic technology*. ISSN 0197-7261. 2020, vol. 45, no. 4, p. 215-226.

216. Rovige, L.; Huijts, J.; Andriyash, I.; Vernier, A.; Tomkus, V.; Girdauskas, V.; Račiukaitis, G.; Dudutis, J.; Stankevič, V.; Gečys, P.; Ouille, M.; Cheng, Z.; Lopez-Martens, R.; Faure, J. Demonstration of stable long-term operation of a kilohertz laser-plasma accelerator // *Physical review accelerators and beams*. ISSN 2469-9888. 2020, vol. 23, art. no. 093401, p. 1-9.

217. Rudzikas, M.; Šetkus, A.; Stange, M.; Ulbikas, J.; Ulyashin, A. Simple interference based colorization of Si based solar cells and panels with ITO/SiNx:H double layer antireflective coatings // *Solar energy*. ISSN 0038-092X. 2020, vol. 207, p. 218-227.

218. Sadaunykas, A.; Zolumskis, A.; Markevičius, A.; Naujalis, E. On-column cryofocusing and analyte enrichment device for gas chromatography systems // *Chemija*. ISSN 0235-7216. 2020, vol. 31, no. 4, p. 284-289.

219. Sakavičius, A.; Agafonov, V.; Bukauskas, V.; Daugalas, T.; Kamarauskas, M.; Lukša, A.; Nargelienė, V.; Niaura, G.; Treideris, M.; Šetkus, A. Long-time drift induced changes in electrical characteristics of graphene–metal contacts // *Lithuanian journal of physics.* ISSN 1648-8504. 2020, vol. 60, no. 4, p. 235-246.

220. Sakavičius, A.; Astromskas, G.; Bukauskas, V.; Kamarauskas, M.; Lukša, A.; Nargelienė, Vi.; Niaura, G.; Ignatjev, I.; Treideris, M.; Šetkus, A. Long distance distortions in the graphene near the edge of planar metal contacts // *Thin solid films*. ISSN 0040-6090. 2020, vol. 698, art. no. 137850, p. 1-10.

221. Samukaitė-Bubnienė, U.; Mazetyte-Stasinskiene, R.; Chernyakova, K.; Karpič, R.; Ramanavičius, A. Time-resolved fluorescence spectroscopy based evaluation of stability of glucose oxidase // *International journal of biological macromolecules*. ISSN 0141-8130. 2020, vol. 163, p. 676-682.

222. Sankauskaitė, A.; Rubežienė, V.; Kubilienė, D.; Abraitienė, A.; Baltušnikaitė-Guzaitienė, J.; Dubinskaitė, K. Investigation of thermal behavior of 3D PET knits with different bioceramic additives // *Polymers*. ISSN 2073-4360. 2020, vol. 12, iss. 6, art. no. 1319, p. 1-12.

223. Szeremeta, A.Z.; Nowok, A.; Sieradzki, A.; Šimėnas, M.; Vilčiauskas, L.; Gagor, A.; Maczka, M.; Paluch, M.; Pawlus, S. Relaxing under pressure with a rigid niccolite formate framework // *Journal of materials chemistry C*. ISSN 2050-7526. 2020, vol. 8, iss. 47, p. 16736-16741.

224. Šapurov, M.; Bleizgys, V.; Baškys, A.; Dervinis, A.; Bielskis, E.; Paulikas, Š.; Paulauskas, N.; Mačaitis, V. Asymmetric compensation of reactive power using thyristor-controlled reactors // *Symmetry: Symmetry in Renewable Energy and Power Systems*. ISSN 2073-8994. 2020, vol. 12, iss. 6, art. no. 880, p. 1-16.

225. Ščajev, P.; Soriūtė, V.; Kreiza, G.; Malinauskas, T.; Stanionytė, S; Onufrijevs, P; Medvids, A; Cheng, H.-H. Temperature dependent carrier lifetime, diffusion coefficient, and diffusion length in Ge0.95Sn0.05 epilayer // *Journal of applied physics*. ISSN 0021-8979. 2020, vol. 128, no. 11, art. no. 115103, p. 1-8.

226. Seliuta, D.; Vyšniauskas, J.; Ikamas, K.; Lisauskas, A.; Kašalynas, I.; Reklaitis, A.; Valušis, G. Symmetric bow-tie diode for terahertz detection based on transverse hot-carrier transport // *Journal of Physics D: Applied Physics*. ISSN 0022-3727. 2020, vol. 53, iss. 27, art. no. 275106, p. 1-7.

227. Šimėnas, M.; Balčiūnas, S.; Wilson, J.N.; Svirskas, Š.; Kinka, M.; Garbaras, A.; Kalendra, V.; Gagor, A.; Szewczyk, D.; Sieradzki, A.; Mzczka, M.; Samulionis, V.; Walsh, A.; Grigalaitis, R.; Banys, J. Suppression of phase transitions and glass phase signatures in mixed cation halide perovskites // *Nature communications*. eISSN 2041-1723. 2020, vol. 11, art. no. 5103, p. 1-9.

228. Šimoliūnienė, M.; Truncaitė, L.; Petrauskaitė, E.; Zajančkauskaitė, A.; Meškys, R.; Skapas, M.; Kaupinis, A.; Valius, M.; Šimoliūnas, E. Pantoea agglomerans-infecting bacteriophage vB_PagS_AAS21: A cold-adapted virus representing a novel genus within the family Siphoviridae // *Viruses*. ISSN 1999-4915. 2020, vol. 12, iss. 4, art. no. 479, p. 1-8.

229. Šimonis, P.; Garjonytė, R.; Stirkė, A. Mediated amperometry as a prospective method for the investigation of electroporation // *Scientific reports*. eISSN 2045-2322. 2020, vol. 10, art. no. 19094, p. 1-8.

230. Sinkevičius, G.; Vengelis, J.; Banys, J.; Masiulis, L.; Grigonis, R.; Baškys, A.; Sirutkaitis, V.; Domarkas, J. Investigation of piezoelectric ringing effects in deuterated potassium dihydrogen phosphate crystals // *Optical engineering*. ISSN 0091-3286. 2020, vol. 59, iss. 3, art. no. 036107, p. 1-11.

231. Sinušaitė, L.; Popov, A.; Antuzevics, A.; Mažeika, K.; Baltrūnas, D.A.; Yang, J.-Ch.; Horng, J. L.; Shi, Sh.; Sekino, T.; Ishikawa, K.; Kareiva, A.; Žarkov, A. Fe and Zn co-substituted beta-tricalcium phosphate (β-TCP): Synthesis, structural, magnetic, mechanical and biological properties // *Materials science & engineering C: materials for biological applications.* ISSN 0928-4931. 2020, vol. 112, art. no. 110918, p. 1-10.

232. Skovorodko, K.; Bareikė, M.; Gudelis, A.; Gricienė, B. Occupational exposure in a PET/CT facility using two different automatic infusion systems // *Physica medica*. ISSN 1120-1797. 2020, vol. 77, p. 169-175.

233. Skuja, L.; Smits, K.; Trukhin, A.; Gahbauer, F.; Ferber, R.; Auzinsh, M.; Busaite, L.; Razinkovas, L.; Mackoit-Sinkevičienė, M.; Alkauskas, A. Dynamics of singlet oxygen molecule trapped in silica glass studied by luminescence polarization anisotropy and density functional theory // *The journal of physical chemistry C.* ISSN 1932-7447. 2020, vol. 124, iss. 13, p. 7244-7253.

234. Skurkytė-Papievienė, V.; Abraitienė, A.; Sankauskaitė, A.; Rubežienė, V.; Dubinskaitė, K. Enhancement of thermal properties of bio-based microcapsules intended for textile applications // *Open chemistry*. ISSN 2391-5420. 2020, vol.18, iss. 1, p. 669-680.

235. Šlekas, G.; Kancleris, Ž.; Urbanovič, A.; Čiegis, R. Comparison of full-wave models of terahertz photoconductive antenna based on ordinary differential equation and Monte Carlo method // *European physical journal plus*. ISSN 2190-5444. 2020, vol. 135, art. no. 85, p. 1-16.

236. Staišiūnas, L.; Leinartas, K.; Juzeliūnas, E.; Bučinskienė, D.; Grigucevičienė, A.; Kalinauskas, P.; Selskis, A.; Stanionytė, S. Anticorrosion performance of hafnium oxide ultrathin films on AZ31 magnesium alloy // *Surface and coatings technology*. ISSN 0257-8972. 2020, vol. 397, art. no. 126046, p. 1-9.

237. Stanchik, A.V.; Tivanov, M.S.; Tyukhov, I.I.; Juškėnas, R.; Korolik, O.V.; Gremenok, V.F.; Saad, A.M.; Naujokaitis, A. Temperature dependence of Raman scattering in the Cu2ZnSnSe4 thin films on a Ta foil substrate // *Solar energy*. ISSN 0038-092X. 2020, vol. 201, p. 480-488.

238. Stankevičius, L.; Tamulevičius, T.; Žutautas, A.; Juodėnas, M.; Juškevičius, K.; Drazdys, R.; Tamulevičius, S. Diffraction efficiency optimization of multilayer dielectric mirror-based gratings for 1030 nm femtosecond lasers // *Optics & laser technology*. ISSN 0030-3992. 2020, vol. 126, art. no. 106071, p. 1-8.

239. Stankevič, V.; Lueg-Althoff, J.; Hahn, M.; Tekkaya, A.E.; Žurauskienė, N.; Dilys, J.; Klimantavičius, J.; Keršulis, S.; Šimkevičius, Č.; Balevičius, S. Magnetic field measurements during magnetic pulse welding using CMR-B-scalar sensors // *Sensors*. ISSN 1424-8220. 2020, vol. 20, iss. 20, art. no. 5925, p. 1-14.

240. Stankevič, V.; Šimonis, P.; Žurauskienė, N.; Stirkė, A.; Dervinis, A.; Bleizgys, V.; Keršulis, S.; Balevičius, S. Compact square-wave pulse electroporator with controlled electroporation efficiency and cell viability // *Symmetry*. ISSN 2073-8994. 2020, vol. 12, iss. 3, art. no. 412, p. 1-14.

241. Stončius, S.; Butkus, E. Chiral cleft-like methanocyclooctadiindoles: synthesis, circular dichroism and TDDFT study // *Tetrahedron letters*. eISSN 0040-4039. 2020, vol. 61, iss. 37, art. no. 152302, p. 1-5.

242. Strazdaitė, S.; Navakauskas, E.; Kirschner, J; Šneideris, T.; Niaura, G. Structure determination of Hen Egg-White Lysozyme aggregates adsorbed to Lipid/Water and Air/Water interfaces // *Langmuir*. ISSN 0743-7463. 2020, vol. 36, iss. 17, p. 4766-4775.

243. Streckaite, S.; Mačernis, M.; Li, F.; Kuthanová T. E.; Litvin, R.; Yang, Ch.; Pascal, A.A.; Valkūnas, L.; Robert, B.; Llansola-Portoles, M.J. Modeling dynamic conformations of organic molecules: alkyne carotenoids in solution // *The journal of physical chemistry A*. ISSN 1089-5639. 2020, vol. 124, iss. 14, p. 2792-2801.

244. Stummer, V.; Flöry, T.; Krizsán, G.; Polónyi, G.; Kaksis, E.; Pugžlys, A.; Hebling, J.; Fülöp, J.A.; Baltuška, A. Programmable generation of terahertz bursts in chirped-pulse laser amplification // *Optica*. ISSN 2334-2536. 2020, vol. 7, iss. 12, p. 1758-1763.

245. Stygienė, L.; Varnaitė-Žuravliova, S.; Abraitienė, A.; Krauledas, S.; Baltušnikaitė-Guzaitienė, J.; Padleckienė, I. Investigation of thermosregulation properties of various ceramic-containing knitted fabric structures // *Journal of industrial textiles*. ISSN 1528-0837. 2020, vol. 50, iss. 5, p. 716-739.

246. Sukackienė, Z.; Antanavičiūtė, K.; Vaičiūnienė, J.; Tamašauskaitė-Tamašiūnaitė, L.; Naujokaitis, A.; Norkus, E. Electroless deposition of nickel boron coatings using morpholine borane as a reducing agent // *Chemija*. ISSN 0235-7216. 2020, vol. 31, no. 1, p. 1-10.

247. Survila, A.; Kanapeckaitė, S.; Gudavičiūtė, L.; Girčienė, O. Impedance of copper electrode in slightly acid Cu(II)-glycine solutions // *Chemija*. ISSN 0235-7216. 2020, vol. 31, no. 2, p. 69-76.

248. Survila, A.; Kanapeckaitė, S. On the application of electrogenerated copper ions in environmental analytical chemistry – The nature and properties of anodic current peaks // *Journal of electroanalytical chemistry*. ISSN 1572-6657. 2020, vol. 862, art. no. 114035, p. 1-6.

249. Skipitytė, R.; Lidén, K.; Eriksson, G.; Kozakaitė, J.; Laužikas, R.; Piličiauskienė, G.; Jankauskas, R. Diet patterns in medieval to early modern (14th–early 20th c.) coastal communities in Lithuania // *Anthropologischer Anzeiger*. ISSN 0003-5548. 2020, vol. 77, no. 4, p. 299-312.

250. Talaikis, M.; Strazdaitė, S.; Žiaunys, M.; Niaura, G. Far-off resonance: multiwavelength Raman spectroscopy probing amide bands of amyloid-β-(37–42) peptide // *Molecules*. ISSN 1420-3049. 2020, vol. 25, iss. 15, art. no. 3556, p. 1-11.

251. Tamašauskaitė-Tamašiūnaitė, L.; Jagminienė, A.; Stankevičienė, I.; Ratautas, K.; Račiukaitis, G.; Norkus, E. Enhancing effect of chloride ions on the autocatalytic process of Ag(I) reduction by Co(II) complexes // *Materials*. ISSN 1996-1944. 2020, vol. 13, iss. 20, art. no. 4556, p. 1-14.

252. Tartėnas, M.; Zubovas, K. Feeding of active galactic nuclei by dynamical perturbations // *Monthly notices of the Royal Astronomical Society*. ISSN 0035-8711. 2020, vol. 492, iss. 1, p. 603-614.

253. Tautkus, S.; Ishikawa, K.; Ramanauskas, R.; Kareiva, A. Zinc and chromium co-doped calcium hydroxyapatite: Sol-gel synthesis, characterization, behaviour in simulated body fluid and phase transformations // *Journal of solid state chemistry*. ISSN 0022-4596. 2020, vol. 284, art. no. 121202, p. 1-9.

254. Tomkus, V.; Girdauskas, V.; Dudutis, J.; Gečys, P.; Stankevič, V.; Račiukaitis, G.; Gallardo G. I.; Guénot, D.; Svensson, J. B.; Persson, A.; Lundh, O. Laser wakefield accelerated electron beams and betatron radiation from multijet gas targets // *Scientific reports*. eISSN 2045-2322. 2020, vol. 10, art. no. 16807, p. 1-17.

255. Tumėnas, S.; Ragaliauskas, T.; Penkauskas, T.; Valanciute, A.; Ambrulevičius, F.; Valinčius, G. Solvent effects on composition and structure of thiolipid molecular anchors for tethering phospholipid bilayers // *Applied surface science*. ISSN 0169-4332. 2020, vol. 509, art. no. 145268, p. 1-9.

256. Turiansky, M. E.; Alkauskas, A.; Van de Walle, C. G. Spinning up quantum defects in 2D materials // *Nature materials*. ISSN 1476-1122. 2020, vol. 19, iss. 5, p. 487-489.

257. Upskuvienė, D.; Šimkūnaitė, D.; Vaičiūnienė, J.; Kepenienė, V.; Selskis, A.; Tamašauskaitė-Tamašiūnaitė, L.; Norkus, E. Investigation of electro-oxidation of glucose at gold nanoparticles/carbon composites prepared in the presence of halide ions // *Chemija*. ISSN 0235-7216. 2020, vol. 31, no. 4, p. 224-237.

258. Vagner, M.; Plaušinaitienė, V.; Lukose, R.; Keršulis, S.; Talaikis, M.; Knašienė, B.; Stanionytė, S.; Kubilius, V.; Motiejuitis, K.; Šaltytė, Z.; Niaura, G.; Naujalis, E.; Žurauskienė, N. PI-MOCVD technology of (La, Sr) (Mn, Co)O_3: From epitaxial to nanostructured films // *Surface and coatings technology*. ISSN 0257-8972. 2020, vol. 385, art. no. 125287, p. 1-8.

259. Vaitekūnas, J.; Gasparavičiūtė, R.; Stankevičiūtė, J.; Urbelis, G.; Meškys, R. Biochemicaland genetic analysis of 4-hydroxypyridine catabolism in arthrobacter sp. strain IN13 // *Microorganisms*. ISSN 2076-2607. 2020, vol. 8, iss. 6, art. no. 888, p. 1-13.

260. Valiūnienė, A.; Gabriūnaitė, I.; Poderytė, M.; Ramanavičius, A. Electroporation of a hybrid bilayer membrane by scanning electrochemical microscope // *Bioelectrochemistry*. ISSN 1567-5394. 2020, vol. 136, art. no. 107617, p. 1-7.

261. Valiūnienė, A.; Petronienė, J. J.; Dulkys, M.; Ramanavičius, A. Investigation of active and inactivated yeast cells by scanning electrochemical impedance microscopy // *Electroanalysis*. ISSN 1040-0397. 2020, vol. 32, iss. 2, p. 367-374.

262. Valiūnienė, A.; Sabirovas, T.; Petronienė, J. J.; Ramanavičius, A. Towards the application of fast Fourier transform - scanning electrochemical impedance microscopy (FFT-SEIM) // *Journal of electroanalytical chemistry*. ISSN 1572-6657. 2020, vol. 864, art. no. 114067, p. 1-6.

263. Valiūnienė, A.; Virbickas, P.; Medvikytė, G.; Ramanavičius, A. Urea biosensor based on electrochromic properties of Prussian blue // *Electroanalysis*. ISSN 1040-0397. 2020, vol. 32, iss. 3, p. 503-509.

264. Van Amerongen, H.; Chmeliov, J. Instantaneous switching between different modes of non-photochemical quenching in plants. Consequences for increasing biomass production // *Biochimica et biophysica acta (BBA) - Bioenergetics*. ISSN 0005-2728. 2020, vol. 1861, iss. 4, art. no. 148119, p. 1-9.

265. Varnaitė-Žuravliova, S.; Savest, N.; Baltušnikaitė-Guzaitienė, J.; Abraitienė, A.; Krumme, A. Electrospinning of chitosan biopolymer and polyethylene oxide blends // *AUTEX research journal*. ISSN 1470-9589. 2020, vol. 20, iss. 4, p. 426-440.

266. Vengalis, B.; Maneikis, A.; Grigaliūnaitė-Vonsevičienė, G.; Juškėnas, R.; Selskis, A. Alternating current susceptibility and magnetisation of nanocrystalline Co_2MnSi Heusler alloy films // *Lithuanian journal of physics*. ISSN 1648-8504. 2020, vol. 60, no. 1, p. 67-77.

267. Vernickaitė, E.; Lelis, M.; Tsyntsaru, N.; Pakštas, V.; Cesiulis, H. XPS studies on the Mo oxide-based coatings electrodeposited from highly saturated acetate bath // *Chemija*. ISSN 0235-7216. 2020, vol. 31, no. 4, p. 203-209.

268. Vertelis, V.; Balevičius, S.; Stankevič, V.; Žurauskienė, N.; Schneider, M. Pulsed magnetic flux penetration dynamics inside a thin-walled superconducting tube // *Journal of applied physics*. ISSN 0021-8979. 2020, vol. 127, iss. 11, art. no. 113901, p. 1-8.

269. Vertelis, V.; Vincent, G.; Schneider, M.; Balevičius, S.; Stankevič, V.; Žurauskienė, N. Magnetic field expulsion from a conducting projectile in a pulsed serial augmented railgun // *IEEE transactions on plasma science*. ISSN 0093-3813. 2020, vol. 48, iss. 3, p. 727-732.

270. Virbickas, P.; Kavaliauskaitė, G.; Valiūnienė, A.; Plaušinaitienė, V.; Rekertaitė, A. I.; Ramanavičius, A. Cobalt hexacyanoferrate based optical sensor for continuous optical sensing of hydrogen peroxide // *Electrochimica acta*. ISSN 0013-4686. 2020, vol. 362, art. no. 137202, p. 1-8.

271. Voitechovič, E.; Vektarienė, A.; Vektaris, G.; Jančienė, R.; Razumienė, J.; Gurevičienė, V. 1,4-Benzoquinone derivatives for enhanced bioelectrocatalysis by fructose dehydrogenase from Gluconobacter japonicus: towards promising D-fructose biosensor development // *Electroanalysis*. eISSN 1521-4109. 2020, vol. 32, iss. 5, p. 1005-1016.

272. Vyšniauskas, A.; Kuimova, M. K. Microviscosity and temperature sensors: The twists and turns of the photophysics of conjugated porphyrin dimers — a SPP/JPP Young Investigator Award paper // *Journal of porphyrinsand phthalocyanines*. ISSN 1088-4246. 2020, vol. 24, iss. 11n12, p. 1372-1386.

273. Wang, Ch.; Lu, Sh.; Li, S.; Wang, S.; Lin, X.; Zhang, J.; Kondrotas, R.; Li, K.; Chen, Ch.; Tang, J. Efficiency improvement of flexible Sb2Se3 solar cells with non-toxic buffer layer via interface engineering // *Nano energy*. ISSN 2211-2855. 2020, vol. 71, art. no. 104577, p. 1-11.

274. Wickramaratne, D.; Dreyer, C.E.; Shen, J.-X.; Lyons, J.L.; Alkauskas, A.; Van de Walle, Ch.G. Deep-level defects and impurities in InGaN alloys // *Physica Status Solidi B: Basic Solid State Physics*. ISSN 0370-1972. 2020, vol. 257, iss. 4, art. no. 1900534, p. 1-6.

275. Willey, R.R.; Valavičius, A.; Goldstein, F.T. Designing with very thin optical films // *Applied optics*. ISSN 1559-128X. 2020, vol.59, no. 5, p. 213-218.

276. Zabielaitė, A.; Balčiūnaitė, A.; Šimkūnaitė, D.; Lichušina, S.; Stalnionienė, I.; Šimkūnaitė-Stanynienė, B.; Naruškevičius, L.; Tamašauskaitė-Tamašiūnaitė, L.; Norkus, E.; Selskis, A.; Pakštas, V. High performance direct N2H4-H2O2 fuel cell using fiber-shaped Co decorated with Pt crystallites as anode electrocatalysts // *Journal of the electrochemical society*. ISSN 0013-4651. 2020, vol. 167, iss. 5, art. no. 054502, p. 1-9.

277. Zabielaitė, A.; Šimkūnaitė, D.; Balčiūnaitė, A.; Šimkūnaitė-Stanynienė, B.; Stalnionienė, I.; Naruškevičius, L.; Upskuvienė, D.; Selskis, A.; Tamašauskaitė-Tamašiūnaitė, L.; Norkus, E. Investigation of stability of gold nanoparticles modified zinc–cobalt coating in an alkaline sodium borohydride solution // *Chemija*. ISSN 0235-7216. 2020, vol. 31, no. 4, p. 210-223.

278. Zdaniauskienė, A.; Charkova, T.; Ignatjev, I.; Melvydas, V.B.; Garjonytė, R.; Matulaitienė, I.; Talaikis, M.; Niaura, G. Shell-isolated nanoparticle-enhanced Raman spectroscopy for characterization of living yeast cells // *Spectrochimica acta. Part A: Molecular and biomolecular spectroscopy*. ISSN 1386-1425. 2020, vol. 240, art. no. 118560, p. 1-8.

279. Zhang, Y.; Liang, W.; Jin, X.; Krattenmacher, M.; Falk, S.; Sakalas, P.; Heinemann, B.; Schröter, M. 3.2-mW ultra-low-power 173–207-GHz amplifier with 130-nm SiGe HBTs operating in saturation // *IEEE journal of solid-state circuits*. ISSN 0018-9200. 2020, vol. 55, iss. 6, p. 1471-1481.

280. Žemaitis, A.; Gaidys, M.; Gečys, P.; Gedvilas, M. Influence of nonlinear and saturable absorption on laser lift-off threshold of an oxide/metal structure // *Optics letters*. ISSN 0146-9592. 2020, vol. 45, no. 22, p. 6166-6169.

281. Žemaitis, A.; Mimidis, A.; Papadopoulos, A.; Gečys, P.; Račiukaitis, G.; Stratakis, E.; Gedvilas, M. Controlling the wettability of stainless steel from highly-hydrophilic to super-hydrophobic by femtosecond laser-induced ripples and nanospikes // *RSC advances*. eISSN 2046-2069. 2020, vol. 10, iss. 62, p. 37956-37961.

282. Zenker, K.; Sirignano, C.; Riccio, A.; Chianese, E.; Calfapietra, C.; Prati, M.V.; Mašalaitė-Nalivaikė, A.; Remeikis, V.; Mook, E.; Meijer, H.A.J.; Dusek, U. δ13 C signatures of organic aerosols: Measurement method evaluation and application in a source study // J*ournal of aerosol science*. ISSN 0021-8502. 2020, vol. 145, art. no. 105534, p. 1-14.

283. Zubovas, K.; Nardini, E. Intermittent AGN episodes drive outflows with a large spread of observable loading factors // *Monthly notices of the Royal Astronomical Society*. ISSN 0035-8711. 2020, vol. 498, iss. 3, p. 3633-3647.

284. Zubrytė, E.; Gefenienė, A.; Kaušpėdienė, D.; Ragauskas, R.; Binkienė, R.; Selskienė, A.; Pakštas, V. Fast removal of Pb(II) and Cu(II) from contaminated water by groundwater treatment waste: impact of sorbent composition // *Separation science and technology*. ISSN 0149-6395. 2020, vol. 55, iss. 16, p. 2855-2868.

Photo L. Galkauskas